AD-A054 415 WESTINGHOUSE DEFENSE AND ELECTRONIC SYSTEMS CENTER B--ETC F/G 9/1
ANALYSIS OF THE PERFORMANCE OF IMAGE GLIDE SLOPE ANTENNA IN THE--ETC(U)
MAR 78 G J MOUSSALLY, R A MOORE, J T GODFREY DOT-FA74WA-3353

UNCLASSIFIED FAA-RD-78-43 NL

| OF |
AD
A054415

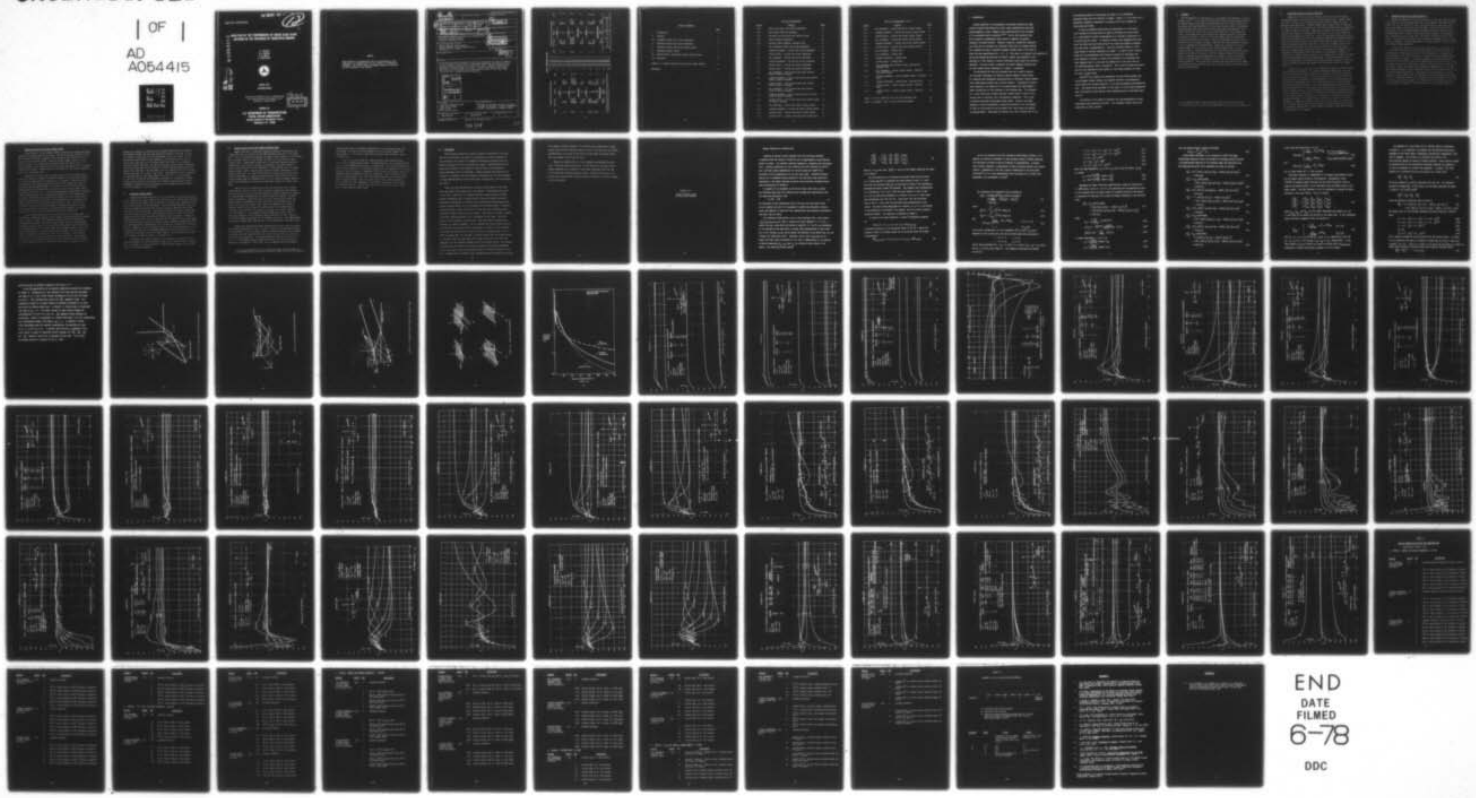

END
DATE
FILMED
6-78
DDC

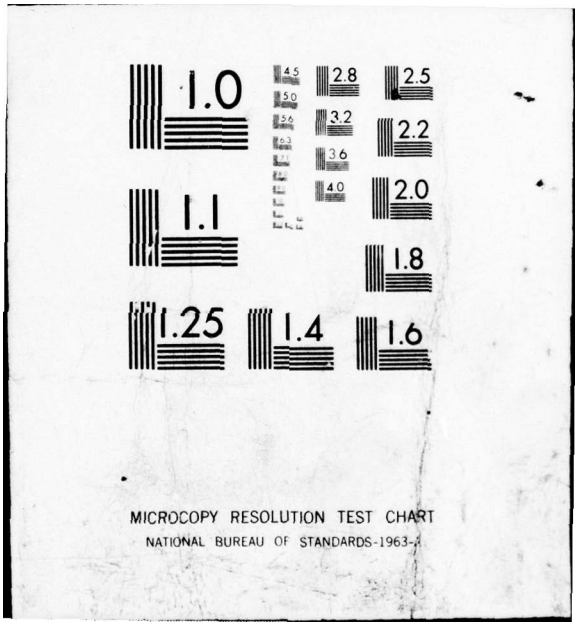
1.0
1.1
1.25
1.4
1.6
1.8
2.0
2.2
2.5
2.8
3.2
3.6
4.0
4.5
5.0
5.6
6.3
MICROCOPY RESOLUTION TEST CHART
NATIONAL BUREAU OF STANDARDS-1963-A

Report No. FAA-RD-78-43

ANALYSIS OF THE PERFORMANCE OF IMAGE GLIDE SLOPE ANTENNA IN THE PRESENCE OF TRUNCATED GROUND

J. T. Godfrey
H. F. Hartley
R. A. Moore
G. J. Moussally

MARCH 1978

INTERIM REPORT

Prepared for

U.S. DEPARTMENT OF TRANSPORTATION
FEDERAL AVIATION ADMINISTRATION
Systems Research & Development Service
Washington, D.C. 20590

NOTICE

Technical Report Documentation Page

1. Report No.	2. Government Accession No.	3. Recipient's Catalog No.
FAA-RD-78-43		

4. Title and Subtitle

ANALYSIS OF THE PERFORMANCE OF IMAGE GLIDE SLOPE ANTENNA IN THE PRESENCE OF TRUNCATED GROUND

5. Report Date: Mar[illegible]78

6. Performing Organization Code

7. Author(s): G. J. Moussally, R. A. Moore, J. T. Godfrey, H. F. Hartley

8. Performing Organization Report No.

9. Performing Organization Name and Address

Westinghouse Defense and Electronic Systems Center
Electronic Systems Division
Baltimore, Maryland 21203

10. Work Unit No. (TRAIS)

11. Contract or Grant No.: DOT-FA74WA-3353

12. Sponsoring Agency Name and Address

Federal Aviation Administration
Systems Research and Development Service
Washington, D.C. 20591

13. Type of Report and Period Covered: Interim Report (2) Modification #5

14. Sponsoring Agency Code: ARD-700

15. Supplementary Notes

12 77 P.

16. Abstract

An analysis has been performed to permit the calculation of fields of dipoles at any orientation over lateral or transverse conducting half-planes and over multiple contiguous strips of arbitrary tilt angle. Computer programs were developed to calculate DDM over terrain types from half-planes and strips. Glide path DDM calculations over typical terrain types for the three image type glide slope systems have been computed.

17. Key Words	18. Distribution Statement
Instrument Landing Systems Glide Slope (Image) Rough Ground Short Ground Planes	Document is available to the U.S. public through the National Technical Information Service, Springfield, Virginia 22161.

19. Security Classif. (of this report)	20. Security Classif. (of this page)	21. No. of Pages	22. Price
UNCLASSIFIED	UNCLASSIFIED	71	

Form DOT F 1700.7 (8-72) Reproduction of completed page authorized

390 358

METRIC CONVERSION FACTORS

Approximate Conversions to Metric Measures

Symbol	When You Know	Multiply by	To Find	Symbol
		LENGTH		
in	inches	*2.5	centimeters	cm
ft	feet	30	centimeters	cm
yd	yards	0.9	meters	m
mi	miles	1.6	kilometers	km
		AREA		
in^2	square inches	6.5	square centimeters	cm^2
ft^2	square feet	0.09	square meters	m^2
yd^2	square yards	0.8	square meters	m^2
mi^2	square miles	2.6	square kilometers	km^2
	acres	0.4	hectares	ha
		MASS (weight)		
oz	ounces	28	grams	g
lb	pounds	0.45	kilograms	kg
	short tons (2000 lb)	0.9	tonnes	t
		VOLUME		
tsp	teaspoons	5	milliliters	ml
Tbsp	tablespoons	15	milliliters	ml
fl oz	fluid ounces	30	milliliters	ml
c	cups	0.24	liters	l
pt	pints	0.47	liters	l
qt	quarts	0.95	liters	l
gal	gallons	3.8	liters	l
ft^3	cubic feet	0.03	cubic meters	m^3
yd^3	cubic yards	0.76	cubic meters	m^3
		TEMPERATURE (exact)		
°F	Fahrenheit temperature	5/9 (after subtracting 32)	Celsius temperature	°C

*1 in = 2.54 (exactly). For other exact conversions and more detailed tables, see NBS Misc. Publ. 286, Units of Weights and Measures, Price $2.25, SD Catalog No. C13.10:286.

Approximate Conversions from Metric Measures

Symbol	When You Know	Multiply by	To Find	Symbol
		LENGTH		
mm	millimeters	0.04	inches	in
cm	centimeters	0.4	inches	in
m	meters	3.3	feet	ft
m	meters	1.1	yards	yd
km	kilometers	0.6	miles	mi
		AREA		
cm^2	square centimeters	0.16	square inches	in^2
m^2	square meters	1.2	square yards	yd^2
km^2	square kilometers	0.4	square miles	mi^2
ha	hectares (10,000 m^2)	2.5	acres	
		MASS (weight)		
g	grams	0.035	ounces	oz
kg	kilograms	2.2	pounds	lb
t	tonnes (1000 kg)	1.1	short tons	
		VOLUME		
ml	milliliters	0.03	fluid ounces	fl oz
l	liters	2.1	pints	pt
l	liters	1.06	quarts	qt
l	liters	0.26	gallons	gal
m^3	cubic meters	35	cubic feet	ft^3
m^3	cubic meters	1.3	cubic yards	yd^3
		TEMPERATURE (exact)		
°C	Celsius temperature	9/5 (then add 32)	Fahrenheit temperature	°F

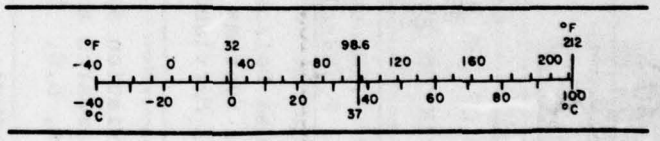

TABLE OF CONTENTS

LIST OF ILLUSTRATIONS

LIST OF ILLUSTRATIONS (cont'd)

I. Introduction

Terrain modeling in electromagnetic scattering problems has traditionally involved separating the terrain under consideration into small enough segments so that a Huygens source approximation to the treatment of the scattered fields is possible.[1,2,3] Use of this technique very often requires an exceedingly large number of segments to properly represent the ground surface. Moreover, numerical integration techniques are often used to calculate the scattered fields from the Huygens sources. This approach can lead to computer programs running times on the order of hours for many applications (ref. 3, p. 70). This paper is concerned with applying the half-plane scattering solutions of Senior[4], Woods[5], and Bromwich[6] to the modeling of a wide variety of terrain conditions using closed form analytic solutions. The use of such a technique can reduce computer running times for many common terrain situations by orders of magnitude.

The motivation for the work presented here was a need to develop more practical techniques (in terms of reduced computer running times) for computing the performance characteristics of instrument landing systems (ILS) glide slope antennas over non-ideal terrain. Practically all glide slope antennas in use today are of the ground-image type which depend on ground reflections for the formation of the guidance beam. The formation of an ideal glide path in space requires a ground plane in front of the antenna that is infinite, flat, and perfectly conducting. Such a case is readily calculated using simple image theory. However, this ideal condition is never encountered in practice and rarely is the flat ground in front of the antenna of such an extent that image theory can provide an accurate model. Many times the terrain is of such a nature that it can

be accurately modeled by half-planes and large (> 2-3 wavelengths) connected strips that are infinite in length. Figure 1-A1 shows some typical geometries frequently encountered in practice which can be modeled by half-planes and strips.

In order to properly characterize the performance of an ILS glide slope antenna on the glide path one needs to calculate the total fields at a large number of points corresponding to an aircraft's position as it is approaching the runway. In addition, several more approaches above and below the glide path and either side of the runway are needed to complete the glide slope characterisation. Thus the scattered fields at a very large number of aircraft positions are needed. In order to have a terrain model that can economically and accurately account for scattering from large segments of terrain, a closed form expression for scattering from these segments that is valid when the segments are in the near field of the radiating antenna system is necessary. Use of the half-plane scattering solution and combining two half-planes to form strips provides the basis for such a terrain model.

Redlich[7,8] has computed the performance of glide slope antennas over limited ground planes, however, his approach involved a two-dimensional terrain model and allowed evaluation of far field performance characteristics only. The terrain model developed in this paper is a fully three dimensional model and allows for near and far field characterization of the glide slope antenna.

Verification of the approach presented has been accomplished by using experimental data obtained by Lucas[13]. Good agreement between theory and experiment has been achieved.

II. APPROACH

The work reported in this Report is a continuation and expansion of that of Godfrey et al[15*]. In the latter work glide path DDM structures associated with the Capture Effect Array image type glide slope ILS over infinite planes and half-planes with edge transverse to the glide path were studied. The studies reported herein deal with all three image type glide slope systems[**] over varied terrain both in front and to the side (lateral) of the antennas and runway. The theory used in the analysis and computer programs is discussed in Appendix I-A herein. Table I-1 lists the various cases for which DDM glide path structures were computed. Section II discusses the results of the computer runs for sloping and rising foreground and their relation to Category I and II tolerance for DDM deviations. Section III discusses the runs for limited lengths of flat foreground with various height steps to a lower foreground plane. Section IV discusses the runs involving sloping and rising ground to the side of the runway. Section V discusses results for various length half-planes with edge parallel to the runway. Section VI includes glide path DDM structures for modified focus of NR and SR systems over the infinite plane[***]. Also results are discussed with modified focus and height with variable azimuth approach angle with all three systems over terrain with sloping lateral ground.

** null reference (NR), sideband reference (SR) and capture effect (CE)

*** modified focus for CE system over infinite plane was treated in reference 15

III. TRUNCATED SLOPING AND RISING FOREGROUND

Figures I-1, I-2 and I-3 show DDM path structures for $\pm 0.6^{\circ}$ tilted foreground pivoted at the antenna for the three image systems. Antenna height and focus are fixed at the standard values used over the large flat plane (infinite plane equivalent). Standard heights were computed from the equations of Table A-1, page A-2 of reference 15. For antenna element position dimensions, see Figures I-28, I-30 and I-32. Positive tilt results in fly-up DDM while negative tilt results in fly-down DDM. The results for run 5 are consistent with those of reference 3, page 3-11. Runs 1,2,3 (positive tilt) show the most deviation from ideal (run 0) for null reference (NR) less for sideband reference (SR), and the least deviation for capture effect (CE) as expected due to the smaller low angle radiation of SR and CE. Run 6 (500' sloping strip) for NR shows the most deviation from the wide strip (10^6 ft) for the same reason. With the standard height of the runs none of the systems meet Category I or II tolerance as indicated by Table I-2; however, by adjustment of height, all systems can be brought within tolerance. The antennas must be raised for rising foreground and lowered for sloping foreground. The gross behaviour of these runs is explained by the fact that with rising ground the antenna patterns are raised resulting in fly-up DDM on-path with the opposite effect for sloping ground.

Figures I-4, I-5, I-6 and I-7 show DDM path structures for tilted foreground pivoted at threshold. For rising foreground, reflections occur from both the horizontal and tilted planes in the vicinity of 3000 feet resulting in the large fly-down signals. This effect decreases for both the SR and CE systems because of decreased low angle radiation. For the sloping ground the DDM follows approximately that of the horizontal plane for a short distance. At longer distances the effect of the lower antenna height above the tilted plane predominates for the NR system, the antenna patterns are raised and fly-up DDM is obtained on-path. For the CE system the decreased low angle radiation results primarily in illumination of the 1100 foot horizontal half-plane giving a small fly-down DDM as in Figure 10 of reference 15. The SR system gives an intermediate result. CE system results for doubled tilt angle are not much different, as expected, as shown in Figure I-7. If the curves are interpreted as the average DDM, all systems meet Category I and II tolerance with the NR the poorest and CE the best. Antenna height adjustments would further improve the performance of all systems.

IV. TRUNCATED STEPPED HALF-PLANE FOREGROUND

Figures I-8 through I-10 show fly-in DDM for a 1000 foot half-plane with a step down to a second plane as indicated in the figures. Runs were made with steps of 10, 20, 30, 50 and 10^7 feet. The result with the last step is the same as that with a single 1000 foot half-plane. The total field arriving at the aircraft in this case was computed by summing the direct field, the reflection from the base plane, the diffraction from the edge, the reflection of edge diffraction from the lower plane, and direct reflection from the lower plane. All systems meet Category I and II guidance tolerances for both average and peak deviations. Further improvement in average deviation could be achieved with antenna height adjustment.

Figures I-11 through I-13 show results with steps at a 500' edge. Now the deviations from the ideal are much larger because the ground currents interrupted by the edge are much larger as shown by Figure 5 of Appendix I-A. It is observed in the latter figure that, at 500 feet from the antenna, the CE ground currents are highest. It would be expected that diffraction effects would be the largest for CE and this is indeed borne out by the results. The CE system has the largest deviation, relative to NR and SR, for 10 feet and 10^7 feet steps. Other step values cause intermediate phasing effects. The only cases meeting Category I and II tolerance are the 10^7 foot step for NR, 10^7 and 20 foot for SR, and none for CE. The effect of the lower plane is to cause oscillations (with range) about the DDM values for the half-plane alone (step = 10^7 feet). Half-plane DDM's can be corrected by height adjustment to zero DDM at long range as shown by Figure 17 of reference 15. Thus some cases can be brought within the Category I and II tolerance by antenna height adjustment.

V. TRUNCATED SLOPING AND RISING LATERAL GROUND

The next series of runs exhibit fly-in structures for sloping and rising ground on the antenna side of the runway. For these cases the antenna is offset 300 feet from the runway centerline and is located on the tilted strip which begins 150 feet from the runway. Standard antenna element heights are used but these heights are perpendicular distances above the tilted plane. If standard heights above runway plane are used, very large far out of of tolerance DDM deviations result. Element offset or Y_s position is for focus at standard height over the runway plane.

Figures I-14 through I-16 are exploratory runs for the three systems showing the effect of varying the extent and angle of a second strip attached to a 200 foot sloping strip as indicated in the figures. A smooth structure is obtained for the large second strip of run 3 with oscillations about the latter run for the limited widths of 200 feet and 0 feet for runs 2 and 1. Tilting upward of the second 200 foot strip as in run 4 adds a small slower oscillation to that of run 3. The CE system compared to NR and SR has slightly larger oscillations in the near region and smaller in the far region due to the larger and smaller edge diffraction currents of the near and far region. Figure I-17 shows fly-in structure for the geometry of run 1 of Figure I-16 with the 200 foot strip tilt angle varied from 0° to 1.72°. At 0° the oscillations are about the standard response of Figure I-16 while, as slope angle is increased, the average is biased below the standard. All runs of Figures I-14 through I-17 are within Category I and II tolerance.

Figures I-18 through I-20 show fly-in results for the three image systems for sloping and rising lateral strips of 200 feet width with variable tilt of 0.86° to 6.88°. The antennas are nominally 300 feet from runway centerline with standard focus and standard height above the sloping plane. Increasing the tilt angle of the ground causes increasing fly-up signals for all systems except for CE at short range for the largest angles. For the NR system angles equal to or greater than about 3° produce out of tolerance average deviations at point C (see Table I-2) and closer. Angles greater than about 6° cause excess deviation at point B and closer. The SR system is similar but is in tolerance for 3.44°. The CE system is within Category I and II tolerance except at threshold for tilt angles of greater than about 6°.

Figures I-21 through I-23 show runs for the same conditions as the previous three figures except that the strip widths are reduced to 150 feet, so that the antenna is positioned over the intersection of the two strips. For the NR system the DDM deviation from standard is now decreased for all angles beyond about 4000 feet, but the larger angles still cause out of tolerance deviations inside 4000 feet. The SR and CE systems show a markedly different behavior with the reduced strip widths in that the DDM deviations go positive beyond about 3000 feet. The SR system is out of tolerance only for tilt angles greater than about 3° at point C and closer. The CE system is out of tolerance at threshold only for tilt angle greater than about 6°. It is of interest to note that, for the SR and CE systems, adjustment of the strips to a width between 150 and 200 feet would yield less derogation beyond point B (zone 2). Adjustment of antenna focus could improve and bring DDM for all tilt angles to within Category I and II tolerance.

VI. TRUNCATED LATERAL GROUND

A series of computer runs were made to investigate the diffraction effects of the single lateral edge formed by the truncation of the infinite plane parallel to the runway on the antenna side as indicated in Figure I-24. Figures I-24 and I-25 show the results for the NR system. The largest DDM deviation occurs when the edge is under the antenna since the edge currents induced by the antenna are largest for this condition. Deviations decrease as the edge is moved away from the antenna and, with 200 feet separation as shown in Figure I-25, small oscillations occur about the standard (infinite plane) structure. Fastest oscillations occur for the 200 foot separation and for aircraft short ground range from threshold because the rate of change of phase difference between the direct and image rays and the diffracted ray from the edge is the highest for these conditions. Similar but larger deviations occur for the CR and CE systems as shown by Figures I-26 and I-27. The largest deviations occur for the SR due to its highest ground current in the near antenna region. CE ground currents are next with SR lowest as shown by Figure 5 of Appendix I-A.

The NR system is within Category I and II tolerance even with the edge under the antenna. For the SR system the edge must be about 15 feet or greater from the antenna to be within tolerance. The CE system requires about 10 feet or more to be within tolerance.

VII. MODIFIED FOCUS, HEIGHT AND AZIMUTH APPROACH ANGLE

Figure I-28, Run 1, shows that modified focusing of the NR array over a large flat plane can result in small DDM deviations from zero on the flight path*. This is achieved by displacing the upper antenna element 1.5 feet further from the runway than the lower element in lieu of 1.13 feet closer as with standard focus. Displacement greater than 1.5 feet will decrease the fly-up DDM (negative sign) but will increase the fly-down in the near threshold region. Runs 1A and 1B show the sensitivity of the modified focus to azimuth approach angles of $\pm 8^{C}$. Runs OA and OB give the azimuth sensitivity of the standard focus case. All azimuth runs result in fly-up signal because large lateral displacements in either direction from the flight path take the receiving antenna under the radiation null of the top antenna element. Displacement of the transmitting antenna from runway center causes the azimuth asymmetry.

Figure I-29 shows modified focus runs for the NR array over sloping lateral ground. Only one large tilted strip was considered in the modified focus runs because the trial and error nature of finding optimum focus becomes too computer-time consuming when two tilted strips are involved. A narrow tilted strip yields oscillations about the large strip and two narrow contiguous strips of different tilt give results not much different from one strip of the same total width. Run 4 shows that modified focus yields a threshold region structure with less deviation from the standard (Run 0) than Run 1 with standard focus; however, both Runs 1 and 4 meet Category I and II tolerance. A top element relative displacement greater than 1.9 feet would bring most of the threshold region DDM closer to zero. Runs 4A and 4B give azimuth sensitivity for the modified focus case. Here DDM polarity changes with azimuth angle polarity due to the diffraction by the edge at YSE.

Figure I-30 shows some SR array modified focus effects over flat ground and sloping lateral ground. Run 1 is over a flarge flat ground plane and with this adjustment of the top element (almost in vertical line with lower element) the flight path DDM deviation from zero is not more than about 1 μa over the entire path into threshold. The derogation from zero here is less than that of Run 1 for the NR system (Figure I-28) but more than that for the CE system (Reference 15, Figure 8). Runs 3, 2, 4, and 5 of Figure I-30 are for sloping

* It is shown in Reference 15 that modified focusing of the CE array can produce essentially zero DDM over the entire flight path into the threshold.

lateral ground and for increasing displacement of the top element away from the runway. All runs are within Category I and II tolerence. Figure I-31 shows glide path structures for $\pm 8^{\circ}$ azimuth approach angle for Runs 1 and 4 of Figure I-31.

Figure I-32 shows results of computed fly-ins using modified focus CE Array with sloping lateral ground. The DDM structure for a standard focused array is given approximately by Run 3 of Figure I-16. The latter run indicates fly-up signal relative to the standard reference over the entire path but is within Category I and II tolerance. Modification of the focus can, however, reduce the deviation from the standard as shown for example by Run 2 of Figure I-32 in which the third element is 0.1 feet (1.89 feet standard) closer to the runway than the second element. Runs 1,3, and 4 are for other focus adjustments. Run 1 is about the best adjustment if zero DDM is considered to be the ideal or reference structure Figure I-33 shows how the structure of Run 1 varies with azimuth approach angle at $\pm 8^{\circ}$.

VIII. Conclusion

The half-plane diffraction analysis reported in Reference 15 has been extended and generalized to permit the calculation of fields of dipoles of any orientation over lateral or transverse conducting half-planes and over multiple contiguous strips of arbitrary tilt angle. Fields diffracted from strips were obtained as the difference between fields of half-planes of length difference equal to stripwidth. Computer programs were modified and extended to incorporate the field equations resulting from the above analysis to enable DDM calculations over terrain types synthesizable from half-planes and strips.

Glide path DDM calculations over typical terrain types for the three image type glide slope systems have been computed. Foreground tilted $\pm 0.6^{\circ}$ at the antenna causes out of otolerance DDM with standard antenna heights; however, performance can be brought within tolerance by height adjustmert. Foreground tilted $\pm 0.86^{\circ}$ at threshold gives within tolerance performance with standard antenna height but can be improved with modified height. Foreground with steps between 10 feet and 10^{7} feet at 1000 feet from the antenna gives performance within tolerance for all systems. With steps at 500 feet, however, the Capture Effect system goes out of tolerance for all steps. The other systems are in tolerance for some cases. Some cases could be brought into tolerance by height adjustment. For the sloping and rising lateral ground it was found that all antennas must be positioned at standard, or near standard height above the tilted plane, rather than above the runway plane, to give within tolerance DDM. For antennas at standard height over the sloping section of a lateral trough the tilt angle must be less than about 3° for the null reference, 3.4° for sideband reference and 6° for capture effect. For antennas positioned over the center of the lateral trough the tilt angle requirement is about the same as above but fly-down signals are obtained over much of the path. Modified focus and height could improve and bring performance with larger

tilt angles to within tolerance. For terrain having effectively a single lateral edge the null reference antenna can be on the edge, but the sideband reference must be at least 15 feet from the edge while the capture effect must be at least 10 feet from the edge.

Effects of modified focus of null reference and sideband reference over a flat plane were investigated. It was found that the upper antenna element position can be adjusted to give small deviations from zero DDM in the glide path threshold approach region. Modified focus runs of all systems over sloping (0.86^{o}) lateral ground were found to be within Category I and II tolerance.

APPENDIX I-A

TERRAIN MODELING USING THE HALF-PLANE GEOMETRY

General Theoretical Considerations

Modeling of general terrain features with the half-plane geometry is possible when the terrain in question can be approximated by semi-infinite planes or strips. The observed radiation depends on a geometric and diffracted term. Analytic expressions for the radiation have been obtained by Senior[4] for a vertical dipole perpendicular to the half-plane and Woods[5] for a horizontal dipole perpendicular to the half-plane edge. Bromwich[6] presents results for a horizontal dipole parallel to the half-plane edge which when calculated in the manner outlined by Senior yield solutions including second order contributions in distance.

In general it is convenient to divide the total field into a direct and reflected term where the reflected term includes the contributions from the image and diffraction, thus

$$\vec{E} = \vec{E}^D + \vec{E}^R . \qquad (1)$$

The advantage of this formulation lies in the fact that the direct field is only counted once and it is necessary to modify the solutions of Senior, Woods, and Bromwich to take this into consideration when summing contributions from more than one strip.

The reflected fields define a set of nine solutions (for a unit dipole), $\mathcal{E}^R_{ij}(x_e;x_0,y_0,z_0,x,y,z)$ where i denotes the field component (i = X,Y,Z), j denotes the axis along which the dipole is parallel (j = X,Y,Z), x_e corresponds to the position of the edge which is always taken perpendicular to the X-axis and in the XY-plane, x_0,y_0, and z_0 denote the position of the dipole and x,y, and z denote the observation point. Locating a set of axes (X_0,Y_0,Z_0) at the dipole such that they are parallel to X,Y, and Z, respectively, it is possible to define components d_{X_0}, d_{Y_0}, and d_{Z_0} for arbitrary orientations of the dipole. The resulting fields satisfy:

$$\begin{pmatrix} E_X^R \\ E_Y^R \\ E_Z^R \end{pmatrix} = \begin{pmatrix} \mathcal{E}_{XX}^R & \mathcal{E}_{XY}^R & \mathcal{E}_{XZ}^R \\ \mathcal{E}_{YX}^R & \mathcal{E}_{YY}^R & \mathcal{E}_{YZ}^R \\ \mathcal{E}_{ZX}^R & \mathcal{E}_{ZY}^R & \mathcal{E}_{ZZ}^R \end{pmatrix} \begin{pmatrix} d_{X_0} \\ d_{Y_0} \\ d_{Z_0} \end{pmatrix} , \tag{2}$$

where $d_k = d\, a_k$ such that $\sum_k a_k^2 = 1$ and d is the complex amplitude and phase of the dipole.

For the situation of an arbitrarily oriented dipole and half-plane it is always possible to transform the space system to axes X, Y, and Z such that the solutions $\mathcal{E}_{ij}^R$ can be calculated in terms of the expressions developed by Senior, Woods, and Bromwich. The simplest such transformation is a translation, $T(x',y',z')$, from the space system to a set of axes fixed in the half-plane followed by a rotation, $A(\alpha,\beta,\gamma)$, which takes the intermediate axes into the XYZ - system such that the half-plane lies in the XY - plane with the half-plane edge perpendicular to the X-axis. The Euler angles specifying the rotation, (α,β,γ), are defined in the convention of Goldstein[9], for example, with the rotation operator similarly defined. The situation is depicted in Figure 2.

In terms of the above operation, a vector $\vec{r}$ transforms according to

$$\vec{r}(x,y,z) = A(\alpha,\beta,\gamma)\; T(x',y',z')\; \vec{r}(x_s,y_s,z_s) . \tag{3}$$

Following calculation of the reflected fields in the XYZ - system the original fields in the space system can be recovered using the inverse transformation

$$\vec{E}^R(x_s,y_s,z_s) = T^{-1}(x',y',z')\; A^{-1}(\alpha,\beta,\gamma)\; \vec{E}^R(x,y,z) . \tag{4}$$

So far the discussion has been confined to half-planes, however, it is possible to extend the procedure to semi-infinite strips by simply combining two half-plane solutions using the principal of superposition. Although this solution technique is approximate in that the ground currents are assumed frozen, a consequence of the dual integral formulation of the half-plane solutions[10], it is a good approximation when the strips are of finite size exceeding a few wavelengths in width[11].

The reflected field component $\mathcal{E}^R_{XX}$ is defined by

$$\mathcal{E}^R_{XX} = -ik/\sqrt{rr_0}\, H_0^{(2)}(kR_1)\sin(\theta/2)\sin(\theta_0/2) - i/2\left(\frac{\partial 2}{\partial x \partial x_0} - k^2\right)\left[\phi_R(\pm) - \phi_S(\pm)\right] + f(S;x,x_0)\,, \tag{5}$$

where

$$\phi_S(\pm) = \pm\int_{\pm\mu_S}^{\infty} H_1^{(2)}(kS\cosh\mu)\,d\mu \tag{6a}$$

$$\phi_R(\pm) = \pm\int_{\pm\mu_R}^{\infty} H_1^{(2)}(kR\cosh\mu)\,d\mu \tag{6b}$$

and

$$f(S;x,x_0) = \begin{cases} \left(\frac{\partial}{\partial x \partial x_0}\right)^2 - k^2 \Big] e^{-ikS}/kS & (0 < \theta < \pi - \theta_0) \\ 0 & (\theta > \pi - \theta_0) \end{cases} \tag{6c}$$

In the above expressions k is the wavenumber, $H_1^{(2)}$ and $H_0^{(2)}$ are Hankel functions of the second kind, the plus and minus signs are determined by

$$\pm: \ \theta \lessgtr \pi - \theta_0 \qquad (S\text{-term})$$

$$\pm: \ \theta \lessgtr \pi + \theta_0 \qquad (R\text{-term})$$

with θ and θ_0 defined by $(x - x_e) = r\cos\theta$, $z = r\sin\theta$, $(x_0 - x_e) = r_0\cos\theta_0$, and $z_0 = r_0\sin\theta_0$ (see Figure 3). The remaining quantities are defined as follows:

$$R = ((x - x_0)^2 + (y - y_0)^2 + (z - z_0)^2)^{\frac{1}{2}} \tag{7a}$$

$$S = ((x - x_0)^2 + (y - y_0)^2 + (z + z_0)^2)^{\frac{1}{2}} \tag{7b}$$

$$r = ((x - x_e)^2 + z^2)^{\frac{1}{2}} \tag{7c}$$

$$r_0 = ((x_0 - x_e)^2 + z_0^2)^{\frac{1}{2}} \tag{7d}$$

$$R_1 = ((r + r_0)^2 + (y - y_0)^2)^{\frac{1}{2}} \tag{7e}$$

where the edge dependence, x_e, is in r, r_0, and R_1 and the limits μ_R and μ_S become

$$\mu_R = \sinh^{-1}\left[2\sqrt{\frac{rr_0}{R}}\ \cos\tfrac{1}{2}(\theta - \theta_0)\right] \tag{8a}$$

$$\mu_S = \sinh^{-1}\left[2\sqrt{\frac{rr_0}{S}}\ \cos\tfrac{1}{2}(\theta + \theta_0)\right] \tag{8b}$$

Expanding the Hankel functions asymptotically, using the substitution $\tau = \sqrt{2ku}\ \sinh\tfrac{1}{2}\mu$ (where u = R or S), and evaluating the non-exponential terms in the integrals about the lower limits (as outlined by Senior) one obtains an expression for Equation (5) in terms of Fresnel integrals of the following form:

$$\begin{aligned}\mathcal{E}^R_{xx} = {} & N_{R_1} \sin\tfrac{1}{2}\theta \sin\tfrac{1}{2}\theta_0 \\ & - k\left[\operatorname{sgn}(\tau_R)\ G_R(|\tau_R|) - \operatorname{sgn}(\tau_S)\ G_S(|\tau_S|)\right] \\ & + 1/k\left[\operatorname{sgn}(\tau_R)\ H_R(|\tau_R|;x,x_0) - \operatorname{sgn}(\tau_S)\ H_S(|\tau_S|;x,x_0)\right] \\ & + f(S;x,x_0)\ ,\end{aligned} \tag{9}$$

where

$$N_{R_1} = \sqrt{\frac{2k}{\pi R_1 rr_0}}\ e^{-i(kR_1 + \pi/4)} \tag{10a}$$

$$G_u(|\tau_u|) = \sqrt{\frac{2}{\pi}}\, e^{i\pi/4} \frac{e^{-iku}}{\sqrt{R_1(R_1 + u)}}\ F(|\tau_u|) \tag{10b}$$

$$H_u(|\tau_u|;m,m_0) = \frac{\partial^2}{\partial m \partial m_0}\ G_u(|\tau_u|) \tag{10c}$$

In these expressions $u = R \text{ or } S$ and

$$\tau_R = 2\sqrt{\frac{krr_0}{R_1 + R}}\ \cos\tfrac{1}{2}(\theta - \theta_0) \tag{11a}$$

$$\tau_S = 2\sqrt{\frac{krr_0}{R_1 + S}}\ \cos\tfrac{1}{2}(\theta + \theta_0) \tag{11b}$$

with the complex Fresnel integral satisfying

$$F(|\tau_u|) = \int_{|\tau_u|}^{\infty} e^{-i\tau^2}\, d\tau \quad . \tag{12}$$

Unlike Senior and Woods it was necessary to retain the image contribution separately since the presence of the edge position prevents a straightforward expansion of the combined image and diffracted term. The remaining reflected field components are given as follows:

$$\mathcal{E}^R_{XY} = 1/k \left[\operatorname{sgn}(\tau_R)\, H_R(|\tau_R|;x,y_0) - \operatorname{sgn}(\tau_S)\, H_S(|\tau_S|;x,y_0) \right] + f(S;x,y_0) \tag{13}$$

$$\mathcal{E}^R_{XZ} = -N_{R_1} \sin\tfrac{1}{2}\Theta \cos\tfrac{1}{2}\Theta_c + 1/k \left[\operatorname{sgn}(\tau_R)\, H_R(|\tau_R|;x,z_0) - \operatorname{sgn}(\tau_S)\, H_S(|\tau_S|;x,z_0) \right] + f(S;x,z_0) \tag{14}$$

$$\mathcal{E}^R_{YX} = 1/k \left[\operatorname{sgn}(\tau_R)\, H_R(|\tau_R|;y,x_0) - \operatorname{sgn}(\tau_S)\, H_S(|\tau_S|;y,x_0) \right] + f(S;y,x_0) \tag{15}$$

$$\mathcal{E}^R_{YY} = -k \left[\operatorname{sgn}(\tau_R)\, G_R(|\tau_R|) - \operatorname{sgn}(\tau_S)\, G_S(|\tau_S|) \right] + 1/k \left[\operatorname{sgn}(\tau_R)\, H_R(|\tau_R|;y,y_0) - \operatorname{sgn}(\tau_S)\, H_S(|\tau_S|;y,y_0) \right] + f(S;y,y_0) \tag{16}$$

$$\mathcal{E}^R_{YZ} = 1/k \left[\operatorname{sgn}(\tau_R)\, H_R(|\tau_R|;y,z_0) - \operatorname{sgn}(\tau_S)\, H_S(|\tau_S|;y,z_0) \right] + f(S;y,z_0) \tag{17}$$

$$\mathcal{E}^R_{ZX} = -N_{R_1} \cos\tfrac{1}{2}\Theta \sin\tfrac{1}{2}\Theta_c + 1/k \left[\operatorname{sgn}(\tau_R)\, H_R(|\tau_R|;z,x_0) - \operatorname{sgn}(\tau_S)\, H_S(|\tau_S|;z,x_0) \right] + f(S;z,x_0) \tag{18}$$

$$\mathcal{E}^R_{ZY} = 1/k \left[\operatorname{sgn}(\tau_R)\, H_R(|\tau_R|;z,y_0) - \operatorname{sgn}(\tau_S)\, H_S(|\tau_S|;z,y_0) \right] + f(S;z,y_0) \tag{19}$$

$$\mathcal{E}^R_{ZZ} = N_{R_1} \cos\tfrac{1}{2}\Theta \cos\tfrac{1}{2}\Theta_c - k \left[\operatorname{sgn}(\tau_R)\, G_R(|\tau_R|) + \operatorname{sgn}(\tau_S)\, G_S(|\tau_S|) \right] + 1/k \left[\operatorname{sgn}(\tau_R)\, H_R(|\tau_R|;z,z_0) - \operatorname{sgn}(\tau_S)\, H_S(|\tau_S|;z,z_0) \right] + g(S;z,z_0) \quad . \tag{20}$$

In the above equations when $0 < \theta < \pi - \theta_c$

$$f(S;m,m_0) = \begin{cases} \left(\frac{\partial^2}{\partial m \partial m_0} - k^2\right) e^{-ikS}/kS & (m = x \text{ or } y \text{ and } m_0 = x_0 \text{ or } y_0, \text{ respectively}) \\ \frac{\partial^2}{\partial m \partial m_0} e^{-ikS}/kS , & (m, m_0 \text{ denote different axes}) \end{cases} \tag{21a}$$

also

$$g(S;z,z_0) = \left(\frac{\partial^2}{\partial z \partial z_0} + k^2\right) e^{-ikS}/kS \quad . \tag{21b}$$

For all other values of θ , f and g vanish.

The direct radiation is independent of the ground plane geometry except for the shadow region defined by this geometry. Consequently, since e^{-ikR}/kR is invariant under rotations one can define the direct fields in terms of any system subject to the requirement that the fields vanish in the shadow region. For most purposes it will be convenient to express the direct radiation in the space system. Thus, one obtains

$$\begin{pmatrix} E^D_{X_s} \\ E^D_{Y_s} \\ E^D_{Z_s} \end{pmatrix} = \begin{pmatrix} \mathcal{E}^D_{X_sX_s} & \mathcal{E}^D_{X_sY_s} & \mathcal{E}^D_{X_sZ_s} \\ \mathcal{E}^D_{Y_sX_s} & \mathcal{E}^D_{Y_sY_s} & \mathcal{E}^D_{Y_sZ_s} \\ \mathcal{E}^D_{Z_sX_s} & \mathcal{E}^D_{Z_sY_s} & \mathcal{E}^D_{Z_sZ_s} \end{pmatrix} \begin{pmatrix} d_{X_{s0}} \\ d_{Y_{s0}} \\ d_{Z_{s0}} \end{pmatrix} , \tag{22}$$

where $d_{X_{s0}}$, $d_{Y_{s0}}$, and $d_{Z_{s0}}$ are the dipole components with respect to a set of axes fixed at the dipole and parallel to the space axes. In the illuminated region the direct component fields are defined by

$$\mathcal{E}^D_{M_sM'_s} = \begin{cases} -\left(\frac{\partial^2}{\partial m_s \partial m'_{s0}} - k^2\right) e^{-ikR}/kR & (M_s = M'_s) \\ -\frac{\partial^2}{\partial m_s \partial m'_{s0}} e^{-ikR}/kR & (M_s \neq M'_s) \end{cases} \tag{23}$$

When $M_s = X_s$, Y_s, or Z_s one has $m_s = x_s, y_s$, or z_s, respectively, and when $M'_s = X_s$, Y_s, or Z_s one has $m'_{s0} = x_{s0}$, y_{s0}, or z_{s0}, respectively. In the space system (x_s, y_s, z_s) defines the observer position while (x_{s0}, y_{s0}, z_{s0}) represents the dipole coordinates analogous to the XYZ system.

The geometry for a half-plane over an infinite plane is illustrated in Figure 4. It is important to recognize that the reflected diffraction component of the fields makes a substantial contribution; consequently, this term is included. The problem is to determine the fields in the four principal regions of practical interest depicted. Since aircraft antenna are sensitive only to the horizontally polarized radiation (Y_s-component) it will be convenient to consider this component. In region I the field consists of a reflected (from the half-plane) and a direct term:

$$E_{Y_s}^{(I)} = E_{Y_s}^{D} + E_{Y_s}^{R} \quad . \tag{24}$$

The direct radiation is given by Equations (22) and (23). The reflected radiation is simply $E_{Y_s}^{R} = d\, \mathcal{E}_{YY}^{R}$ where d is the dipole amplitude and phase. In region II the fields satisfy

$$E_{Y_s}^{(II)} = E_{Y_s}^{D} + E_{Y_s}^{R} - E_{Y_s}^{R'} \quad , \tag{25}$$

where the reflected diffraction term is given by

$$E_{Y_s}^{R'} = -d\,k \left[\operatorname{sgn}(\tau_{R'})\, G_{R'}(|\tau_{R'}|) - \operatorname{sgn}(\tau_{S'})\, G_{S'}(|\tau_{S'}|) \right] \tag{26}$$
$$+ d/k \left[\operatorname{sgn}(\tau_{R'})\, H_{R'}(|\tau_{R'}|; y, y_0) - \operatorname{sgn}(\tau_{S'})\, H_{S'}(|\tau_{S'}|; y, y_0) \right] .$$

The primes refer to the indicated distances and angles depicted in Figure 4 where

$$R' = ((x - x_0)^2 + (y - y_0)^2 + (z + 2h + z_0)^2)^{\frac{1}{2}} \tag{27a}$$

$$S' = ((x - x_0)^2 + (y - y_0)^2 + (z + 2h - z_0)^2)^{\frac{1}{2}} \tag{27b}$$

$$r' = ((x - x_e)^2 + (z + 2h)^2)^{\frac{1}{2}} \tag{27c}$$

$$r_0' = r_0 \tag{27d}$$

$$R_1' = ((r' + r_0')^2 + (y - y_0)^2)^{\frac{1}{2}} \tag{27e}$$

with h being the height of the half-plane above the infinite plane. In region III the fields are the same as in region II except the half-plane's image term vanishes ($\theta > \pi - \theta_e$). Finally, in region IV the fields are the same as in region III except they include the reflected direct term (from the infinite plane).

$$E_{Y_s}^{(IV)} = E_{Y_s}^{(III)} + d\, f(R'; y, y_0) \quad , \tag{28}$$

where $f(R';y,y_0)$ is defined in Equations (21a) with $S = R'$.

To see the applicability of the general presentation consider the situation of Figure 1a. Contributions to the reflected field come from the half-plane with edge at $x_e = 0$ and a strip rotated according to $A(-\frac{\pi}{2},\psi,\frac{\pi}{2})$ with edges at 0 and x'. The solutions only involve the $\mathcal{E}^R_{YY}$ component fields. The situation of Figure 1b is simply treated as previously discussed in the half-plane over the infinite plane case. In Figure 1d a lateral edge is illustrated with edge at $y_{se} = -y'$. One simply rotates the space system through the transformation $A(-\frac{\pi}{2},0,0)$ with only the $\mathcal{E}^R_{XX}$ component fields entering the calculation. Figure 1c corresponds to a rotated half-plane, $A(-\frac{\pi}{2},0,0)$ representing the transformation needed, with edge at $y_{se} = -y'$. In addition a tilted strip contributes where the required transformation for modeling the strip is $A(-\pi,-\phi,\frac{\pi}{2})\ T(0,-y',0)$. In general since only the Y_s component of the total fields is needed for modeling aircraft antennas the $\mathcal{E}^R_{XX}$, $\mathcal{E}^R_{ZZ}$, $\mathcal{E}^R_{XZ}$, and $\mathcal{E}^R_{ZX}$ component fields will be required for this case. In all cases the antenna dipoles are parallel to the Y_s - axis.

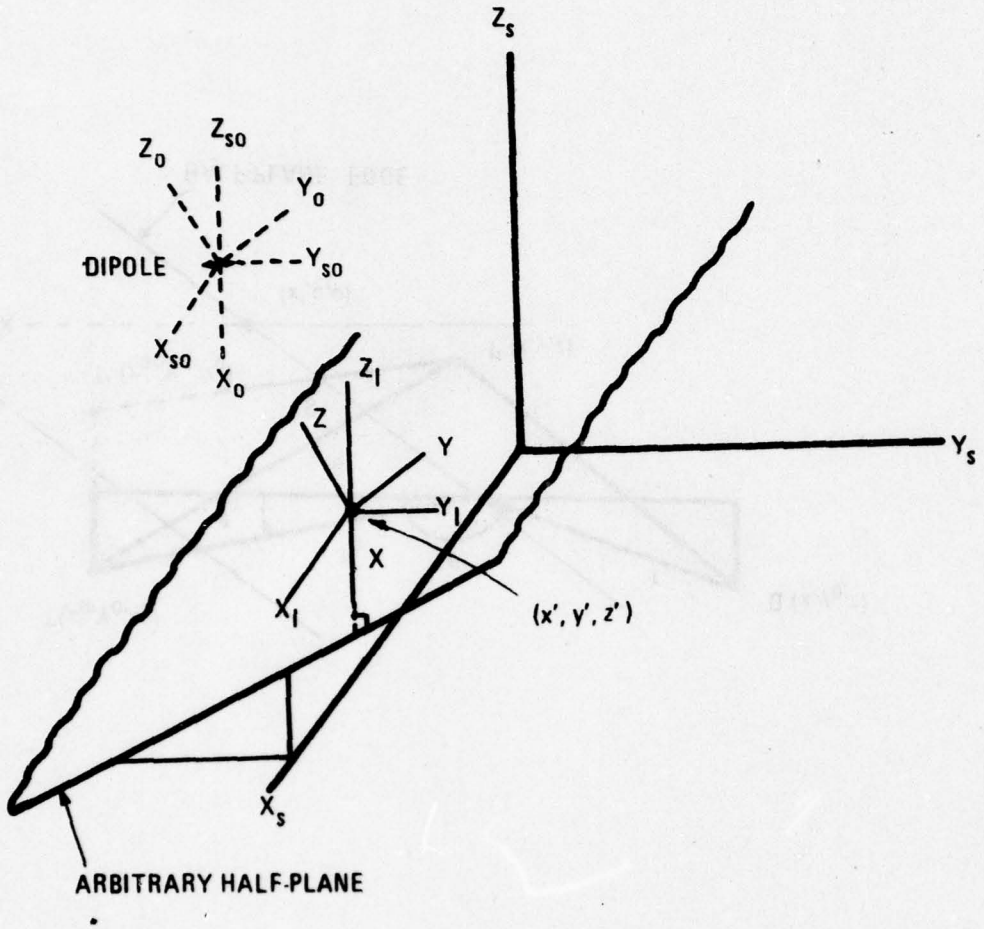

FIGURE I-A2 SPACE, HALF-PLANE, AND DIPOLE COORDINATES

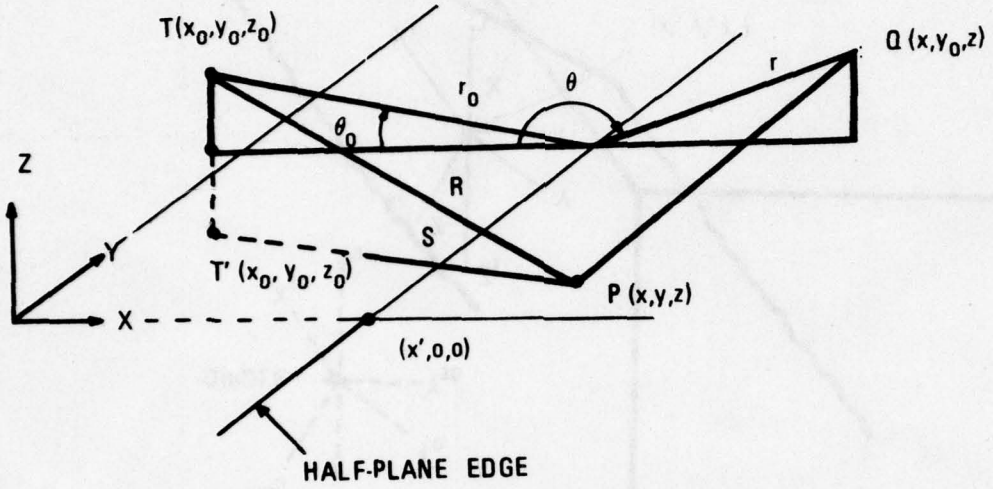

FIGURE I-A3 HALF-PLANE DIFFRACTION VARIABLES

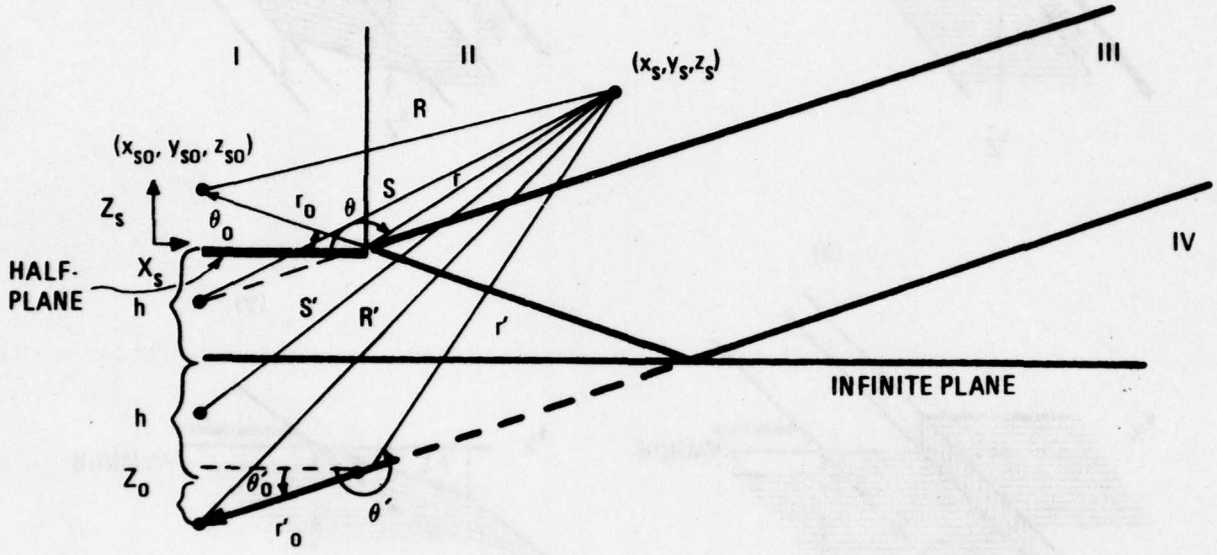

FIGURE I--A4 VARIABLES FOR HALF--PLANE OVER INFINITE PLANE

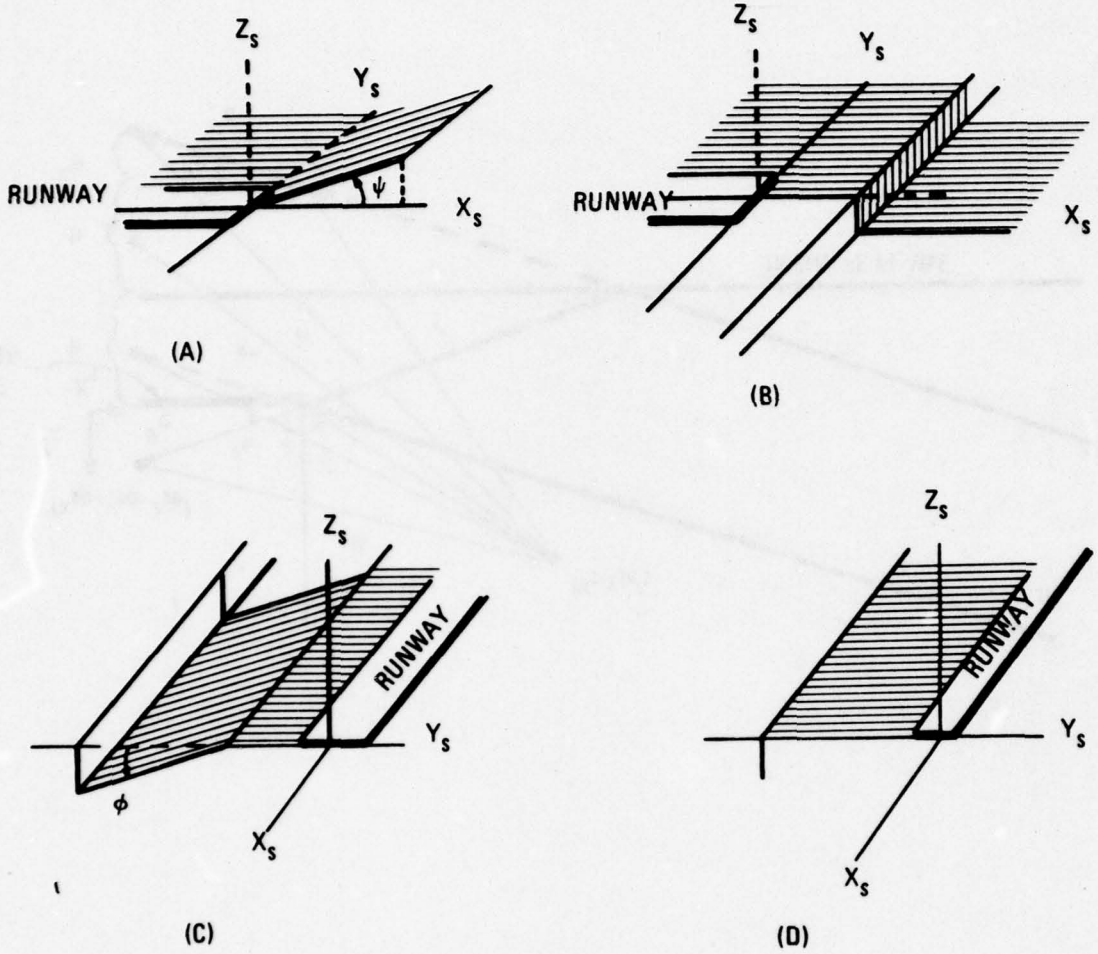

FIGURE I--A1 TYPICAL TERRAIN GEOMETRICS

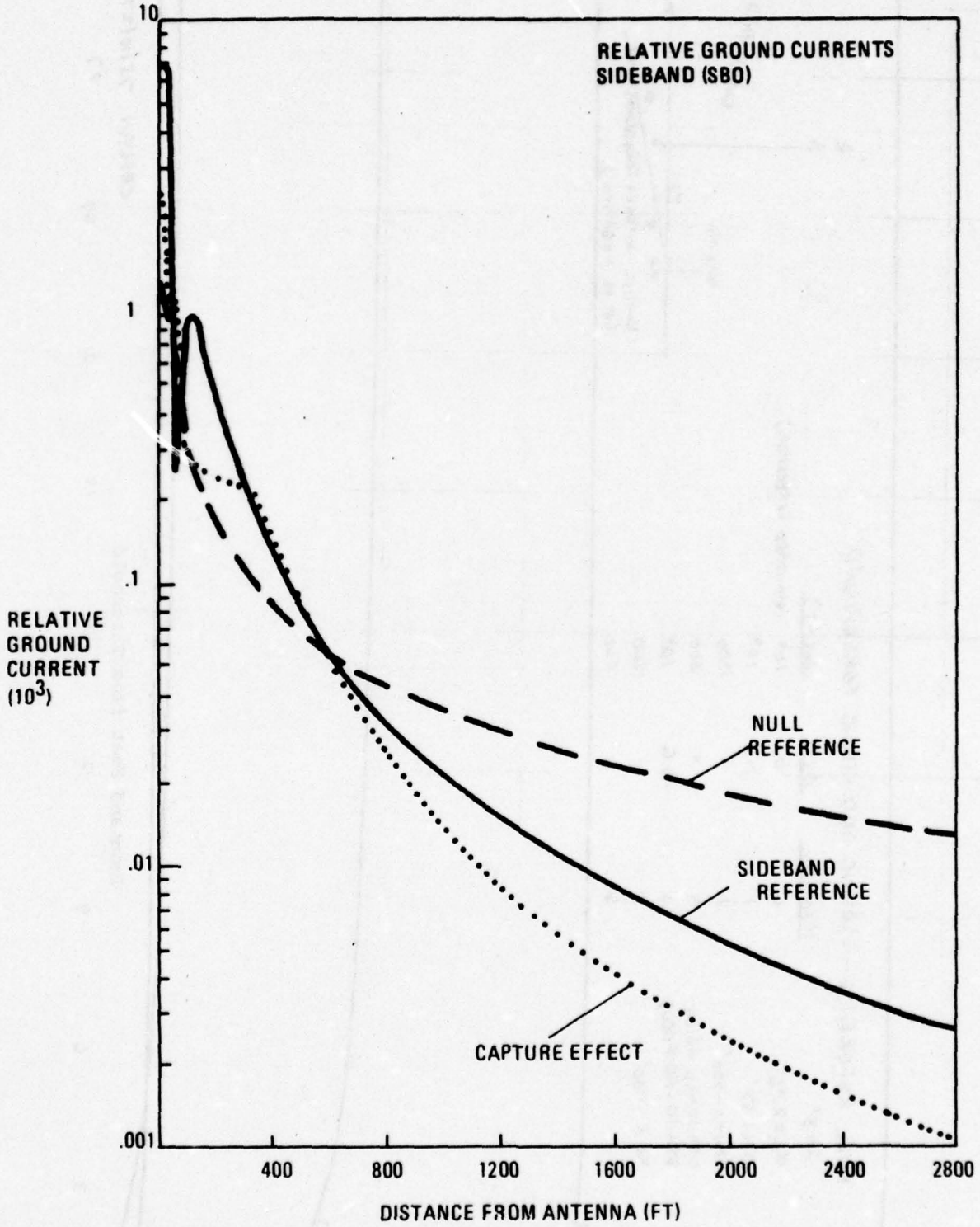
RELATIVE GROUND CURRENTS
SIDEBAND (SBO)
10
1
.1
.01
.001
RELATIVE
GROUND
CURRENT
(10^3)
NULL
REFERENCE
SIDEBAND
REFERENCE
CAPTURE EFFECT
400
800
1200
1600
2000
2400
2800
DISTANCE FROM ANTENNA (FT)

FIGURE I-A5

FIGURE I-1

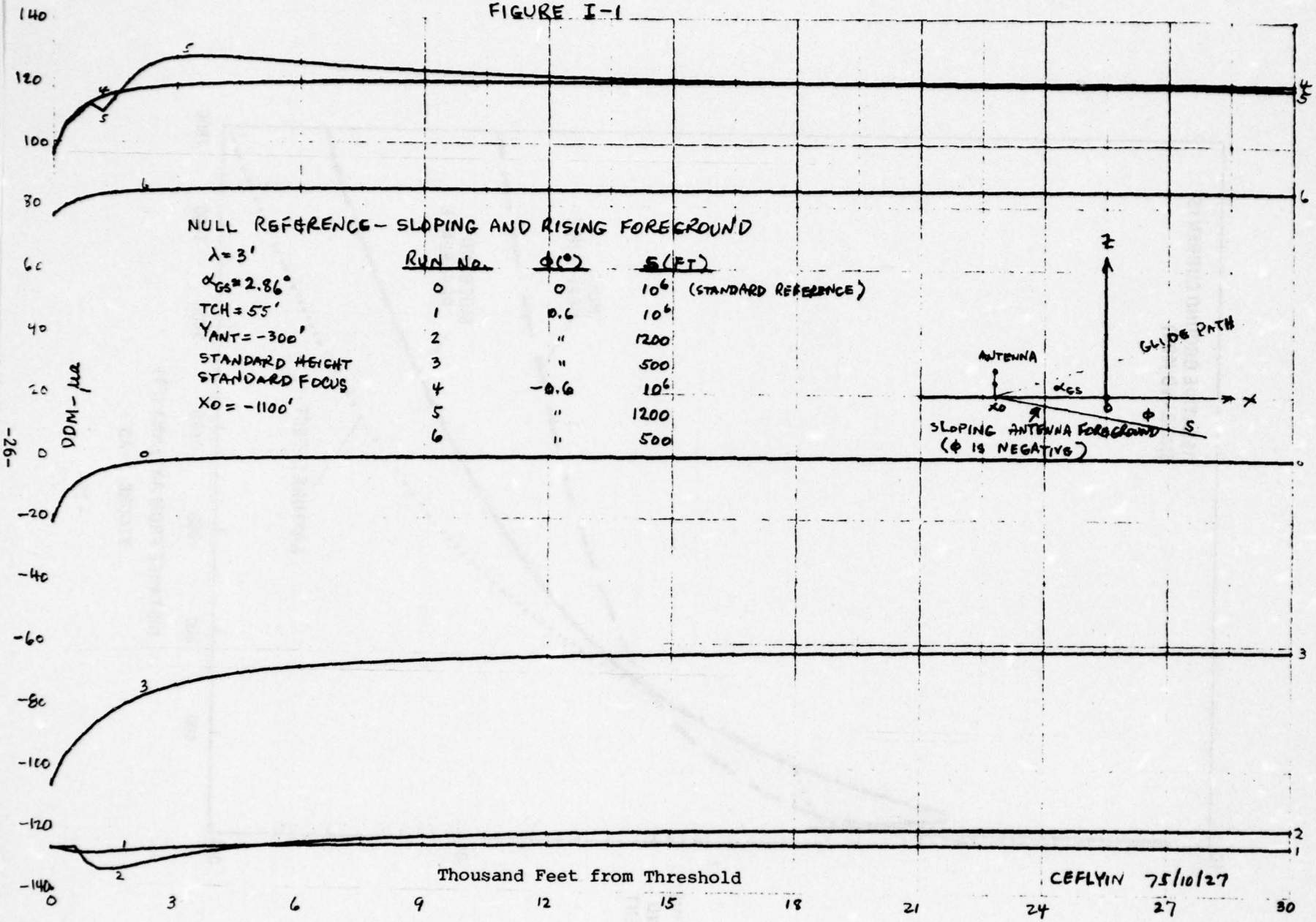

NULL REFERENCE - SLOPING AND RISING FOREGROUND

$\lambda = 3'$

$\alpha_{GS} = 2.86°$

TCH = 55'

$Y_{ANT} = -300'$

STANDARD HEIGHT

STANDARD FOCUS

$X_0 = -1100'$

RUN No.	ϕ(°)	S(FT)
0	0	10^6 (STANDARD REFERENCE)
1	0.6	10^6
2	"	1200
3	"	500
4	-0.6	10^6
5	"	1200
6	"	500

FIGURE I-2

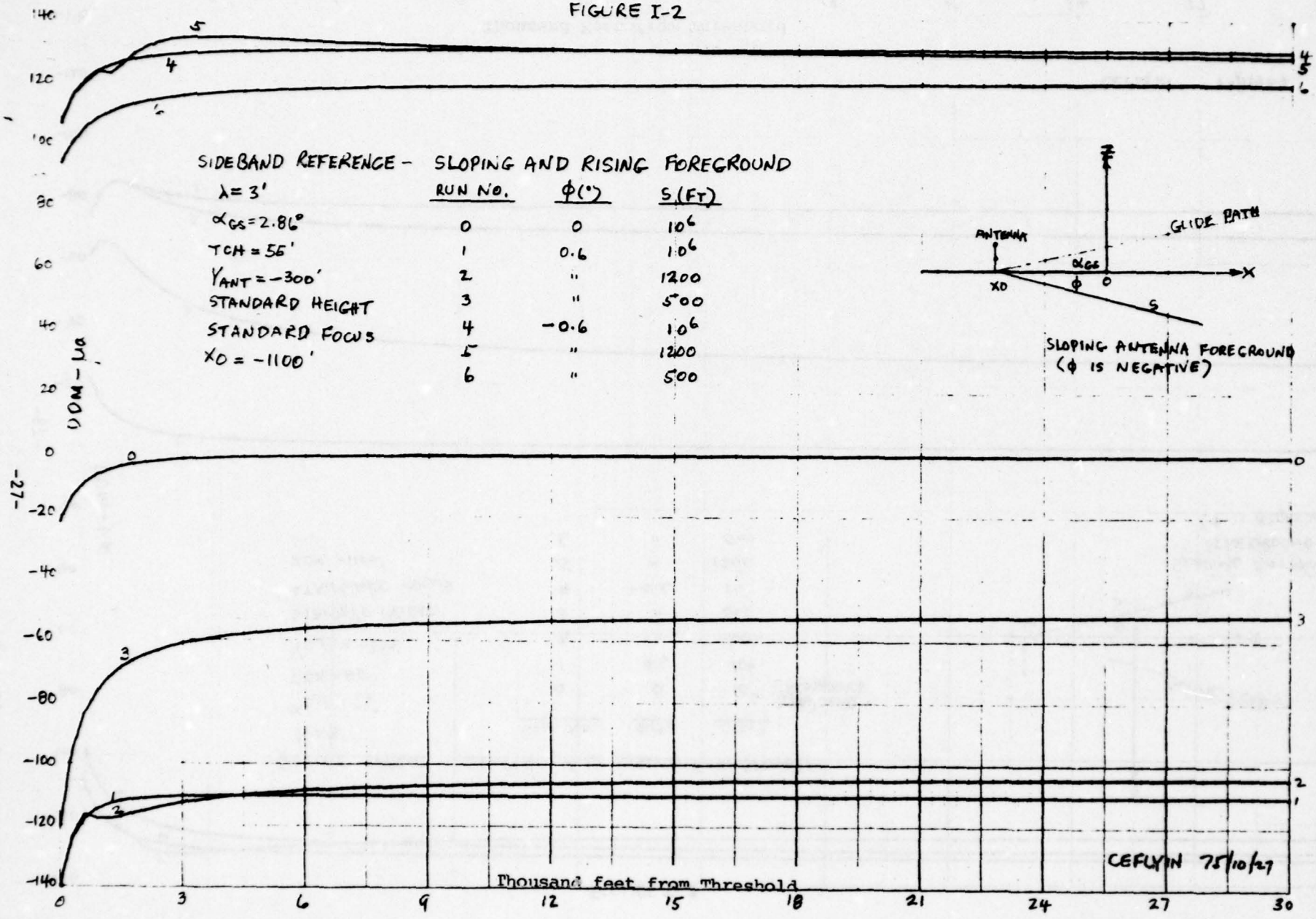
SIDEBAND REFERENCE - SLOPING AND RISING FOREGROUND
λ = 3'
α_{GS} = 2.86°
TCH = 56'
Y_{ANT} = −300'
STANDARD HEIGHT
STANDARD FOCUS
XO = −1100'
RUN NO. | φ(°) | S(FT)
0 | 0 | 10^6
1 | 0.6 | 10^6
2 | " | 1200
3 | " | 500
4 | −0.6 | 10^6
5 | " | 1200
6 | " | 500
ANTENNA
GLIDE PATH
α_{GS}
XO
φ
0
X
S
SLOPING ANTENNA FOREGROUND
(φ IS NEGATIVE)
DDM - Ua
140
120
100
80
60
40
20
0
-20
-40
-60
-80
-100
-120
-140
0
3
6
9
12
15
18
21
24
27
30
Thousand feet from Threshold
CEFLYIN 75/10/27

FIGURE I-3

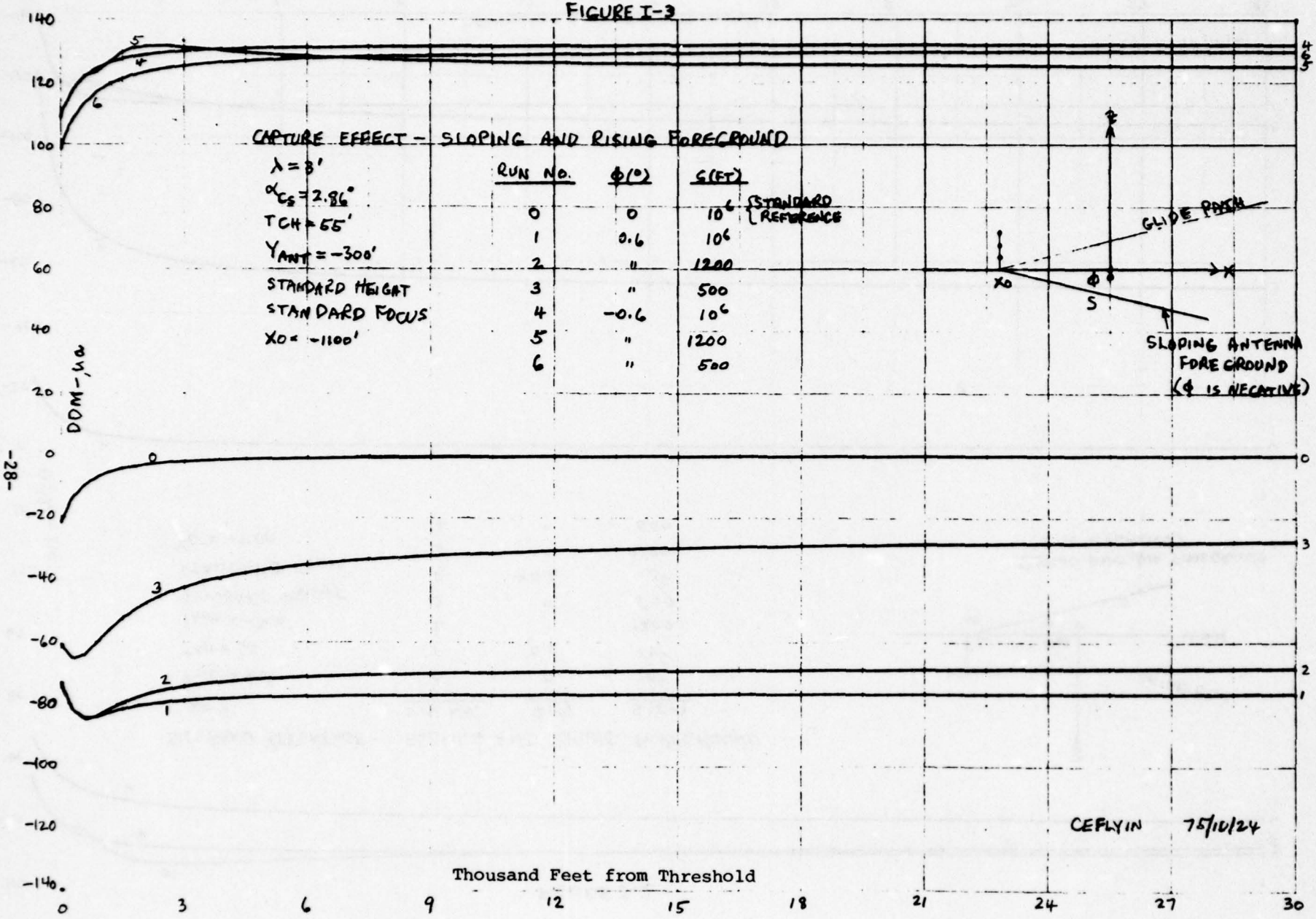
CAPTURE EFFECT - SLOPING AND RISING FORECROUND
$\lambda = 3'$
$\alpha_{GS} = 2.86°$
TCH = 55'
$Y_{ANT} = -300'$
STANDARD HEIGHT
STANDARD FOCUS
$X_0 = -1100'$
RUN NO. | Φ(°) | G(FT)
0 | 0 | 10^6 {STANDARD REFERENCE
1 | 0.6 | 10^6
2 | " | 1200
3 | " | 500
4 | -0.6 | 10^6
5 | " | 1200
6 | " | 500
GLIDE PATH
X_0
Φ
S
SLOPING ANTENNA FORE GROUND (Φ IS NEGATIVE)
DDM-μa
140
120
100
80
60
40
20
0
-20
-40
-60
-80
-100
-120
-140
-28-
0
3
6
9
12
15
18
21
24
27
30
Thousand Feet from Threshold
CEFLYIN 75/10/24

FIGURE I-4

NULL REFERENCE - SLOPING AND RISING FOREGROUND

$\lambda = 3'$
$\alpha_{GS} = 2.86°$
TCH = 55'
$Y_{ANT} = -300'$
STANDARD HEIGHT
STANDARD FOCUS
$X_0 = -1100'$

RUN NO.	ϕ(°)	S(FT)
0	0	10^6
1	0.86	10^6
2	"	1000
3	"	500
4	-0.86	10^6
5	"	1000
6	"	500

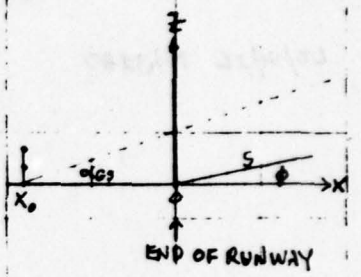

FIGURE I-5

SIDEBAND REFERENCE - SLOPING AND RISING FOREGROUND

$\lambda = 3'$

$\alpha_{GS} = 2.86°$

TCH = 55'

$Y_{ANT} = -306'$

STANDARD HEIGHT

STANDARD FOCUS

$X_0 = -1100'$

RUN. No.	ϕ(°)	S(FT)
0	0	10^6
1	0.86°	10^6
2	"	1000
3	"	500
4	-0.86°	10^6
5	"	1000
6	"	500

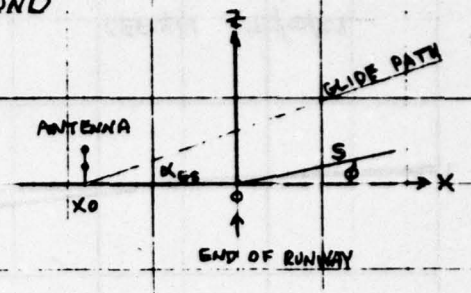

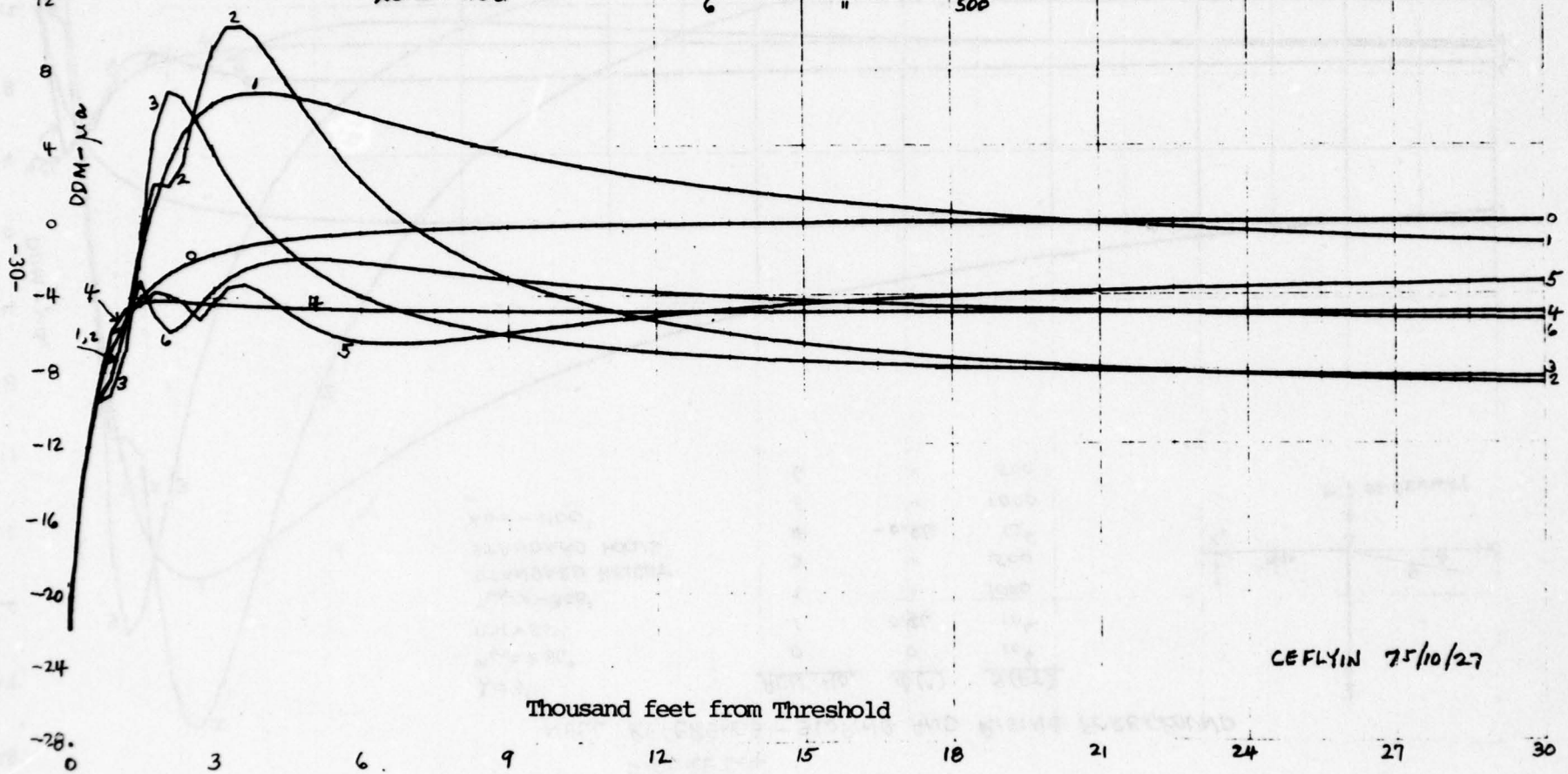

FIGURE I-4

NULL REFERENCE - SLOPING AND RISING FOREGROUND

$\lambda = 3'$
$\alpha_{GS} = 2.86°$
TCH = 55'
$Y_{ANT} = -300'$
STANDARD HEIGHT
STANDARD FOCUS
$X_0 = -1100'$

RUN NO.	ϕ(°)	S(FT)
0	0	10^6
1	0.86	10^6
2	"	1000
3	"	500
4	-0.86	10^6
5	"	1000
6	"	500

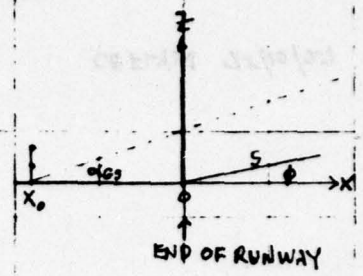

DDM-μa

28 24 20 16 12 8 4 0 -4 -8 -12 -16 -20 -24 -28

0 3 6 9 12 15 18 21 24 27 30

Thousand feet from Threshold

GEFLYN 75/10/27

FIGURE I-5

SIDEBAND REFERENCE - SLOPING AND RISING FOREGROUND

$\lambda = 3'$

$\alpha_{GS} = 2.86°$

TCH = 55'

$Y_{ANT} = -300'$

STANDARD HEIGHT

STANDARD FOCUS

$X_0 = -1100'$

RUN. No.	ϕ(°)	S(FT)
0	0	10^6
1	0.86°	10^6
2	"	1000
3	"	500
4	-0.86°	10^6
5	"	1000
6	"	500

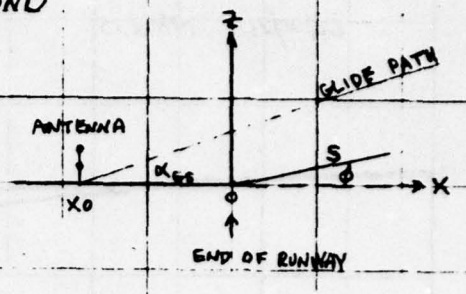

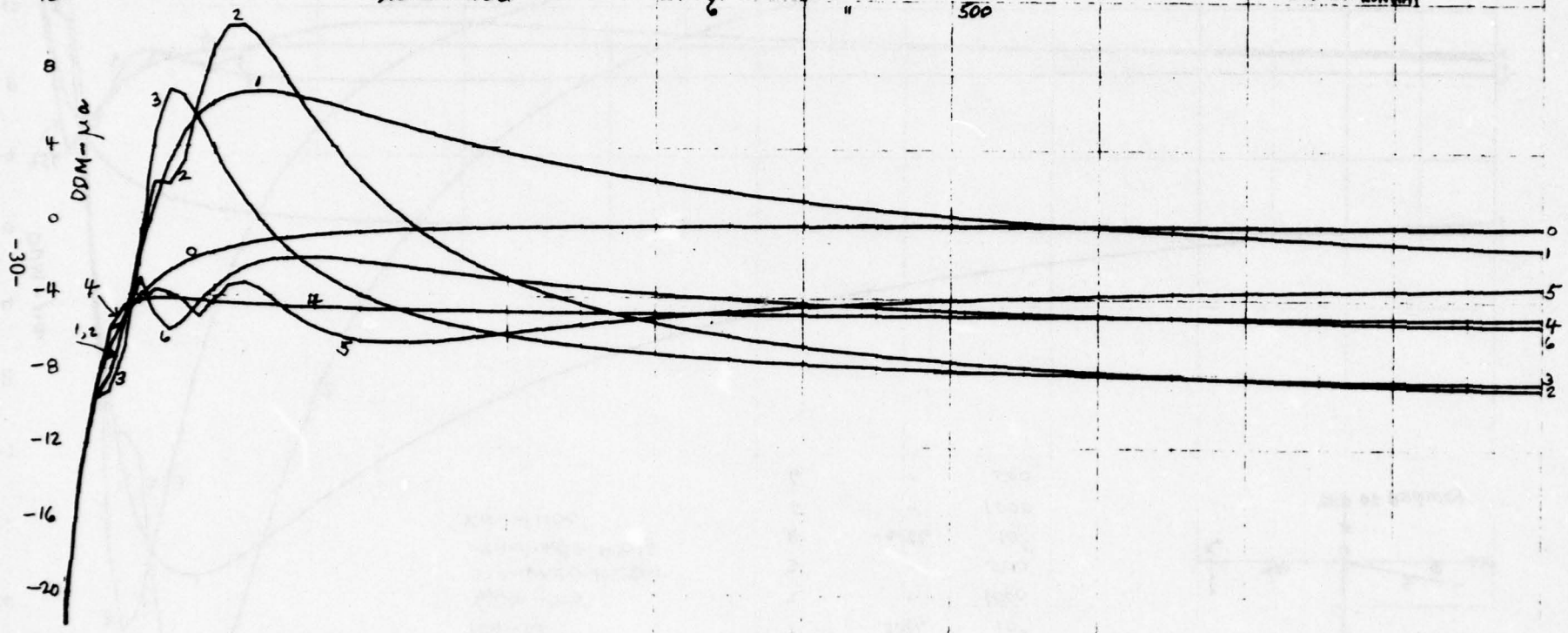

CEFLYIN 75/10/27

FIGURE I-6

CAPTURE EFFECT - SLOPING AND RISING FOREGROUND

$\lambda = 3'$
$\alpha_{GS} = 2.86°$
TCH = 55'
$Y_{ANT} = -300'$
STANDARD HEIGHT
" FOCUS
$X_0 = -1100'$

RUN NO.	ϕ(°)	S(FT)
0	0	10^6
1	0.86	10^6
2	"	1000
3	"	500
4	-0.86	10^6
5	"	1000
6	"	500

0 IS STANDARD REFERENCE RUN

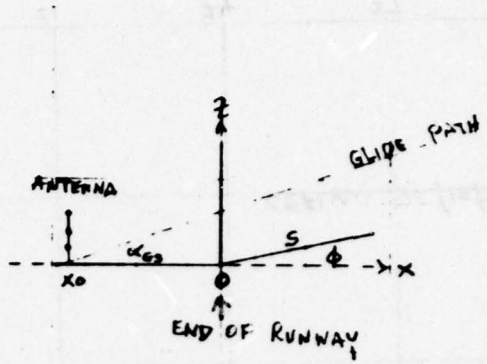

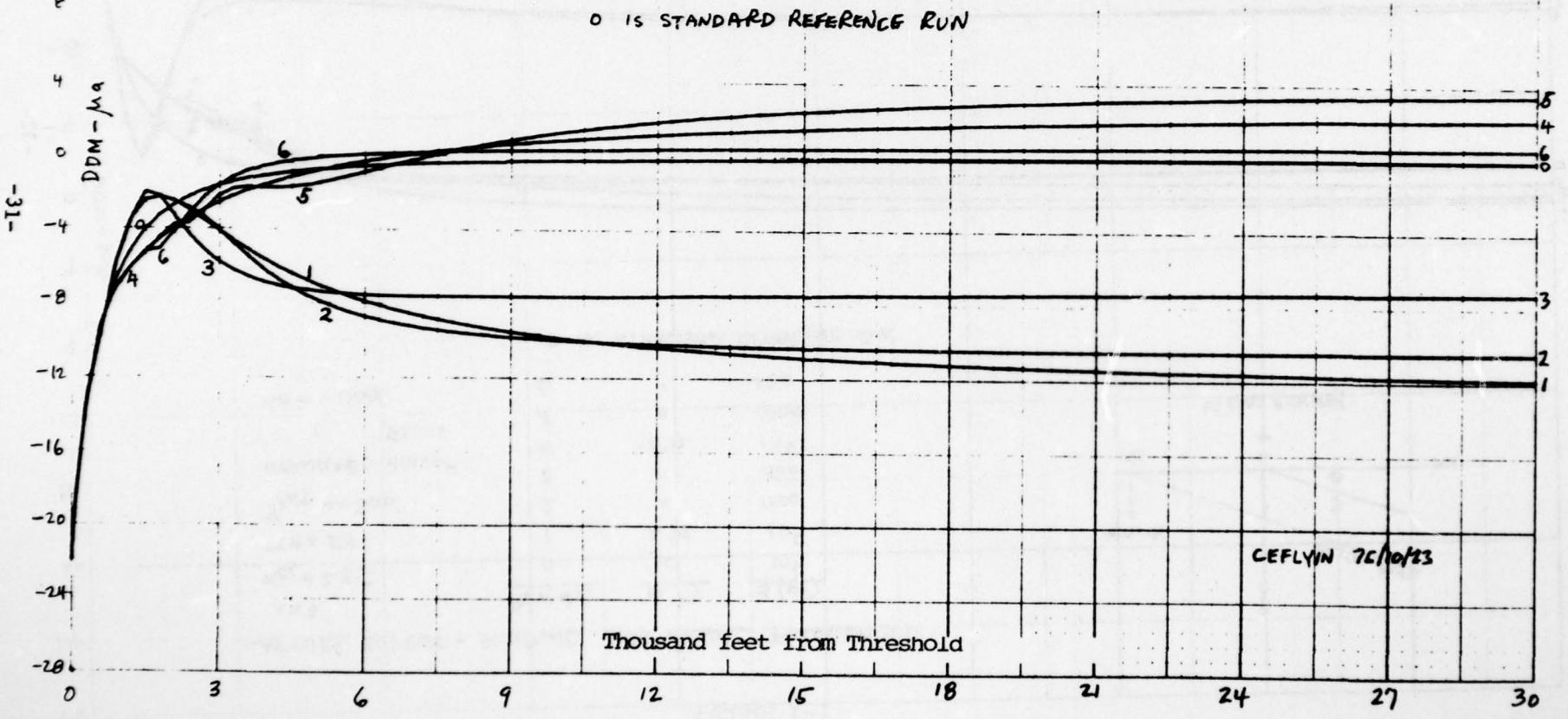

FIGURE I-7

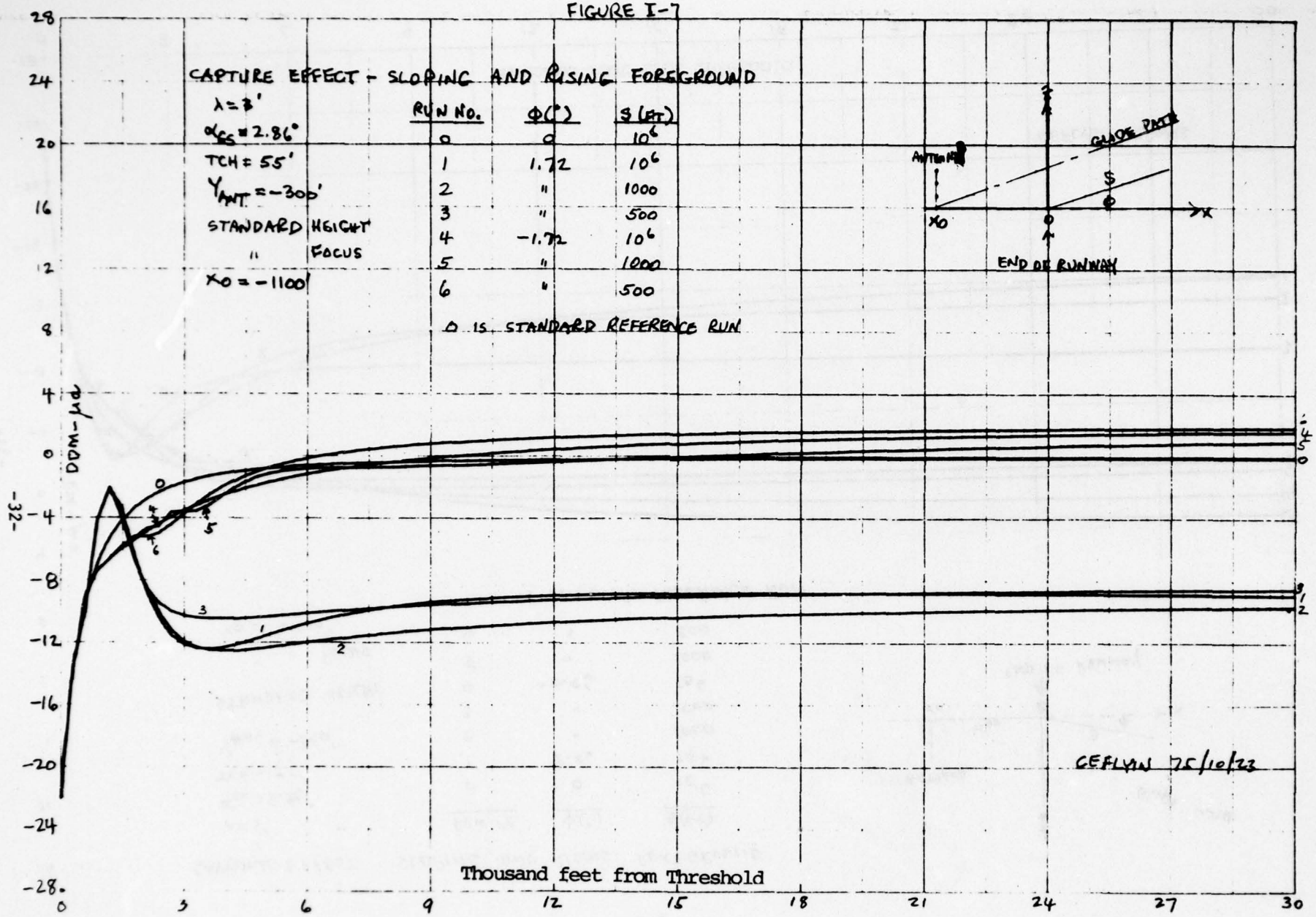
CAPTURE EFFECT - SLOPING AND RISING FOREGROUND
λ = 3'
α_GS = 2.86°
TCH = 55'
Y_ANT = -300'
STANDARD HEIGHT
" FOCUS
X0 = -1100'
RUN NO. Φ(°) S(FT)
0 0 10^6
1 1.72 10^6
2 " 1000
3 " 500
4 -1.72 10^6
5 " 1000
6 " 500
0 IS STANDARD REFERENCE RUN
ANTENNA
GLIDE PATH
X0
END OF RUNWAY
DDM-μd
28
24
20
16
12
8
4
0
-4
-8
-12
-16
-20
-24
-28.
-32-
0
3
6
9
12
15
18
21
24
27
30
Thousand feet from Threshold
CEFLYIN 75/10/23

FIGURE I-8

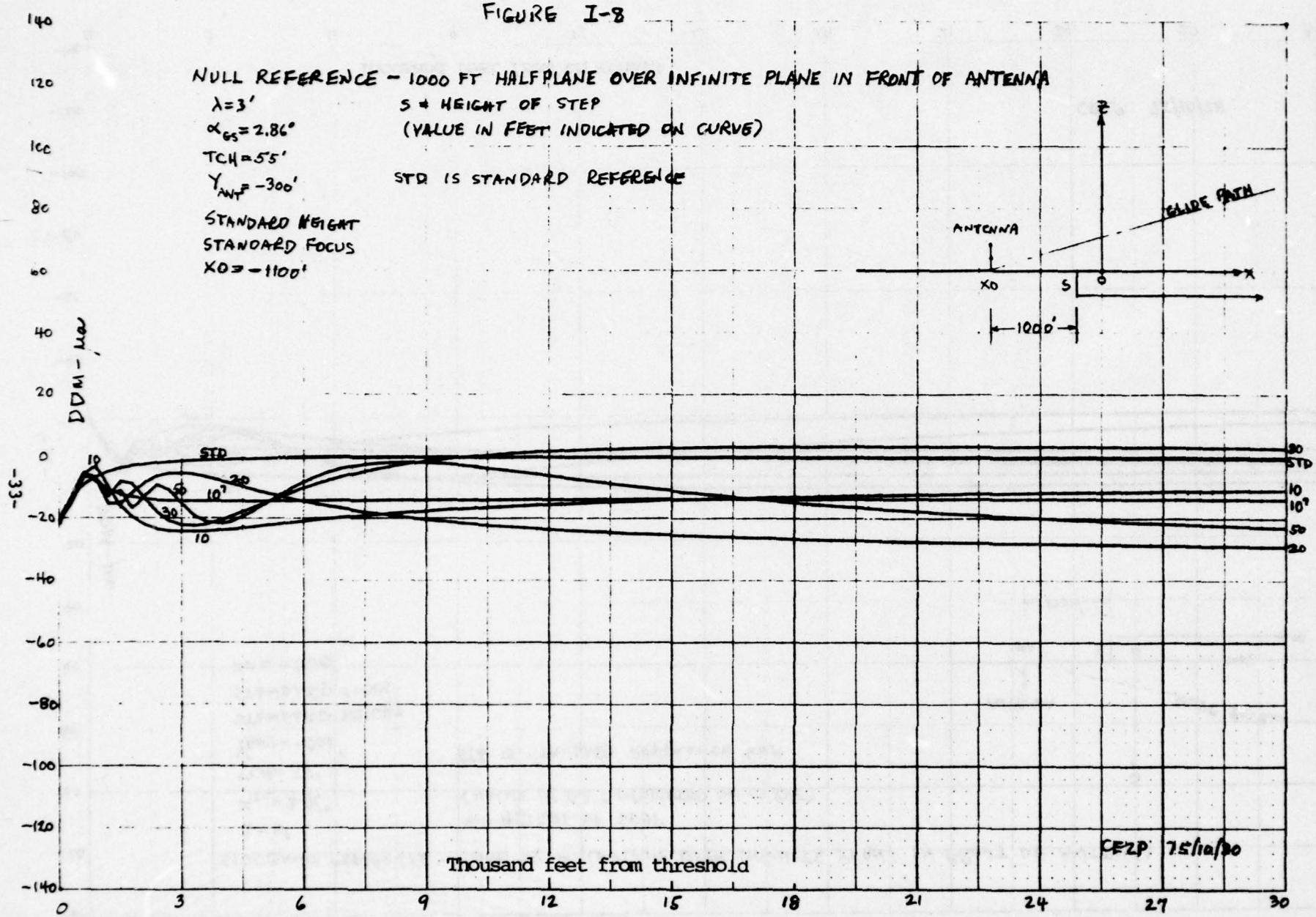
NULL REFERENCE - 1000 FT HALFPLANE OVER INFINITE PLANE IN FRONT OF ANTENNA
λ=3'
α_{GS}=2.86°
TCH=55'
Y_{ANT}=-300'
STANDARD HEIGHT
STANDARD FOCUS
XO=-1100'
S = HEIGHT OF STEP
(VALUE IN FEET INDICATED ON CURVE)
STD IS STANDARD REFERENCE
ANTENNA
GLIDE PATH
XO
S
1000'
DDM - μa
STD
10
20
50
10²
30
140
120
100
80
60
40
20
0
-20
-40
-60
-80
-100
-120
-140
0
3
6
9
12
15
18
21
24
27
30
Thousand feet from threshold
CEZP 75/10/30

FIGURE I-9

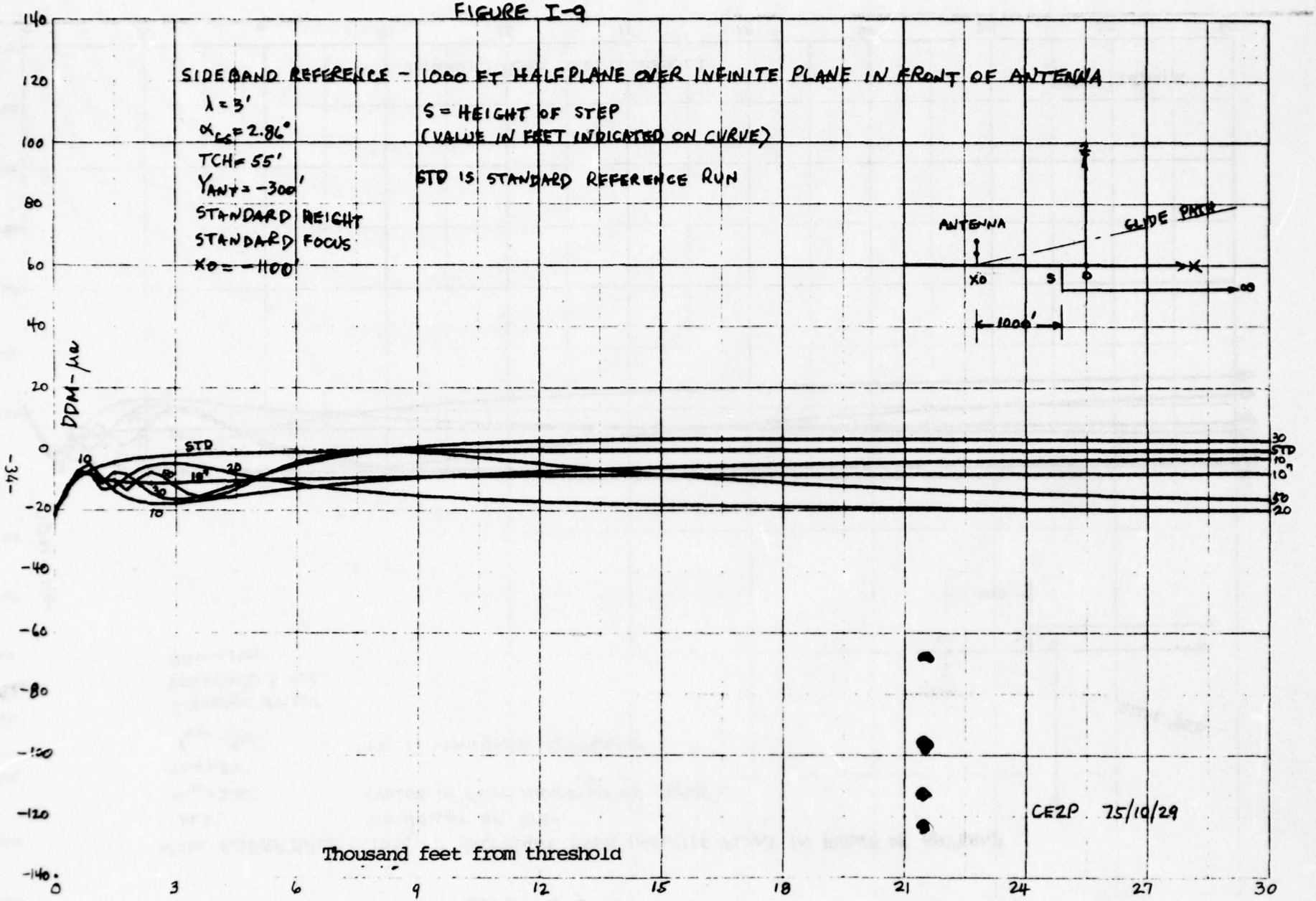
SIDEBAND REFERENCE - 1000 FT HALFPLANE OVER INFINITE PLANE IN FRONT OF ANTENNA
λ = 3'
α_{GS} = 2.86°
TCH = 55'
Y_{ANT} = -300'
STANDARD HEIGHT
STANDARD FOCUS
XO = -1100'
S = HEIGHT OF STEP
(VALUE IN FEET INDICATED ON CURVE)
STD IS STANDARD REFERENCE RUN
ANTENNA
GLIDE PATH
XO
S
1000'
∞
DDM-μa
STD
10
5
10
20
30
10
30
10
5
10
20
-40
-60
-80
-100
-120
-140
Thousand feet from threshold
0
3
6
9
12
15
18
21
24
27
30
CE2P 75/10/29

FIGURE I-10

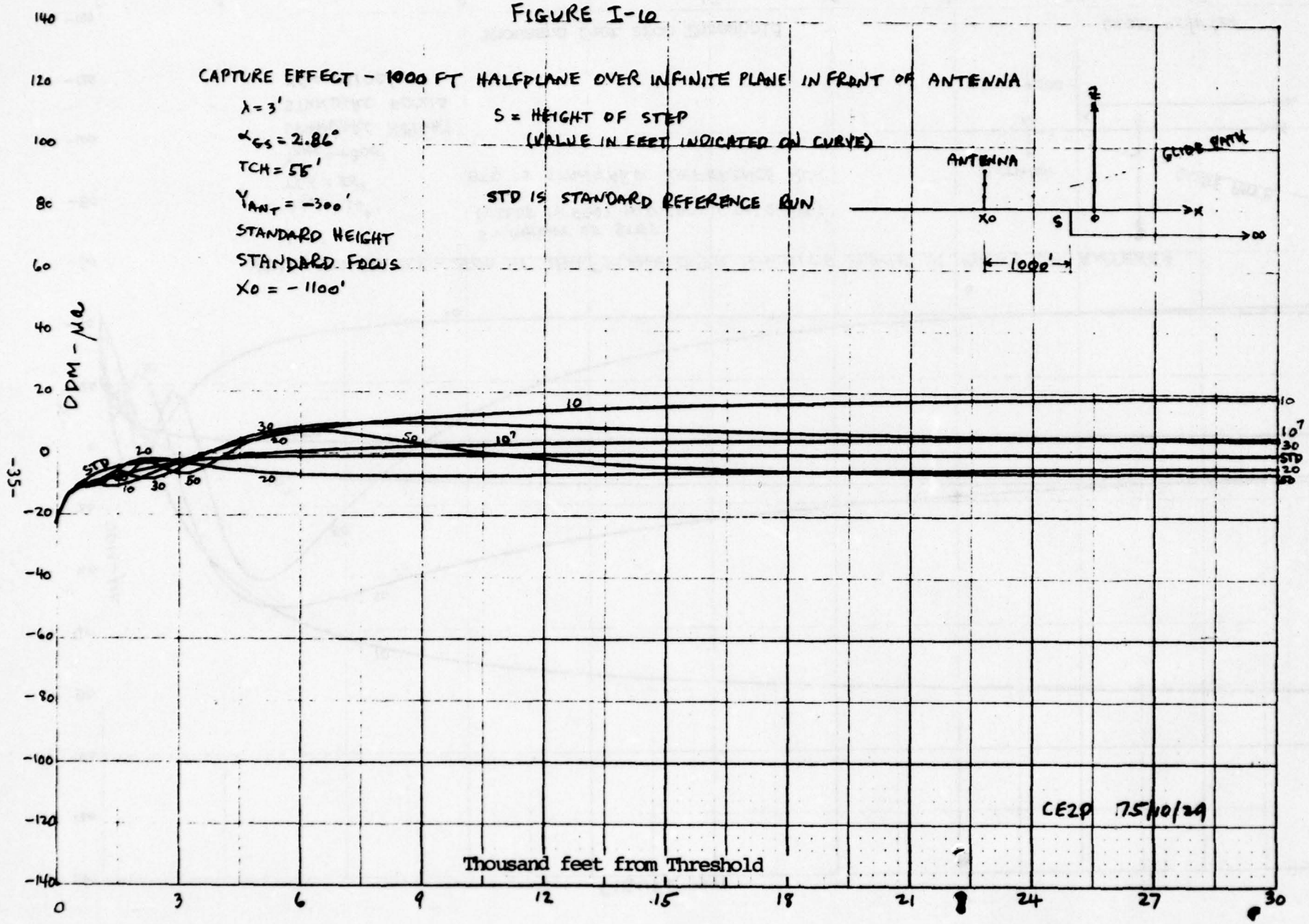
CAPTURE EFFECT - 1000 FT HALFPLANE OVER INFINITE PLANE IN FRONT OF ANTENNA
λ = 3'
α_{GS} = 2.86°
TCH = 55'
Y_{ANT} = -300'
STANDARD HEIGHT
STANDARD FOCUS
XO = -1100'
S = HEIGHT OF STEP
(VALUE IN FEET INDICATED ON CURVE)
STD IS STANDARD REFERENCE RUN
ANTENNA
GLIDE PATH
XO
S
1000'
DDM - MD
Thousand feet from Threshold
CE2D 75/10/29
-35-

FIGURE I-11

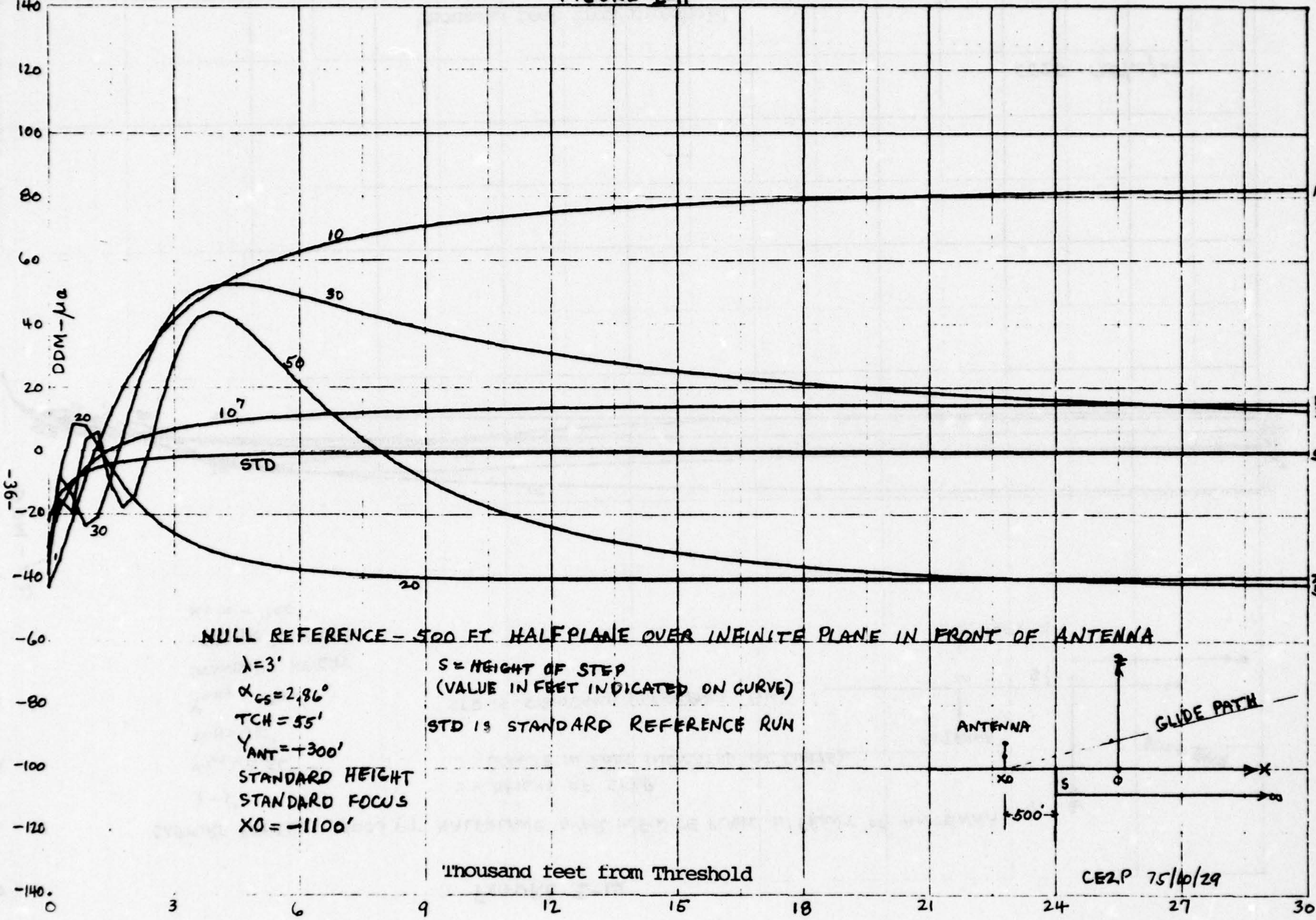

140
120
100
80
60
40
20
0
-20
-40
-60
-80
-100
-120
-140
DDM-μa
10
30
50
20
10'
STD
NULL REFERENCE - 500 FT HALFPLANE OVER INFINITE PLANE IN FRONT OF ANTENNA
λ=3'
α_{GS}=2.86°
TCH=55'
Y_{ANT}=+300'
STANDARD HEIGHT
STANDARD FOCUS
XO=-1100'
S = HEIGHT OF STEP
(VALUE IN FEET INDICATED ON CURVE)
STD IS STANDARD REFERENCE RUN
ANTENNA
GLIDE PATH
XO
S
O
500'
Z
X
CE2P 75/10/29
Thousand feet from Threshold
0
3
6
9
12
15
18
21
24
27
30

FIGURE I-12

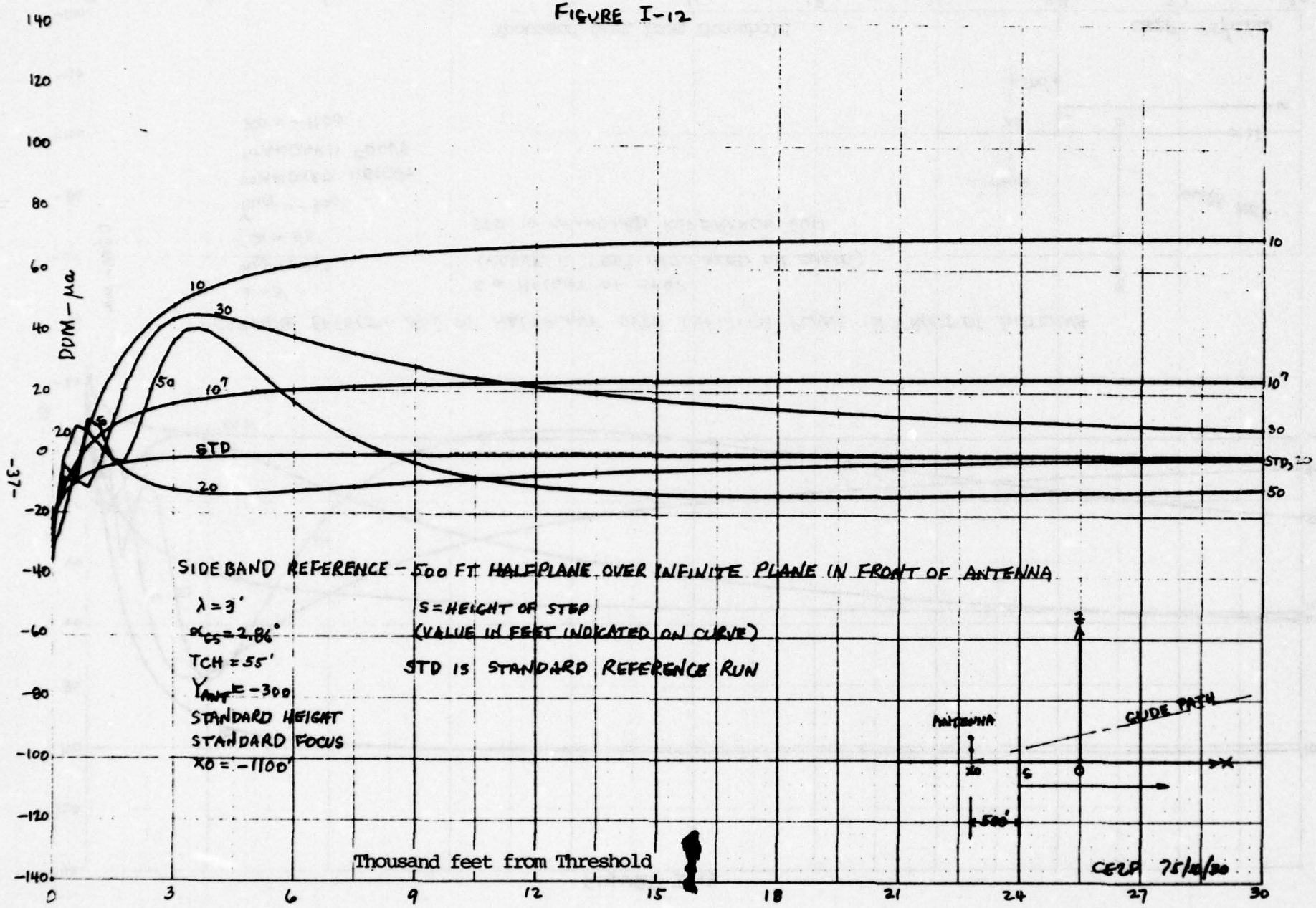
DDM – μa
140
120
100
80
60
40
20
0
-20
-40
-60
-80
-100
-120
-140
0
3
6
9
12
15
18
21
24
27
30
10
30
50a
10⁷
STD
20
10
10⁷
30
STD, 20
50
SIDEBAND REFERENCE – 500 FT HALFPLANE OVER INFINITE PLANE IN FRONT OF ANTENNA
λ = 3'
α_GS = 2.86°
TCH = 55'
Y_ANT = -300
STANDARD HEIGHT
STANDARD FOCUS
XO = -1100'
S = HEIGHT OF STEP
(VALUE IN FEET INDICATED ON CURVE)
STD IS STANDARD REFERENCE RUN
ANTENNA
GLIDE PATH
XO
S
500'
Thousand feet from Threshold
CEDP 75/12/30

FIGURE I-13

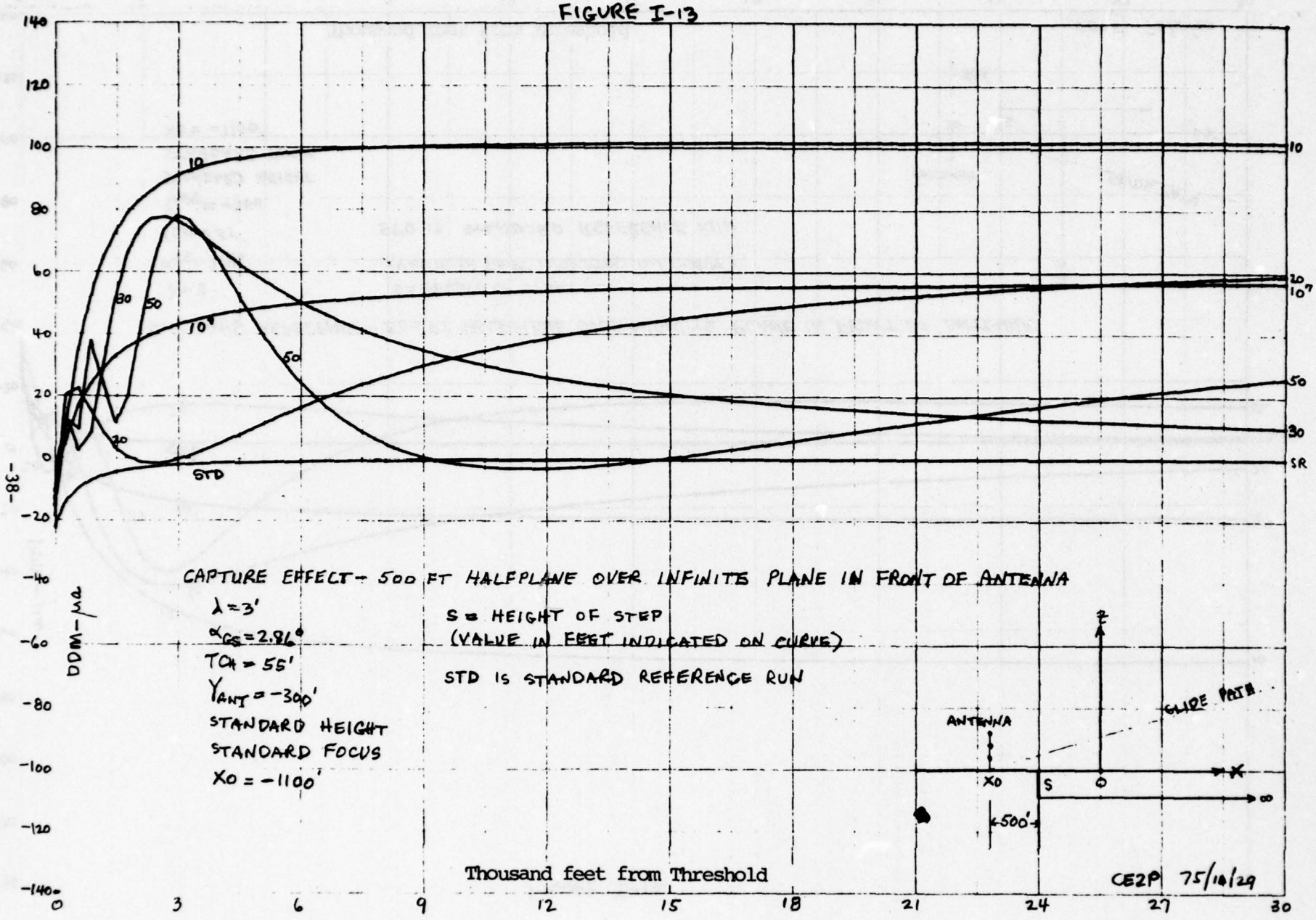
140
120
100
80
60
40
20
0
-20
-40
-60
-80
-100
-120
-140
DDM-VOD
0
3
6
9
12
15
18
21
24
27
30
Thousand feet from Threshold
10
80
50
10'
60
20
STD
10
20
10'
50
30
SR
CAPTURE EFFECT - 500 FT HALFPLANE OVER INFINITE PLANE IN FRONT OF ANTENNA
λ = 3'
α_GS = 2.86°
TCH = 55'
Y_ANT = -300'
STANDARD HEIGHT
STANDARD FOCUS
X0 = -1100'
S = HEIGHT OF STEP
(VALUE IN FEET INDICATED ON CURVE)
STD IS STANDARD REFERENCE RUN
ANTENNA
GLIDE PATH
X0
S
0
500'
∞
CE2P 75/10/29

FIGURE I-14

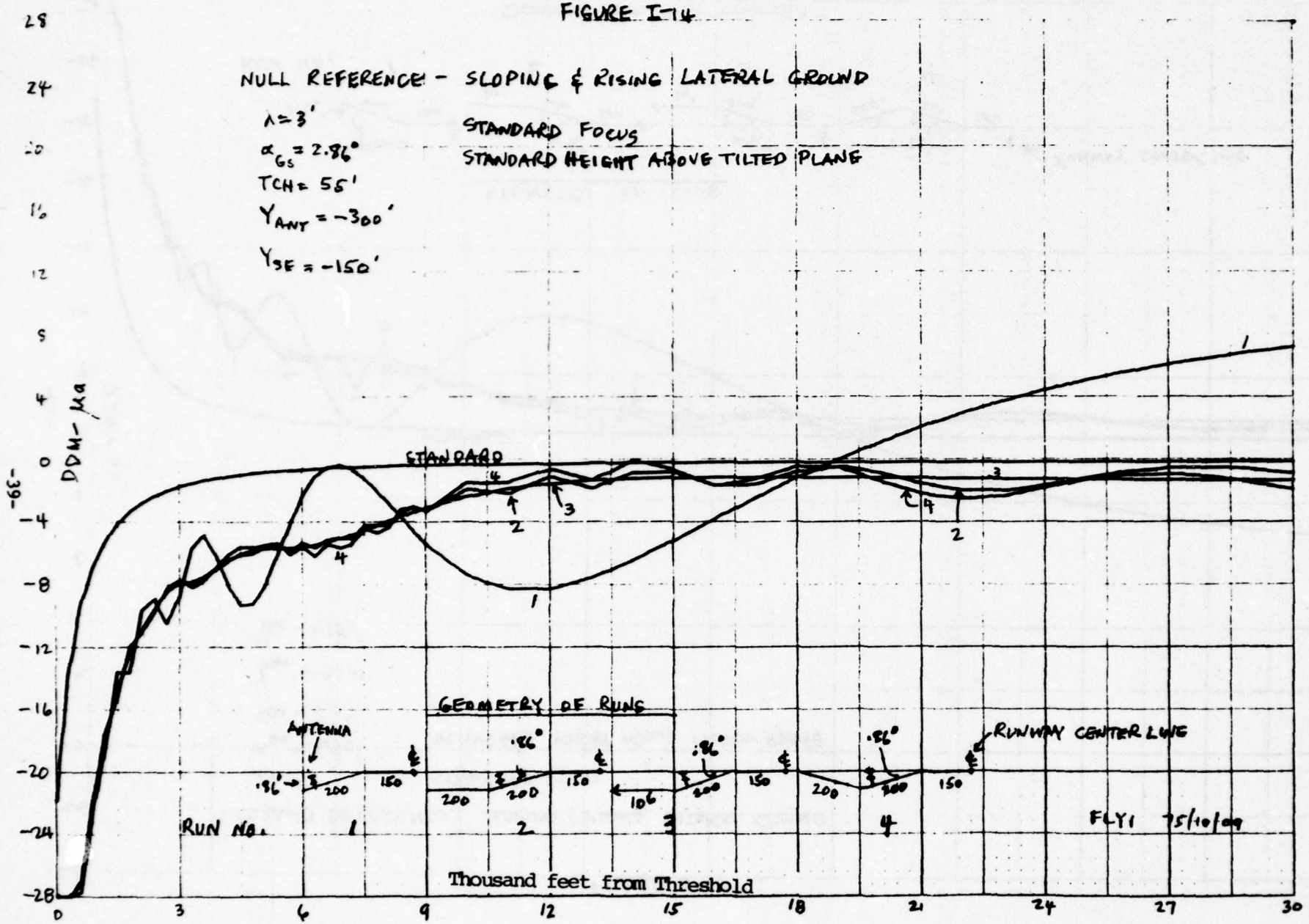
NULL REFERENCE - SLOPING & RISING LATERAL GROUND
λ = 3'
α_{GS} = 2.86°
TCH = 55'
Y_{ANT} = -300'
Y_{SE} = -150'
STANDARD FOCUS
STANDARD HEIGHT ABOVE TILTED PLANE
DDM - μa
STANDARD
GEOMETRY OF RUNS
ANTENNA
.86°
RUNWAY CENTERLINE
200
150
100
RUN NO.
FLY
Thousand feet from Threshold

FIGURE I-15

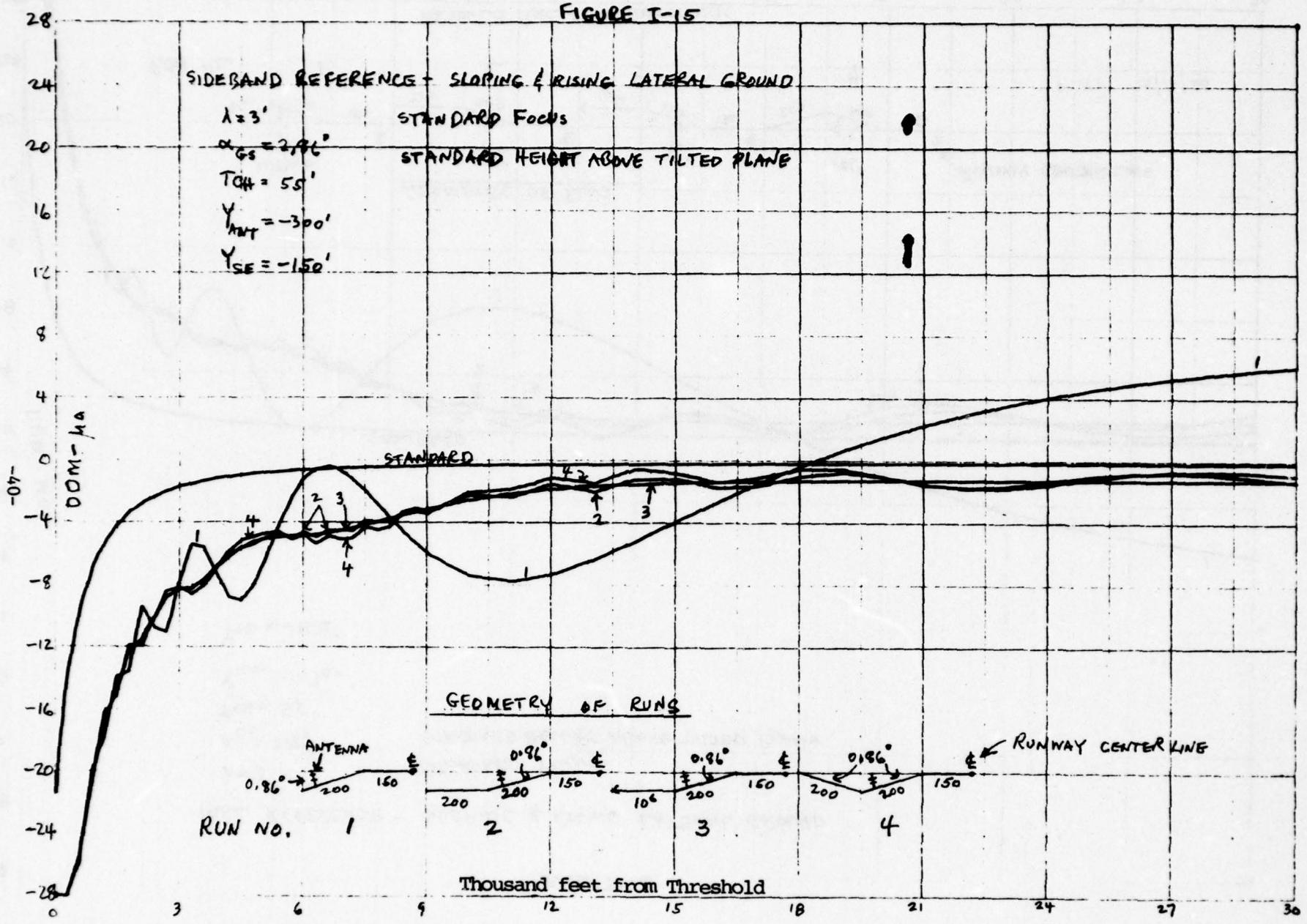
SIDEBAND REFERENCE + SLOPING & RISING LATERAL GROUND
λ = 3'
α_{GS} = 2.86°
TCH = 55'
Y_{ANT} = -300'
Y_{SE} = -150'
STANDARD FOCUS
STANDARD HEIGHT ABOVE TILTED PLANE
STANDARD
DDM-μa
28
24
20
16
12
8
4
0
-4
-8
-12
-16
-20
-24
-28
-40
GEOMETRY OF RUNS
ANTENNA
0.86°
200
160
150
200
104
RUNWAY CENTERLINE
RUN NO. 1 2 3 4
Thousand feet from Threshold
0
3
6
9
12
15
18
21
24
27
30

FIGURE I-16

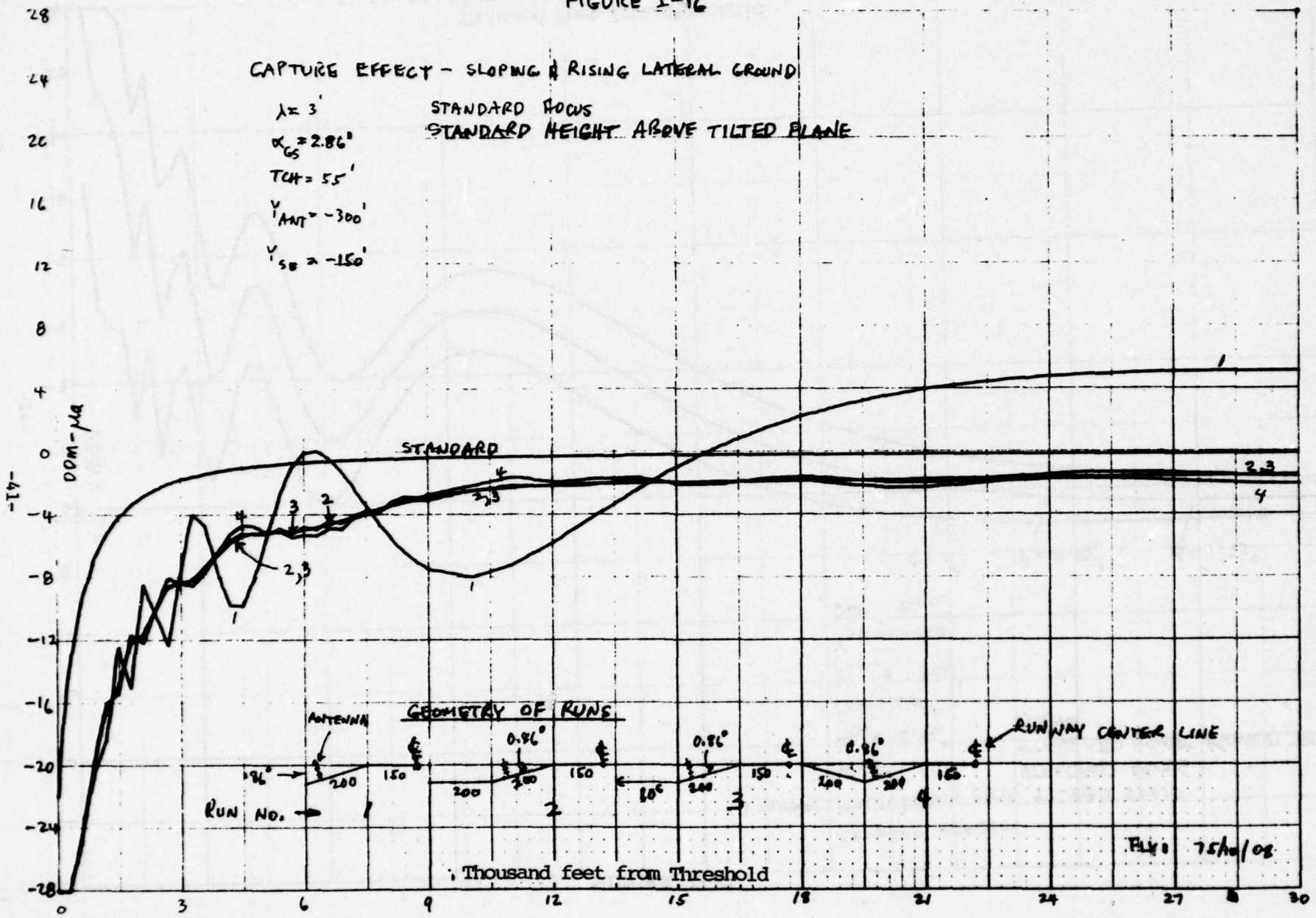
CAPTURE EFFECT - SLOPING & RISING LATERAL GROUND
λ = 3'
α_{GS} = 2.86°
TCH = 55'
Y_{ANT} = -300'
Y_{SB} = -150'
STANDARD FOCUS
STANDARD HEIGHT ABOVE TILTED PLANE
STANDARD
DDM-μa
-41-
GEOMETRY OF RUNS
ANTENNA
RUNWAY CENTER LINE
0.86°
RUN NO.
Thousand feet from Threshold
FAA 75/no/08

FIGURE I-17

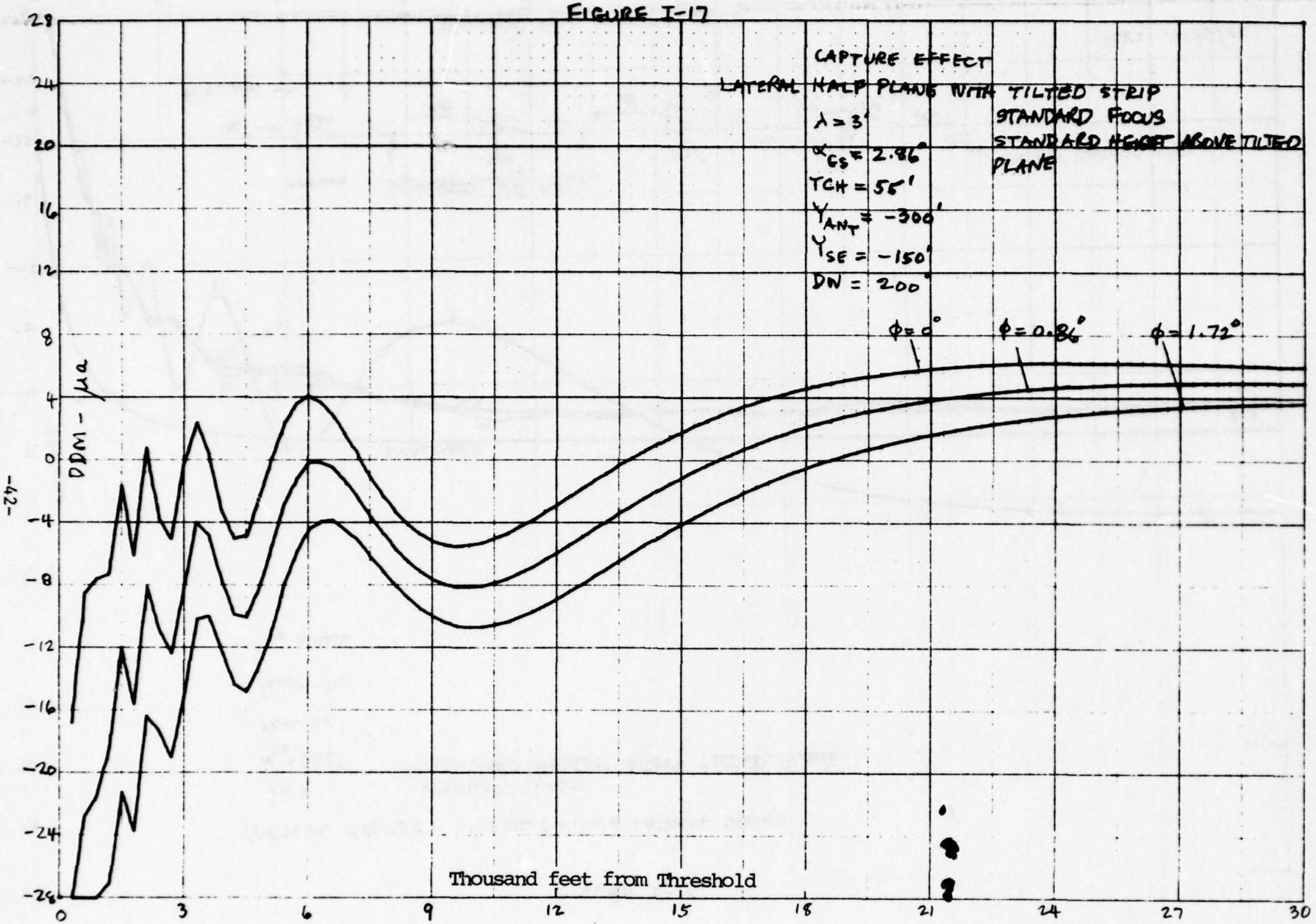
CAPTURE EFFECT
LATERAL HALF PLANE WITH TILTED STRIP
STANDARD FOCUS
STANDARD HEIGHT ABOVE TILTED PLANE
λ = 3'
α_GS = 2.86°
TCH = 55'
Y_ANT = -300'
Y_SE = -150'
DW = 200'
φ = 0°
φ = 0.86°
φ = 1.72°
DDM - μa
Thousand feet from Threshold
28
24
20
16
12
8
4
0
-4
-8
-12
-16
-20
-24
-28
0
3
6
9
12
15
18
21
24
27
30

FIGURE I-18

NULL REFERENCE - SLOPING AND RISING LATERAL GROUND

$\lambda = 3'$
$\alpha_{GS} = 2.86°$
TCH = 55'
$Y_{ANT} = -300'$
$Y_{SE} = -150'$

S1 = 200'
S2 = 200'
STANDARD FOCUS
STANDARD HEIGHT ABOVE PLANE S1

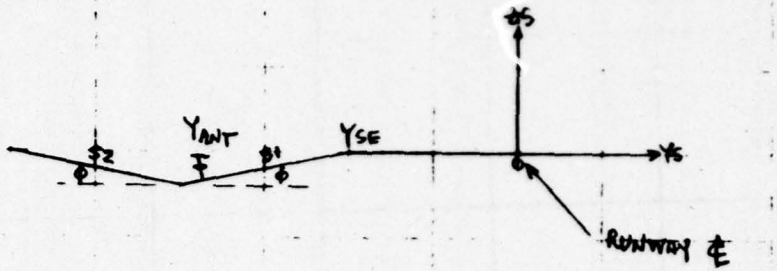

FIGURE I-19

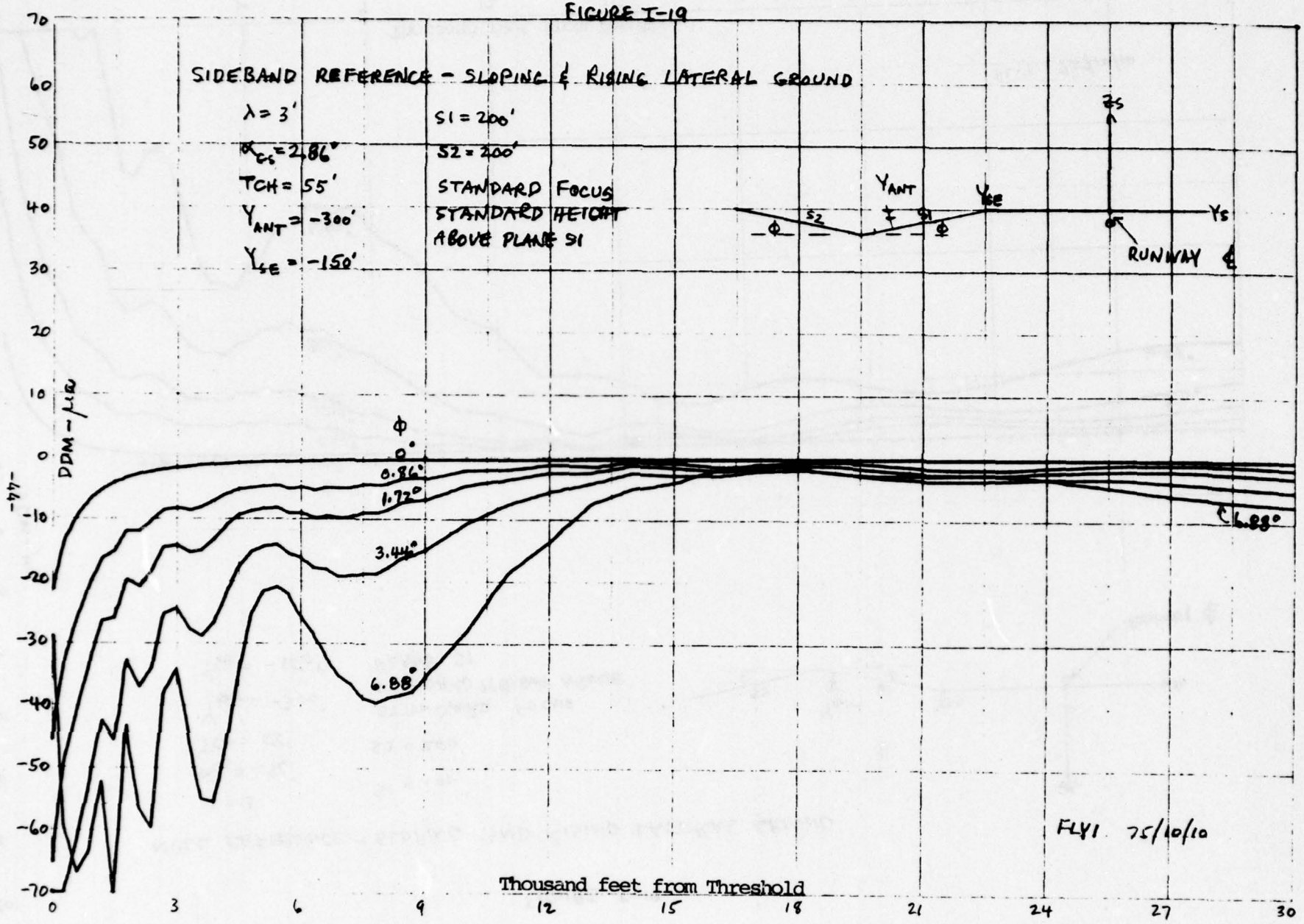
SIDEBAND REFERENCE - SLOPING & RISING LATERAL GROUND
λ = 3'
α_{CS} = 2.86°
TCH = 55'
Y_{ANT} = -300'
Y_{SE} = -150'
S1 = 200'
S2 = 200'
STANDARD FOCUS
STANDARD HEIGHT
ABOVE PLANE S1
Y_{ANT}
Y_{SE}
S2
S1
Φ
Φ
Zs
Ys
RUNWAY
DDM - μA
Φ
0°
0.86°
1.72°
3.44°
6.88°
6.88°
-10
-20
-30
-40
-50
-60
-70
70
60
50
40
30
20
10
0
0
3
6
9
12
15
18
21
24
27
30
Thousand feet from Threshold
FLY1 75/10/10

FIGURE I-20

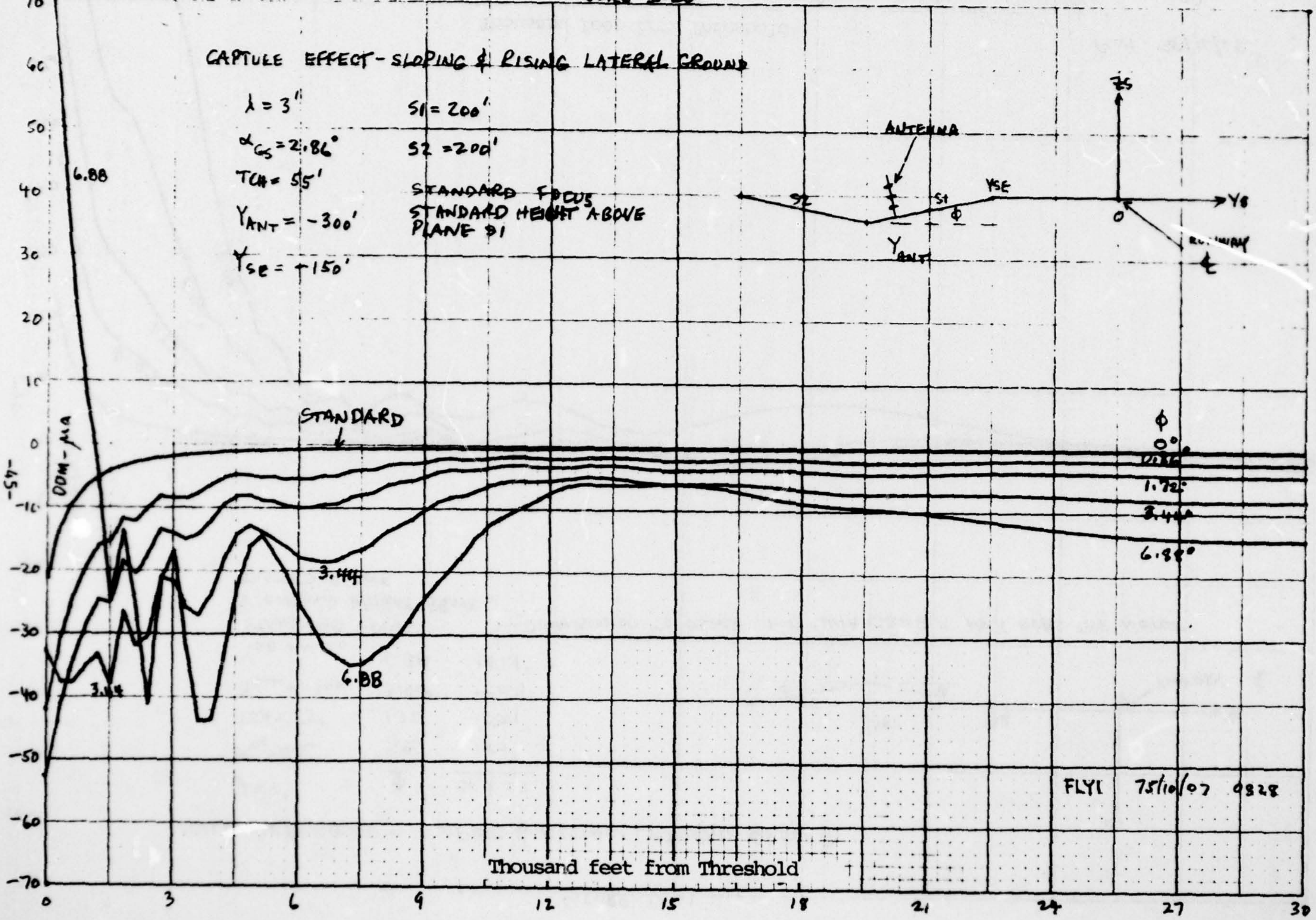

CAPTURE EFFECT - SLOPING & RISING LATERAL GROUND
λ = 3'
α_{GS} = 2.86°
TCH = 55'
Y_{ANT} = -300'
Y_{SE} = +150'
S1 = 200'
S2 = 200'
STANDARD FOCUS
STANDARD HEIGHT ABOVE PLANE Φ1
ANTENNA
S2
S1
Φ
YSE
Y_{ANT}
ZS
YS
O
RUNWAY
DDM - μA
STANDARD
6.88
3.44
Φ
0°
0.86°
1.72°
3.44°
6.88°
Thousand feet from Threshold
FLY1 75/10/07 0828

FIGURE I-21

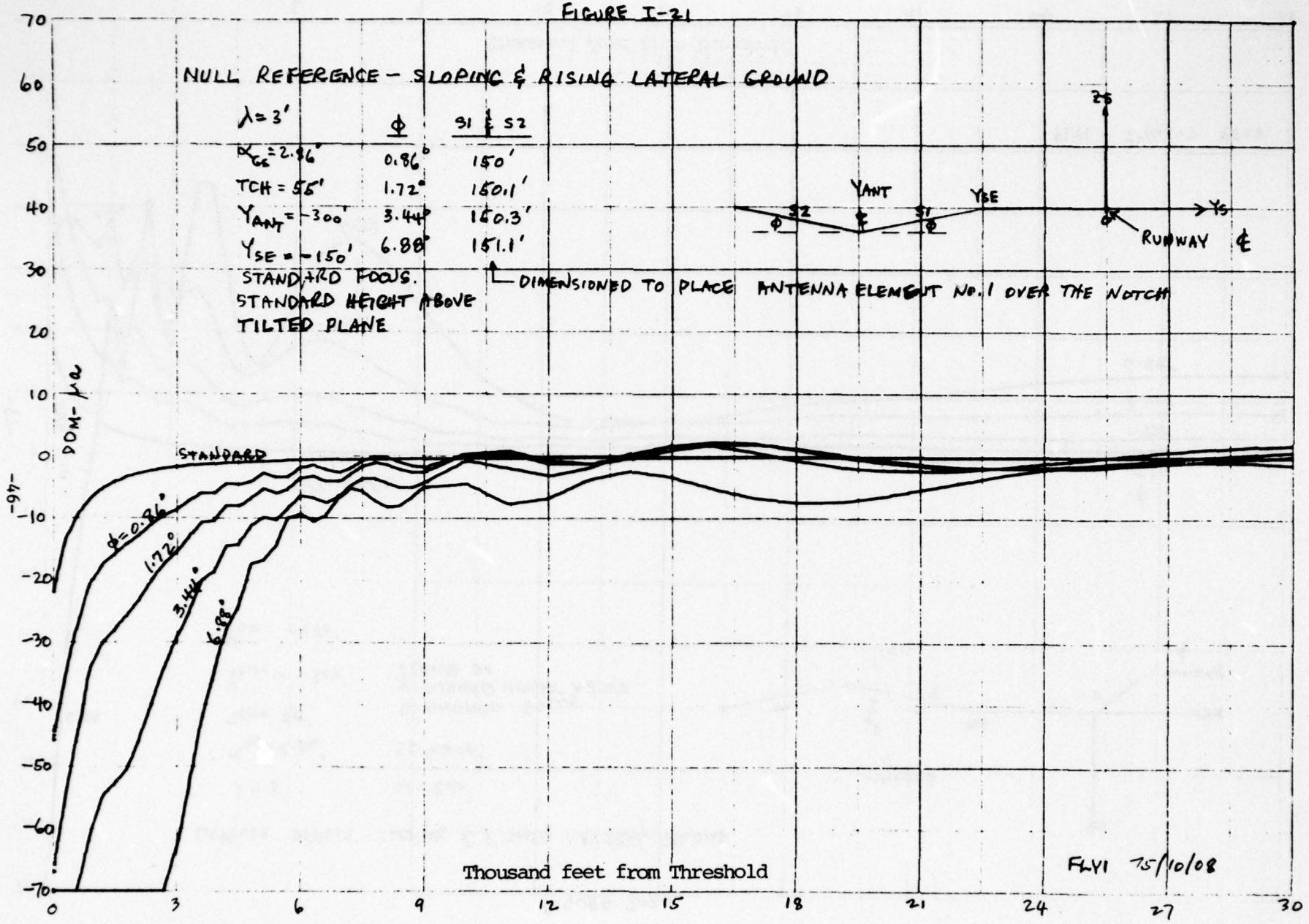
NULL REFERENCE - SLOPING & RISING LATERAL GROUND
λ = 3'
Φ
S1 & S2
α_GS = 2.96°
0.86°
150'
TCH = 55'
1.72°
150.1'
Y_ANT = -300'
3.44°
150.3'
Y_SE = -150'
6.88°
151.1'
STANDARD FOCUS.
STANDARD HEIGHT ABOVE TILTED PLANE
DIMENSIONED TO PLACE ANTENNA ELEMENT NO. 1 OVER THE NOTCH
Y_ANT
Y_SE
S2
S1
Φ
Z_S
Y_S
RUNWAY ℄
DDM-μa
STANDARD
Φ=0.86°
1.72°
3.44°
6.88°
-46-
Thousand feet from Threshold
FLVI 75/10/08

FIGURE I-22

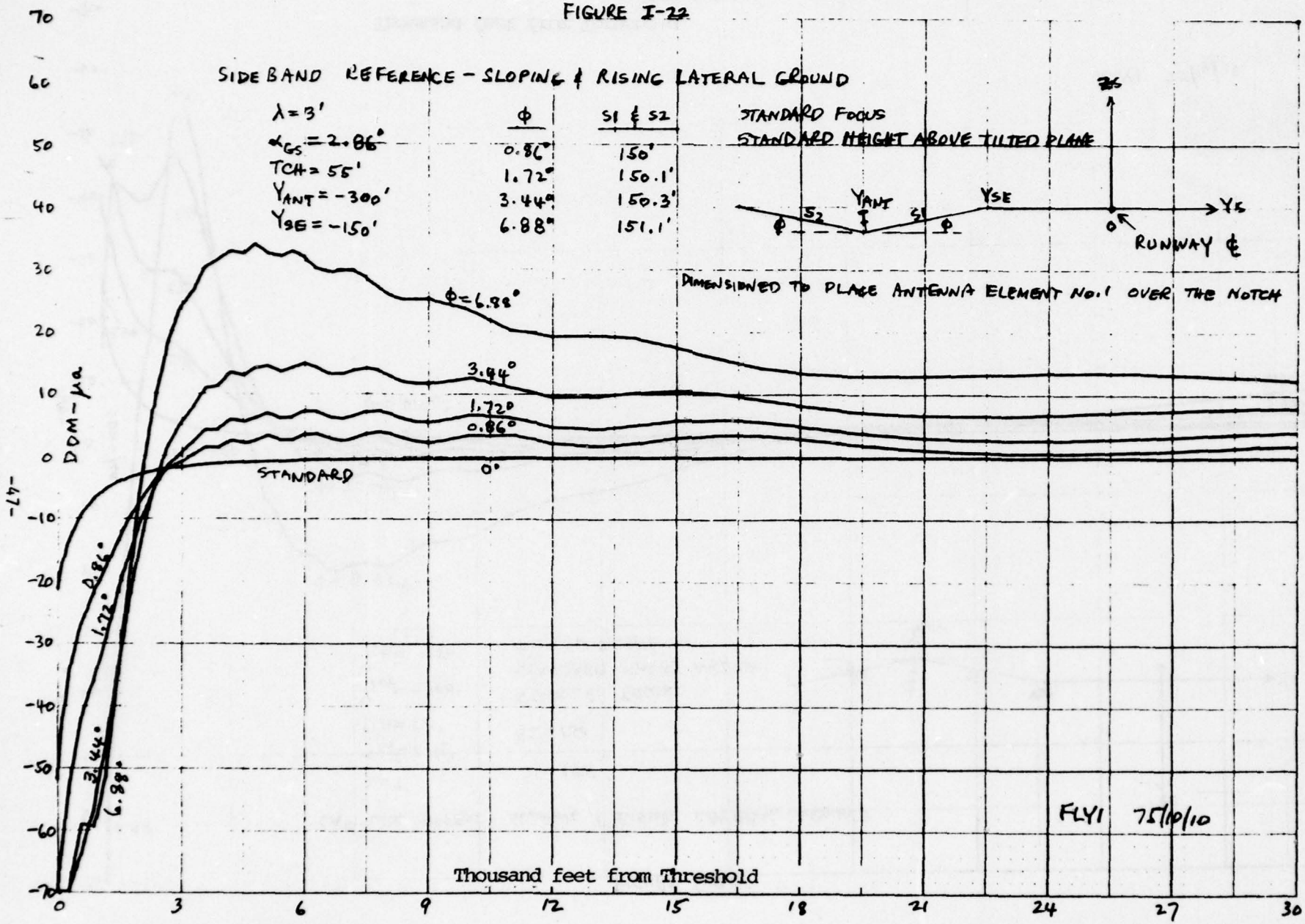
SIDE BAND REFERENCE - SLOPING & RISING LATERAL GROUND
λ = 3'
α_GS = 2.86°
TCH = 55'
Y_ANT = -300'
Y_SE = -150'
Φ
0.86°
1.72°
3.44°
6.88°
S1 & S2
150'
150.1'
150.3'
151.1'
STANDARD FOCUS
STANDARD HEIGHT ABOVE TILTED PLANE
Z
Y_ANT
Y_SE
Y
S2
S1
Φ
0
RUNWAY ℄
DIMENSIONED TO PLACE ANTENNA ELEMENT No.1 OVER THE NOTCH
Φ=6.88°
3.44°
1.72°
0.86°
0°
STANDARD
DDM-μa
Thousand feet from Threshold
FLY1 75/10/10

FIGURE I-23

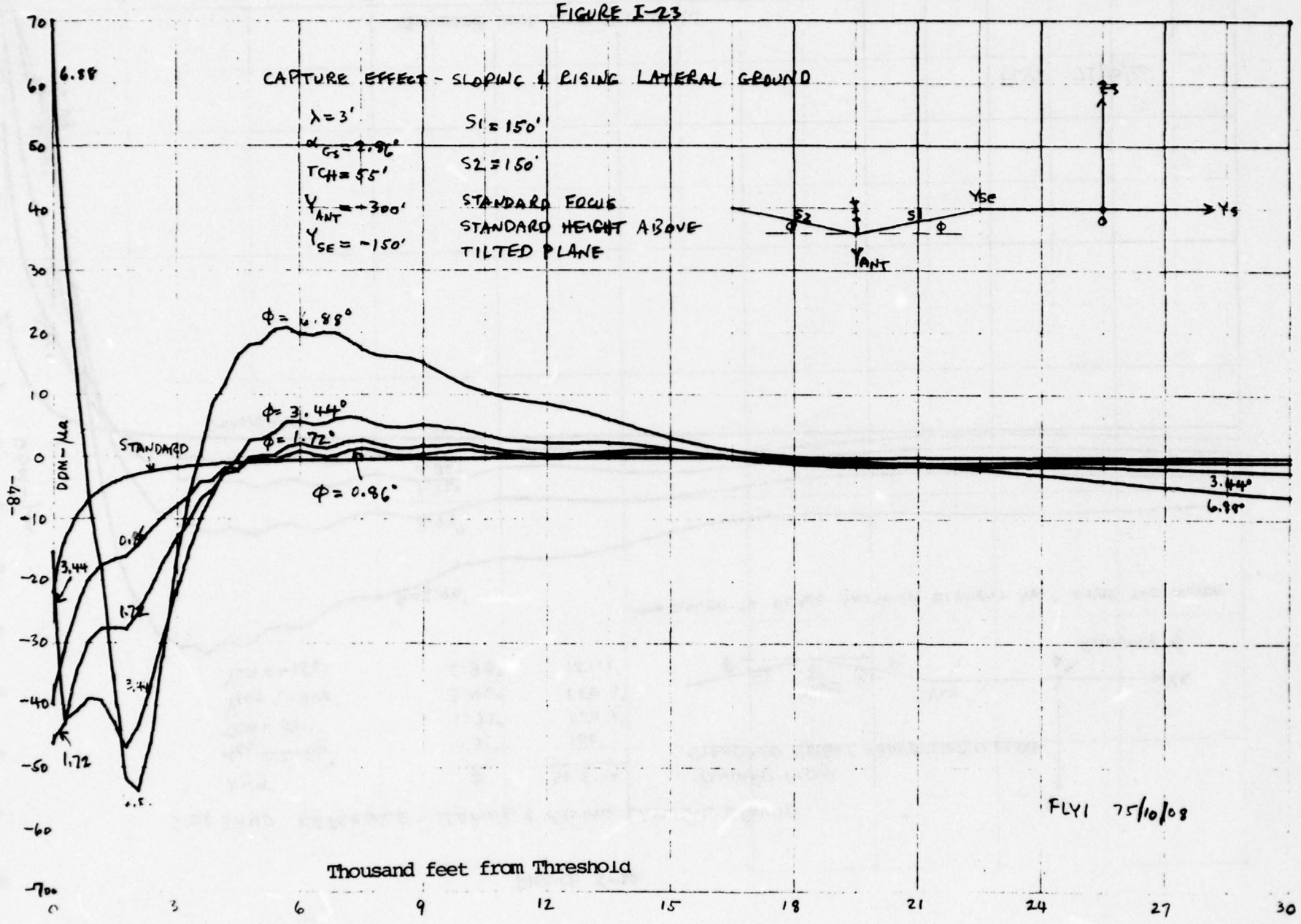

FLY1 75/10/08

FIGURE I-24

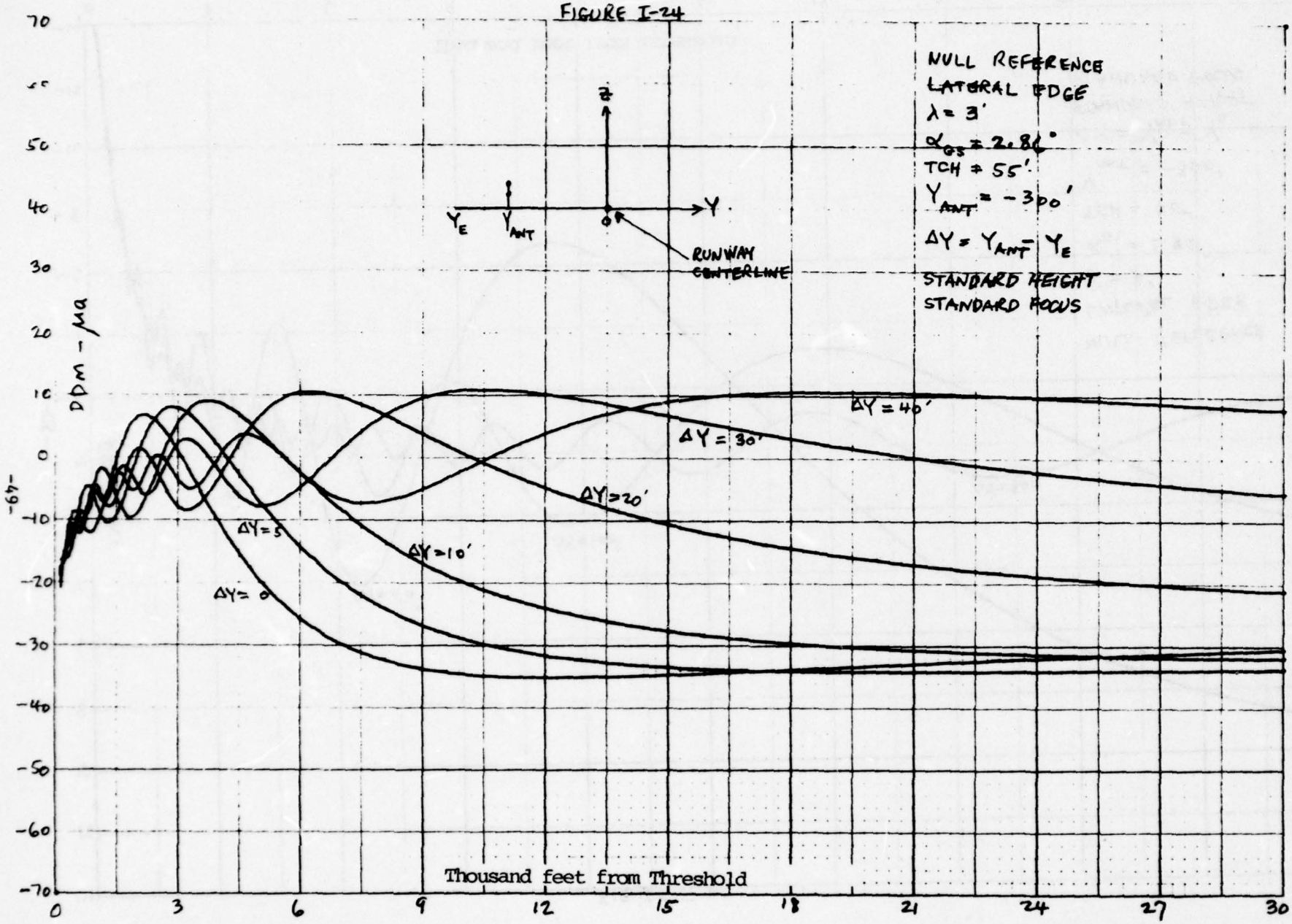

CEL/GEFLYHO 75/09/23 1429

FIGURE I-25

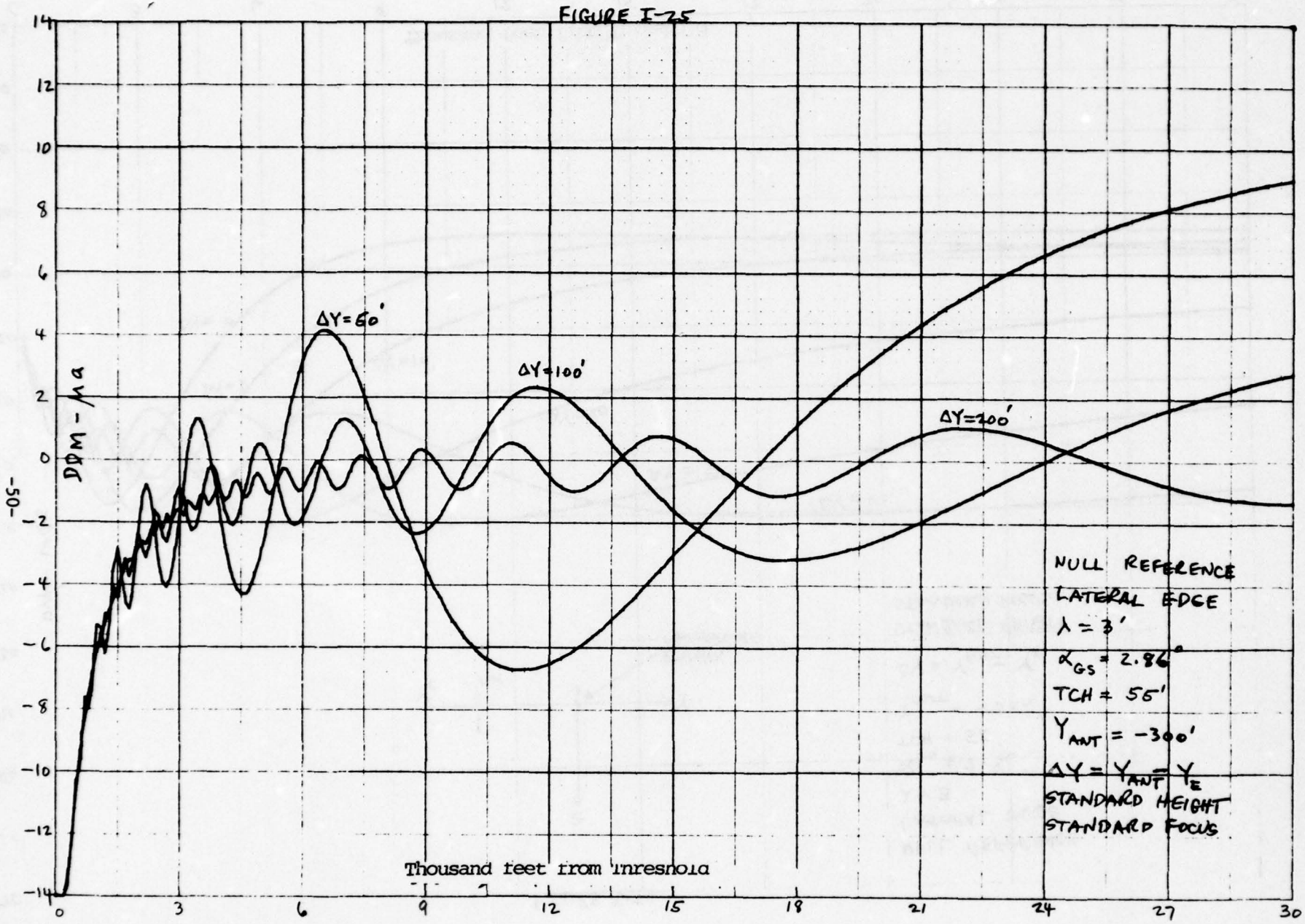
ΔY=60'
ΔY=100'
ΔY=200'
DDM-μa
-50-
Thousand feet from Inresnoia
NULL REFERENCE
LATERAL EDGE
λ = 3'
α_{GS} = 2.86°
TCH = 55'
Y_{ANT} = -300'
ΔY = Y_{ANT} - Y_E
STANDARD HEIGHT
STANDARD FOCUS

FIGURE I-26

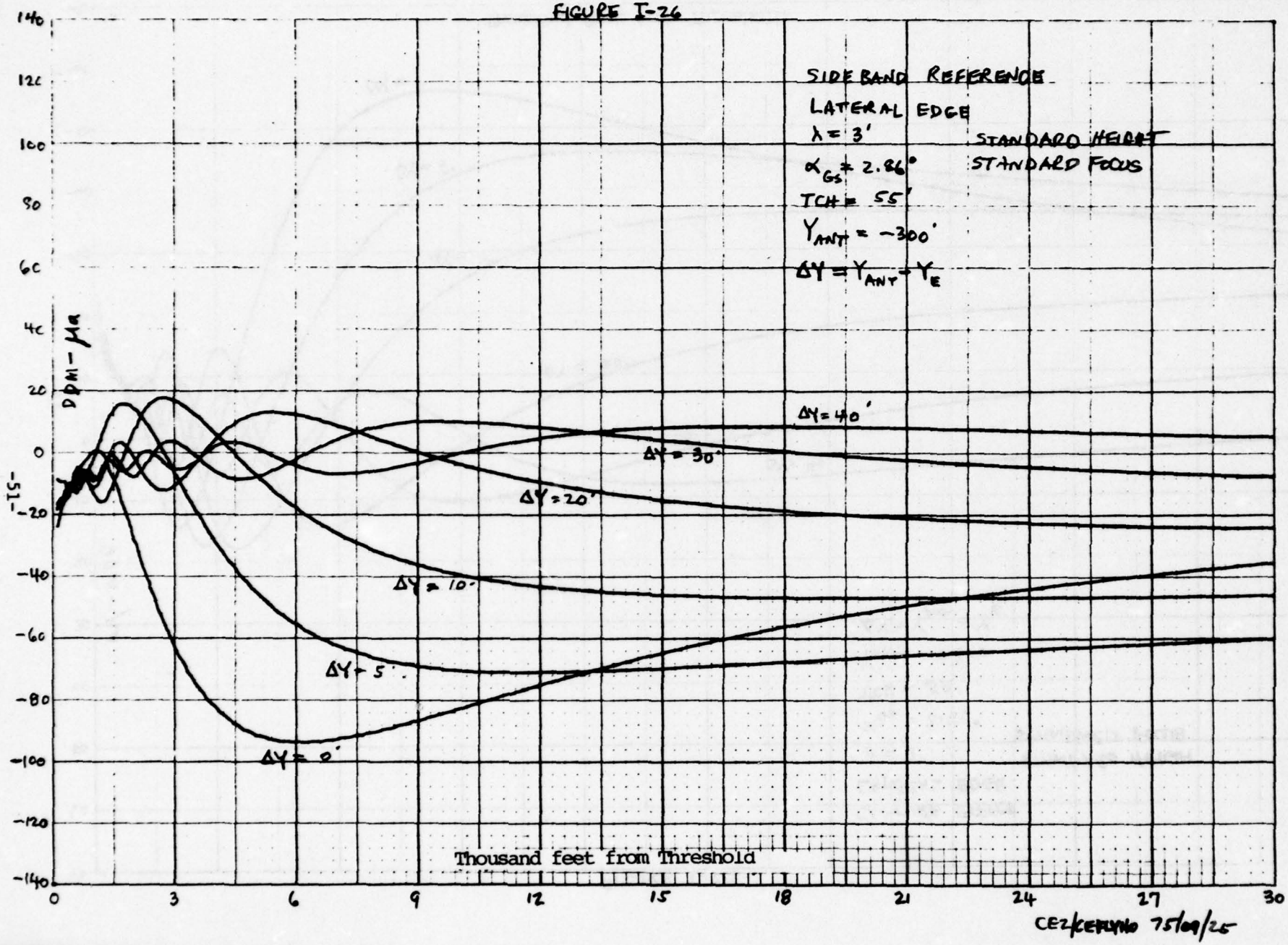
SIDEBAND REFERENCE
LATERAL EDGE
λ = 3'
STANDARD HEIGHT
STANDARD FOCUS
α_{GS} = 2.86°
TCH = 55'
Y_{ANT} = -300'
$\Delta Y = Y_{ANT} - Y_E$
DDM - μa
-.155
ΔY = 40'
ΔY = 30'
ΔY = 20'
ΔY = 10'
ΔY = 5'
ΔY = 0'
Thousand feet from Threshold
140
120
100
80
60
40
20
0
-20
-40
-60
-80
-100
-120
-140
0
3
6
9
12
15
18
21
24
27
30
CEZ/KEFLYNG 75/09/25

FIGURE I-27

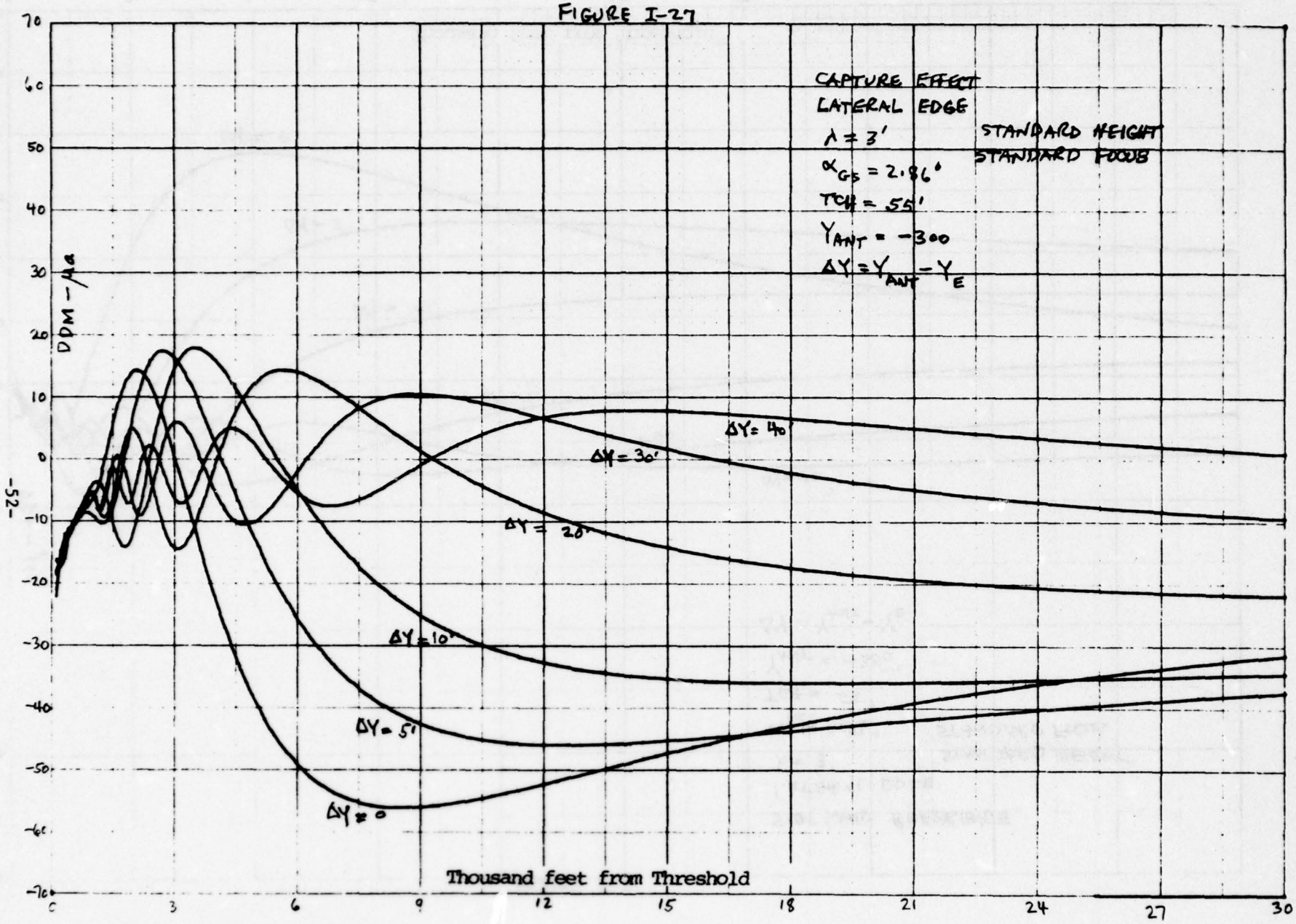
CAPTURE EFFECT
LATERAL EDGE
λ = 3'
STANDARD HEIGHT
STANDARD FOOD
α_{GS} = 2.86°
TCH = 55'
Y_{ANT} = -300
$\Delta Y = Y_{ANT} - Y_E$
DDM - dB
ΔY = 40'
ΔY = 30'
ΔY = 20'
ΔY = 10'
ΔY = 5'
ΔY = 0
Thousand feet from Threshold
70
60
50
40
30
20
10
0
-10
-20
-30
-40
-50
-60
-70
0
3
6
9
12
15
18
21
24
27
30

FIGURE I-28

NULL REFERENCE OVER INFINITE PLANE, MODIFIED AND STANDARD FOCUS

$\lambda = 3'$
$\alpha_{GS} = 2.86°$
TCH = 55'
$Y_{ANT} = -300'$
$X0 = -1100.9'$

RUN NO.	YA1	ZA1	YA2	ZA2	REMARKS
0	-300.0	15.03	-29887	30.06	STANDARD FOCUS, 0° AZIMUTH
0A	"	"	"	"	" " -8° "
0B	"	"	"	"	" " 8° "
1	"	"	-30150	"	MODIFIED " 0° "
1A	"	"	"	"	" " -8° "
1B	"	"	"	"	" " 8° "

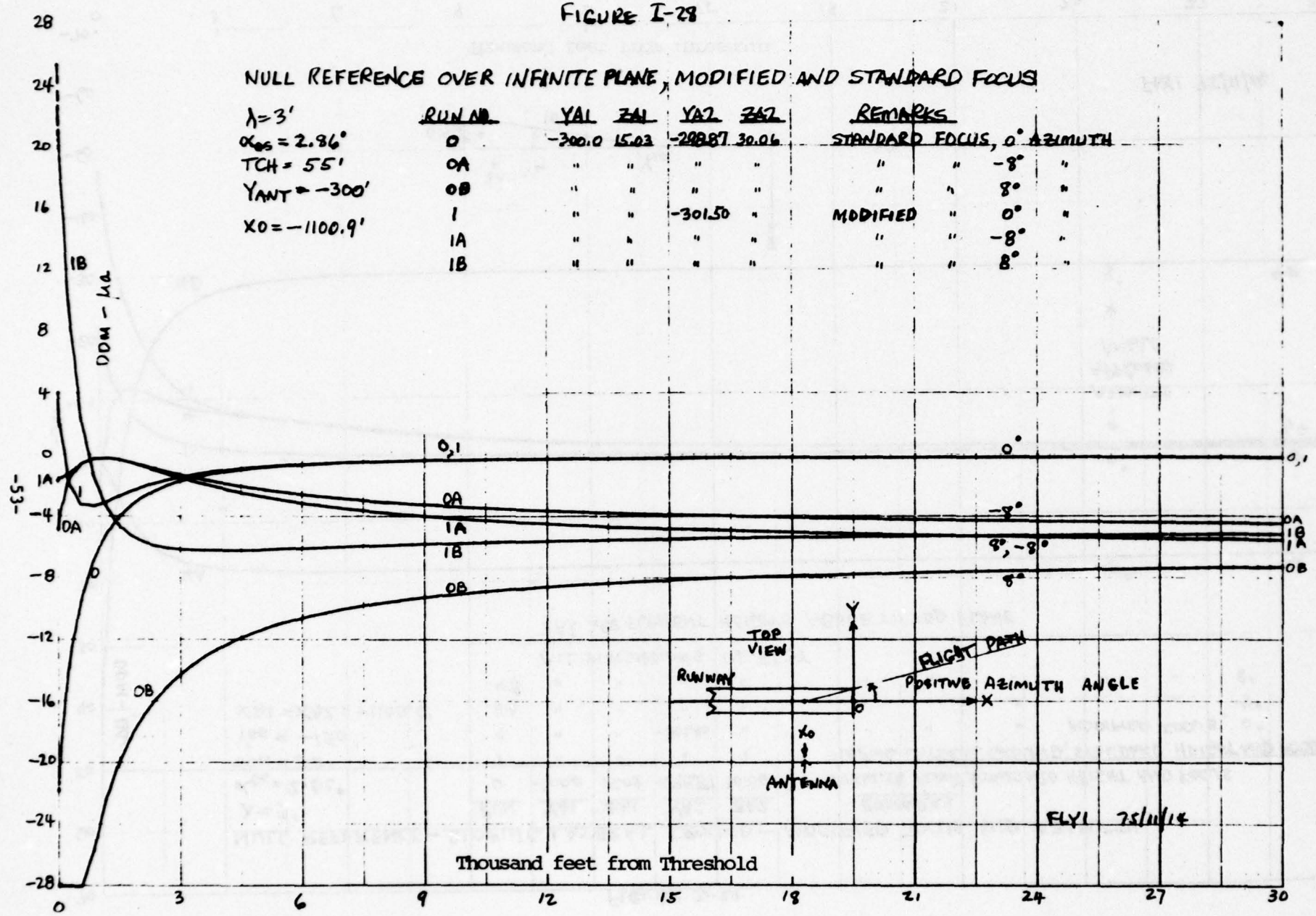

FIGURE I-29

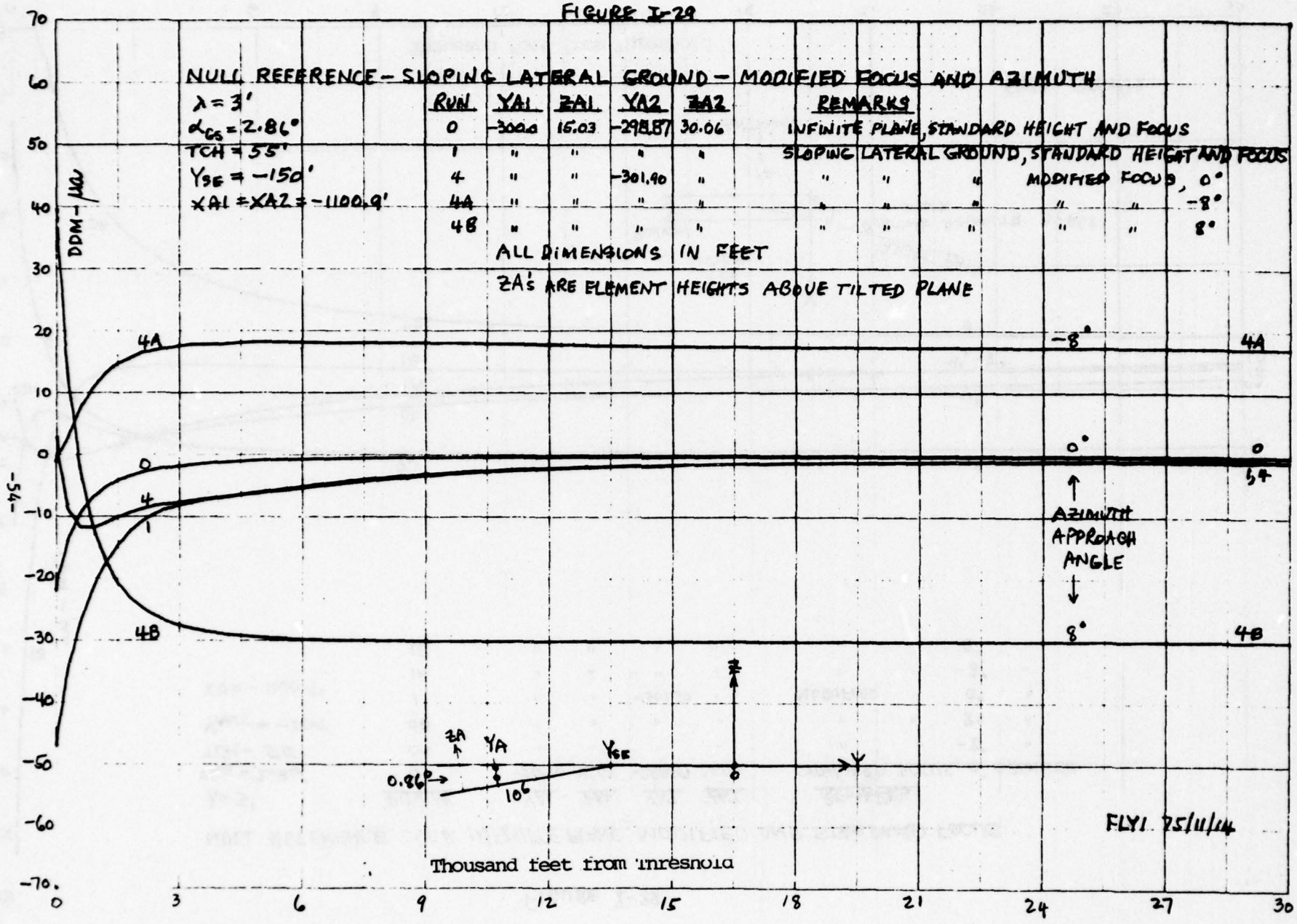
NULL REFERENCE – SLOPING LATERAL GROUND – MODIFIED FOCUS AND AZIMUTH
λ = 3'
α_{GS} = 2.86°
TCH = 55'
Y_{GE} = −150'
XA1 = XA2 = −1100.9'
RUN YA1 ZA1 YA2 ZA2 REMARKS
0 −3000 16.03 −298.87 30.06 INFINITE PLANE, STANDARD HEIGHT AND FOCUS
1 " " " " SLOPING LATERAL GROUND, STANDARD HEIGHT AND FOCUS
4 " " −301.90 " " " " " MODIFIED FOCUS, 0°
4A " " " " " " " " " " −8°
4B " " " " " " " " " " 8°
ALL DIMENSIONS IN FEET
ZA's ARE ELEMENT HEIGHTS ABOVE TILTED PLANE
DDM – μa
4A
0
4
1
4B
−8°
0°
8°
AZIMUTH APPROACH ANGLE
ZA
YA
Y_{GE}
0.86°
10^6
Thousand feet from threshold
FLY! 75/11/14

FIGURE I-30

SIDEBAND REFERENCE - SLOPING LATERAL GROUND - MODIFIED FOCUS

$\lambda = 3'$
$\alpha_{GS} = 2.86°$
TCH = 55'
$Y_{ANT} = -300'$
$Y_{SE} = +150'$
(EXCEPT RUNS 0 AND 1)

RUN NO.	YA1	ZA1	YA2	ZA2	REMARKS
0	-300.0	7.52	-298.25	22.65	INFINITE PLANE, STANDARD HEIGHT & FOCUS
1	"	7.52	-299.97	22.65	" " , MODIFIED FOCUS
2	"	7.53	-300.50	22.58	SEE DIAGRAM BELOW
3	"	"	-300.30	"	"
4	"	"	-300.60	"	"
5	"	"	-300.90	"	"

XA1 = XA2 = -1100.93
ALL DIMENSIONS IN FEET
ZA's ARE HEIGHT ABOVE TILTED PLANE

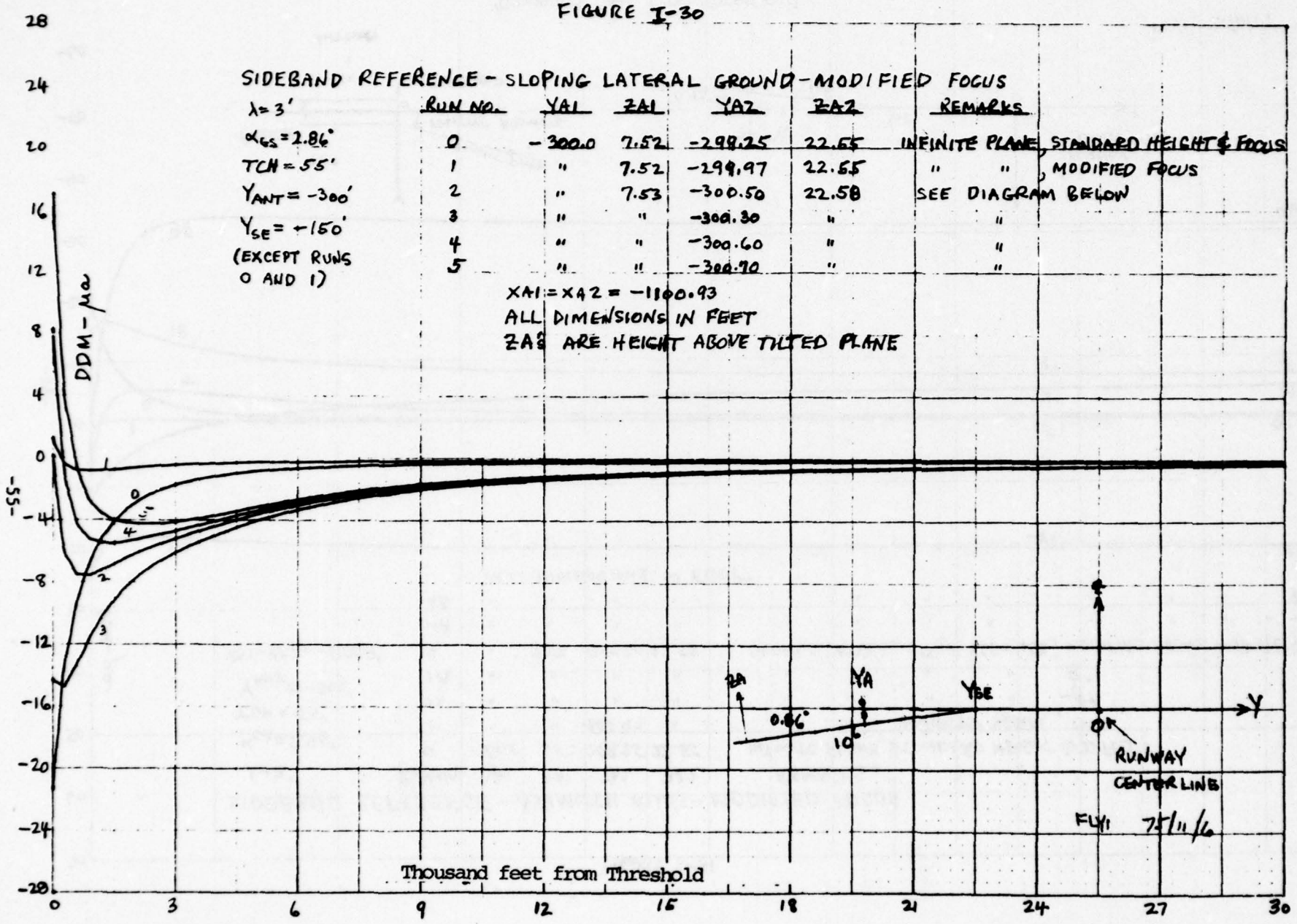

FIGURE I-31

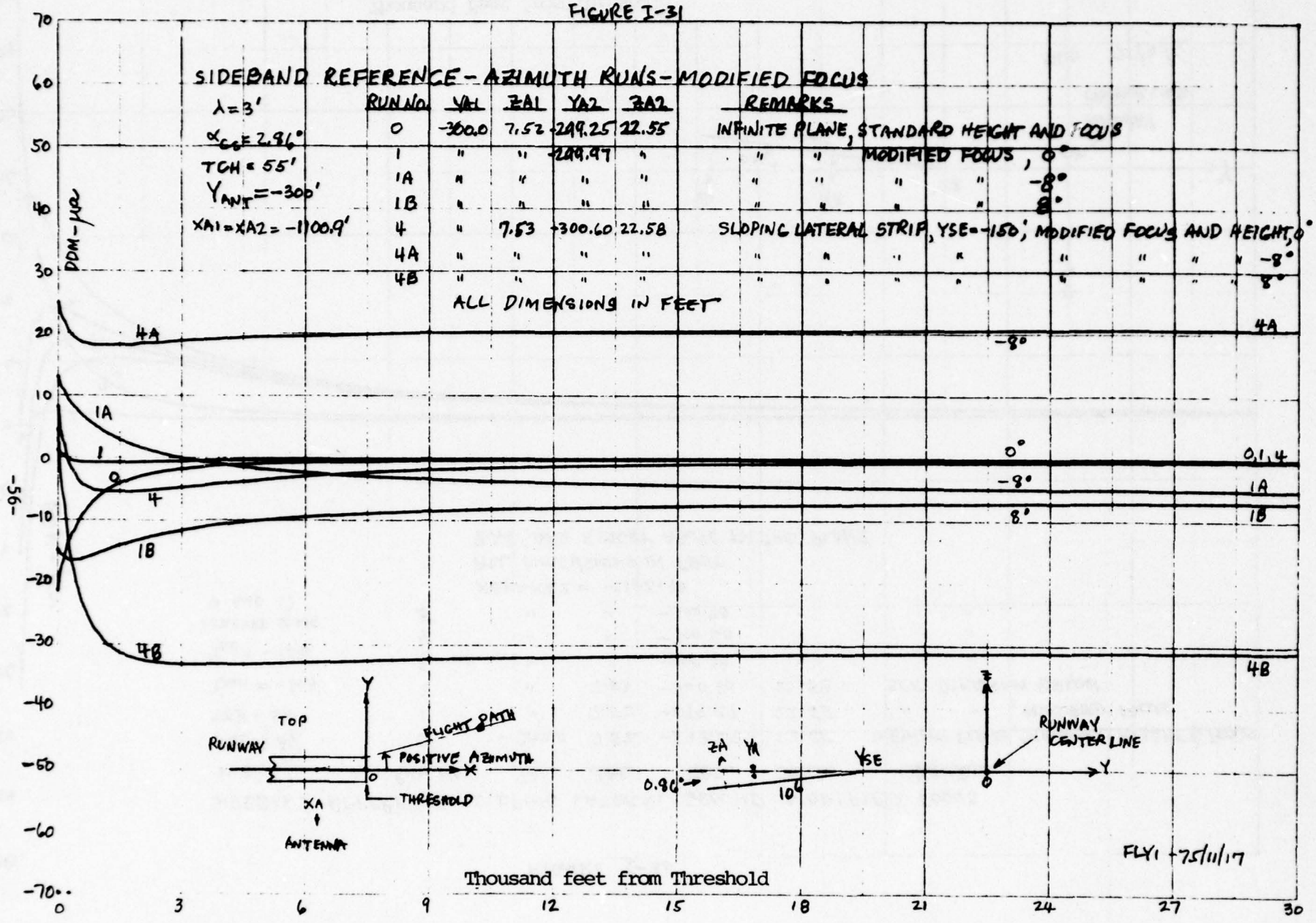
SIDEBAND REFERENCE - AZIMUTH RUNS - MODIFIED FOCUS
λ = 3'
α_{GS} = 2.96°
TCH = 55'
Y_{ANT} = -300'
XA1 = XA2 = -1100.9'
RUN No. YA1 ZA1 YA2 ZA2 REMARKS
0 -300.0 7.52 +299.25 22.55 INFINITE PLANE, STANDARD HEIGHT AND FOCUS
1 " " +299.97 " " " MODIFIED FOCUS, 0°
1A " " " " " " " -8°
1B " " " " " " " 8°
4 " 7.53 +300.60 22.58 SLOPING LATERAL STRIP, YSE = -150', MODIFIED FOCUS AND HEIGHT, 0°
4A " " " " " " " -8°
4B " " " " " " " 8°
ALL DIMENSIONS IN FEET
DDM - μa
4A
1A
1
0
4
1B
4B
-8°
0°
-8°
8°
4A
0, 1, 4
1A
1B
TOP
RUNWAY
FLIGHT PATH
POSITIVE AZIMUTH
THRESHOLD
XA
ANTENNA
ZA
YA
YSE
0.96°
10°
RUNWAY CENTER LINE
FLY1 - 75/11/17
Thousand feet from Threshold
70
60
50
40
30
20
10
0
-10
-20
-30
-40
-50
-60
-70
0
3
6
9
12
15
18
21
24
27
30

FIGURE I-32

CAPTURE EFFECT - SLOPING LATERAL GROUND - MODIFIED FOCUS

$\lambda = 3'$

$\alpha_{GG} = 2.86°$

TCH = 55'

$Y_{ANT} = -300'$ (YA2)

$Y_{SE} = -150'$

RUN NO.	YA1	ZA1	YA2	ZA2	YA3	ZA3	REMARKS
0	-301.13	15.03	-300.0	30.06	-248.11	45.09	STANDARD REFERENCE
1	-301.20	16.05	-300.0	30.10	-300.50	45.15	MODIFIED FOCUS & HEIGHT
2	-301.10	15.05	-300.0	30.10	-299.90	45.15	"
3	-301.20	15.05	-300.0	30.10	-300.40	45.15	"
4	-300.00	15.05	-300.0	30.10	-300.00	45.15	"

XA1 = XA2 = XA3 = -1100.93

ALL DIMENSIONS IN FEET

ZA's ARE HEIGHT ABOVE TILTED PLANE

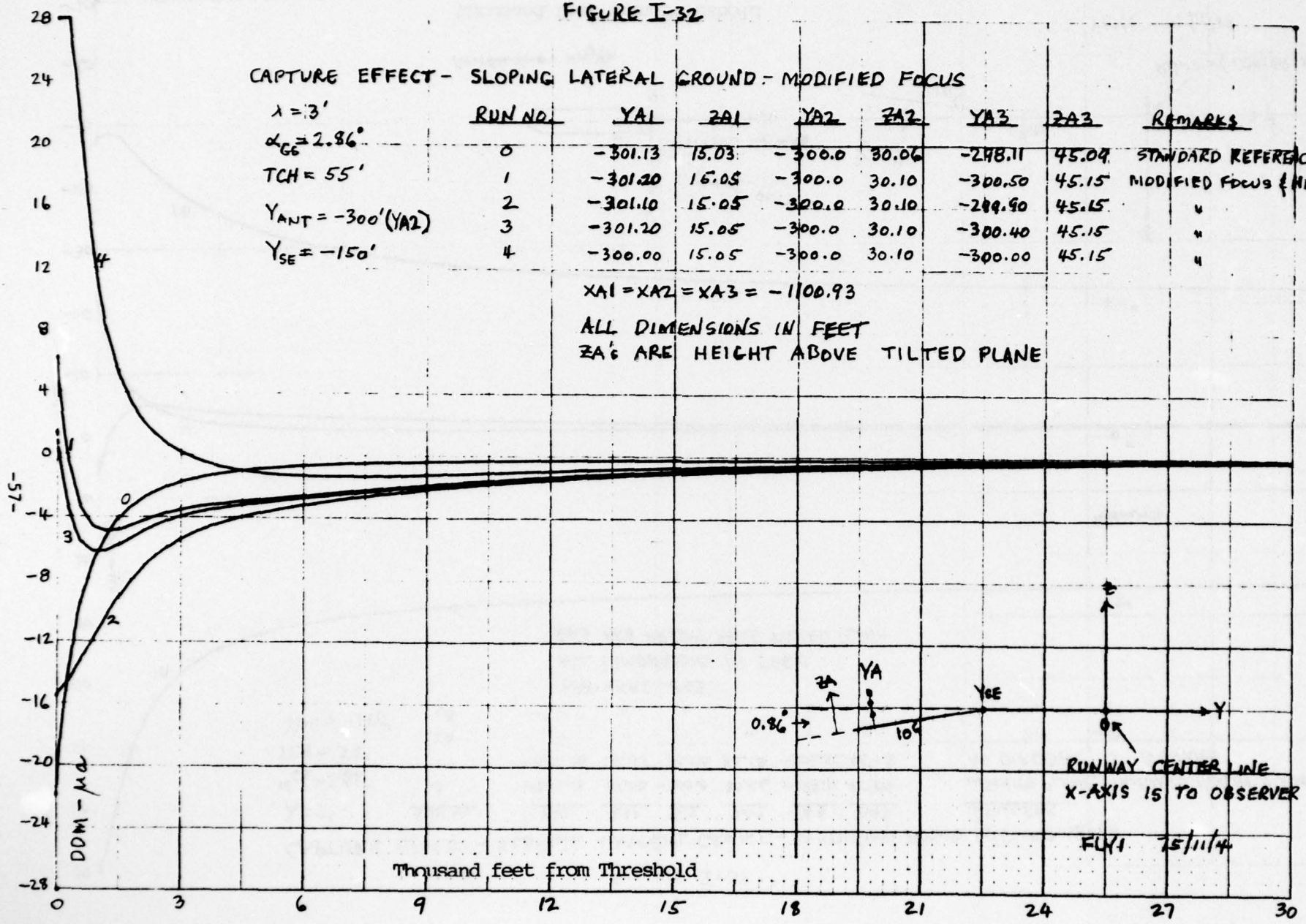

FLY1 75/11/4

FIGURE I-33

CAPTURE EFFECT - SLOPING LATERAL GROUND - MODIFIED FOCUS AND AZIMUTH

$\lambda = 3'$
$\alpha_{CS} = 2.86°$
TCH = 55'
YSE = -150'

RUN No.	YA1	ZA1	YA2	ZA2	YA3	ZA3	REMARKS
0	-301.13	15.03	-300.0	30.06	-298.11	45.09	INFINITE PLANE, STANDARD HEIGHT & FOCUS
1	-301.20	15.05	-300.0	30.10	-300.50	46.15	AS DIAGRAM, 0° AZIMUTH
1A	"	"	"	"	"	"	" -8° "
1B	"	"	"	"	"	"	" 8° "

XA1 = XA2 = XA3
ALL DIMENSIONS IN FEET
ZA's ARE HEIGHT ABOVE TILTED PLANE

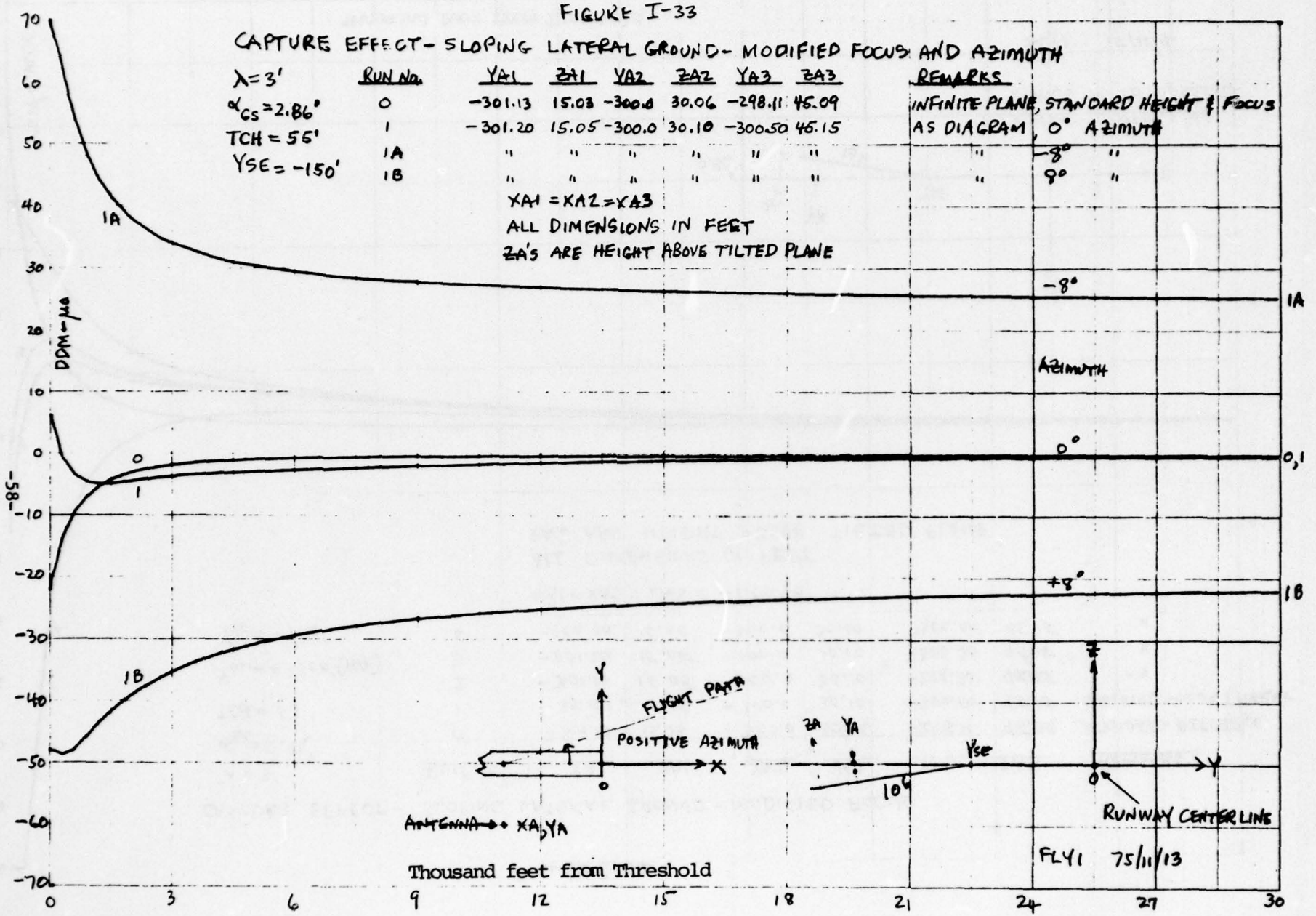

TABLE I-1

LIST OF COMPUTED GLIDE PATH DDM STRUCTURE RUNS

Total Number of Runs = 187

A. TERRAIN: SLOPING AND RISING FOREGROUND - 59 RUNS

Antenna	Figure	Run	Description
NULL REFERENCE, standard height and focus	I-1	0	standard reference (large flat plane, focused)
		1	10^6 ft. strip rising at 0.6° starting at antenna
		2	1200 ft. strip rising at 0.6° starting at antenna
		3	500 ft. strip rising at 0.6° starting at antenna
		4	10^6 ft. strip sloping at 0.6° starting at antenna
		5	1200 ft. strip sloping at 0.6° starting at antenna
		6	500 ft. strip sloping at 0.6° starting at antenna
SIDEBAND REFERENCE, standard height and focus	I-2	0	standard reference (large flat plane, focused)
		1	10^6 ft. strip rising at 0.6° starting at antenna
		2	1200 ft. strip rising at 0.6° starting at antenna
		3	500 ft. strip rising at 0.6° starting at antenna
		4	10^6 ft. strip sloping at 0.6° starting at antenna
		5	1200 ft. strip sloping at 0.6° starting at antenna
		6	500 ft. strip sloping at 0.6° starting at antenna
CAPTURE EFFECT, standard height and focus	I-3	0	standard reference (large flat plane, focused)
		1	10^6 ft. strip rising at 0.6° starting at antenna
		2	1200 ft strip rising at 0.6° starting at antenna
		3	500 ft. strip rising at 0.6° starting at antenna
		4	10^6 ft. strip sloping at 0.6° starting at antenna
		5	1200 ft. strip sloping at 0.6° starting at antenna
		6	500 ft. strip sloping at 0.6° starting at antenna

Antenna	Figure	Run	Description
NULL REFERENCE, standard height and and focus	I-4	0	standard reference
		1	10^6 ft. strip rising at 0.86° starting at threshold
		2	1000 ft. strip rising at 0.86° starting at threshold
		3	500 ft. strip rising at 0.86° starting at threshold
		4	10^6 ft. strip sloping at 0.86° starting at threshold
		5	1000 ft. strip sloping at 0.86° starting at threshold
		6	500 ft. strip sloping at 0.86° starting at threshold
SIDEBAND REFERENCE, standard height and focus	I-5	0	standard reference
		1	10^6 ft. strip rising at 0.86° starting at threshold
		2	1000 ft. strip rising at 0.86° starting at threshold
		3	500 ft. strip rising at 0.86° starting at threshold
		4	10^6 ft. strip sloping at 0.86° starting at threshold
		5	1000 ft. strip sloping at 0.86° starting at threshold
		6	500 ft. strip sloping at 0.86° starting at threshold
CAPTURE EFFECT, standard height and focus	I-6	0	standard reference
		1	10^6 ft. strip rising at 0.86° starting at threshold.
		2	1000 ft. strip rising at 0.86° starting at threshold
		3	500 ft. strip rising at 0.86° starting at threshold
		4	10^6 ft. strip sloping at 0.86° starting at threshold
		5	1000 ft. strip sloping at 0.86° starting at threshold
		6	500 ft. strip sloping at 0.86° starting at threshold

Antenna	Figure	Run	Description
CAPTURE EFFECT, standard height and focus	I-7	0	standard reference
		1	10^6 ft. strip rising at 1.72° starting at threshold
		2	1000 ft. strip rising at 1.72° starting at threshold
		3	500 ft. strip rising at 1.72° starting at threshold
		4	10^6 ft. strip sloping at 1.72° starting at threshold
		5	1000 ft. strip sloping at 1.72° starting at threshold
		6	500 ft. strip sloping at 1.72° starting at threshold

B. TERRAIN: STEP DOWN IN ANTENNA FOREGROUND - 36 RUNS

Antenna	Figure	Run	Description
NULL REFERENCE, standard height and focus	I-8	SR	standard reference
		10	10 ft. step at 1000 ft. from antenna
		20	20 ft. step at 1000 ft. from antenna
		30	30 ft. step at 1000 ft. from antenna
		50	50 ft. step at 1000 ft. from antenna
		10^7	10^7 ft. step at 1000 ft. from antenna
SIDEBAND REFERENCE, standard height and focus	I-9	SR	standard reference
		10	10 ft. step at 1000 ft. from antenna
		20	20 ft. step at 1000 ft. from antenna
		30	30 ft. step at 1000 ft. from antenna
		50	50 ft. step at 1000 ft. from antenna
		10^7	10^7 ft. step at 1000 ft. from antenna

Antenna	Figure	Run	Description
CAPTURE EFFECT, standard height and focus	I-10	SR	standard reference
		10	10 ft. step at 1000 ft. from antenna
		20	20 ft. step at 1000 ft. from antenna
		30	30 ft. step at 1000 ft. from antenna
		50	50 ft. step at 1000 ft. from antenna
		10^7	10^7 ft. step at 1000 ft. from antenna
NULL REFERENCE, standard height and focus	I-11	SR	standard reference
		10	10 ft. step at 500 ft. from antenna
		20	20 ft. step at 500 ft. from antenna
		30	30 ft. step at 500 ft..from antenna
		50	50 ft. step at 500 ft. from antenna
		10^7	10^7 ft. step at 500 ft. from antenna
SIDEBAND REFERENCE, standard height and focus	I-12	SR	standard reference
		10	10 ft. step at 500 ft. from antenna
		20	20 ft. step at 500 ft. from antenna
		30	30 ft. step at 500 ft. from antenna
		50	50 ft. step at 500 ft. from antenna
		10^7	10^7 ft. step at 500 ft. from antenna
CAPTURE EFFECT, standard height and focus	I-13	SR	standard reference
		10	10 ft. step at 500 ft. from antenna
		20	20 ft. step at 500 ft. from antenna
		30	30 ft. step at 500 ft. from antenna
		50	50 ft. step at 500 ft. from antenna
		10^7	10^7 ft. step at 500 ft. from antenna

C. TERRAIN: SLOPING AND RISING FOREGROUND - 48 RUNS

Antenna	Figure	Run	Description
NULL REFERENCE, standard focus. Standard height above tilted plane.	I-14	0	standard reference
		1	200 ft. 0.86° sloping strip
		2	200 ft. 0.86° sloping strip plus 200 ft. horizontal strip
		3	200 ft. 0.86° sloping strip plus 10^6 ft. horizontal strip
		4	200 ft. 0.86° sloping strip plus 200 ft. 0.86° rising strip
SIDEBAND REFERENCE, standard focus. Standard height above tilted plane	I-15	0	standard reference
		1	200 ft. 0.86° sloping strip
		2	200 ft. 0.86° sloping strip plus 200 ft. horizontal strip
		3	200 ft. 0.86° sloping strip plus 10^6 ft. horizontal strip
		4	200 ft. 0.86° sloping strip plus 200 ft. 0.86° rising strip
CAPTURE EFFECT, standard focus. Standard height above tilted plane	I-16	0	standard reference
		1	200 ft. 0.86° sloping strip
		2	200 ft. 0.86° sloping strip plus 200 ft. horizontal strip
		3	200 ft. 0.86° sloping strip plus 10^6 ft. horizontal strip
		4	200 ft. 0.86° sloping strip plus 200 ft. 0.86° rising strip.

Antenna	Figure	Run	Description
CAPTURE EFFECT, standard focus. Standard height above tilted plane	I-17	0	150 ft. lateral edge plus 200 ft. strip at 0° slope
		0.86	150 ft. lateral edge plus 200 ft. strip at 0.86° slope
		1.72	150 ft. lateral edge plus 200 ft. strip at 1.72° slope
NULL REFERENCE, standard focus. Standard height above tilted plane	I-18	0	standard reference
		0.86	Lateral trough, 200 ft. sides at 0.86° angle
		1.72	Lateral trough, 200 ft. sides at 1.72° angle
		3.44	Lateral trough, 200 ft. sides at 3.44° angle
		6.88	Lateral trough, 200 ft. sides at 6.88° angle
SIDEBAND REFERENCE, standard focus. Standard height above tilted plane	I-19	0	standard reference
		0.86	lateral trough, 200 ft. sides at 0.86° angle
		1.72	lateral trough, 200 ft. sides at 1.72° angle
		3.44	lateral trough, 200 ft. sides at 3.44° angle
		6.88	lateral trough, 200 ft. sides at 6.88° angle
CAPTURE EFFECT, standard focus. Standard height above tilted plane	I-20	0	standard reference
		0.86	lateral trough, 200 ft. sides at 0.86° angle
		1.72	lateral trough, 200 ft. sides at 1.72° angle
		3.44	lateral trough, 200 ft. sides at 3.44° angle
		6.88	lateral trough, 200 ft. sides at 6.88° angle

Antenna	Figure	Run	Description
NULL REFERENCE, Standard focus. Standard height above tilted plane	I-21	0	standard reference
		0.86	lateral trough, 150 ft. sides, at 0.86° angle
		1.72	lateral trough, 150 ft. sides, at 1.72° angle
		3.44	lateral trough, 150 ft. sides, at 3.44° angle
		6.88	lateral trough, 150 ft. sides, at 6.88° angle
SIDEBAND REFERENCE, standard focus. Standard height above tilted plane	I-22	0	standard reference
		0.86	lateral trough, 150 ft. sides, at 0.86° angle
		1.72	lateral trough, 150 ft. sides, at 1.72° angle
		3.44	lateral trough, 150 ft. sides, at 3.44° angle
		6.88	lateral trough, 150 ft. sides, at 6.88° angle
CAPTURE EFFECT, standard focus. Standard height above tilted plane	I-23	0	standard reference
		0.86	lateral trough, 150 ft. sides, at 0.86° angle
		1.72	lateral trough, 150 ft. sides, at 1.72° angle
		3.44	lateral trough, 150 ft. sides, at 3.44° angle
		6.88	lateral trough, 150 ft. sides, at 6.88° angle

D. TERRAIN: **LATERAL EDGE - 21 RUNS**

Antenna	Figure	Run	Description
NULL REFERENCE, standard height and focus	I-24	0	lateral edge 0 ft. from antenna
		5	lateral edge 5 ft. from antenna
		10	lateral edge 10 ft. from antenna
		20	lateral edge 20 ft. from antenna
		30	lateral edge 30 ft. from antenna
		40	lateral edge 40 ft. from antenna

Antenna	Figure	Run	Description
NULL REFERENCE, standard height and focus	I-25	50	lateral edge 50 ft. from antenna
		100	lateral edge 100 ft. from antenna
		200	lateral edge 200 ft. from antenna
SIDEBAND REFERENCE, standard height and focus	I-26	0	lateral edge 0 ft. from antenna
		5	lateral edge 5 ft. from antenna
		10	lateral edge 10 ft. from antenna
		20	lateral edge 20 ft. from antenna
		30	lateral edge 30 ft. from antenna
		40	lateral edge 40 ft. from antenna
CAPTURE EFFECT, standard height and focus	I-27	0	lateral edge 0 ft. from antenna
		5	lateral edge 5 ft. from antenna
		10	lateral edge 10 ft. from antenna
		20	lateral edge 20 ft. from antenna
		30	lateral edge 30 ft. from antenna
		40	lateral edge 40 ft. from antenna

E. TERRAIN: FLAT AND SLOPING LATERAL GROUND - 33 RUNS

Antenna	Figure	Run	Description
NULL REFERENCE, standard and modified focus	I-28	0	standard reference. Infinite plane, standard height and focus. 0° azimuth
		0A	standard reference. Infinite plane, standard height and focus. -8° azimuth.
		0B	standard reference. Infinite plane, standard height and focus. 8° azimuth.
		1	infinite plane, standard height, modified focus, 0°
		1A	infinite plane, standard height, modified focus, -8°
		1B	infinite plane, standard height, modified focus, 8°

Antenna	Figure	Run	Description
NULL REFERENCE, standard and modified focus	I-29	0	standard reference
		1	10^6 ft. lateral strip, standard height and focus
		4	10^6 ft. lateral strip, modified focus, 0°
		4A	10^6 ft. lateral strip, modified focus, -8°
		4B	10^6 ft. lateral strip, modified focus, 8°
SIDEBAND REFERENCE, modified focus and height	I-30	0	standard reference
		1	infinite plane, standard height, modified focus
		2	10^6 ft lateral strip, modified height and focus
		3	10^6 ft. lateral strip, same height and different focus
		4	10^6 ft. lateral strip, same height and different focus
		5	10^6 ft. lateral strip, same height and different focus
SIDEBAND REFERENCE, modified focus and height	I-31	0	standard reference
		1	infinite plane, standard height, modified focus, 0° azimuth
		1A	infinite plane, standard height, modified focus, -8° azimuth
		1B	infinite plane, standard height, modified focus, 8° azimuth
		4	sloping 10^6 ft. lateral strip, modified height and focus, 0° azimuth
		4A	sloping 10^6 ft. lateral strip, modified height and focus, -8° azimuth
		4B	sloping 10^6 ft. lateral strip, modified height and focus, 8° azimuth.

Antenna	Figure	Run	Description
CAPTURE EFFECT, modified focus and height	I-32	0	standard reference
		1	sloping 10^6 ft. lateral strip, modified height and focus
		2	sloping 10^6 ft. lateral strip, modified height and focus
		3	sloping 10^6 ft. lateral strip, modified height and focus
		4	sloping 10^6 ft. lateral strip, modified height and focus
CAPTURE EFFECT, modified focus and height	I-33	0	standard reference
		1	sloping 10^6 ft. lateral strip, modified height and focus, 0° azimuth
		1A	sloping 10^6 ft. lateral strip, modified height and focus, -8° azimuth
		1B	sloping 10^6 ft. lateral strip, modified height and focus, 8° azimuth

TABLE I-2

CATEGORY I AND II GLIDE SLOPE DDM TOLERANCE

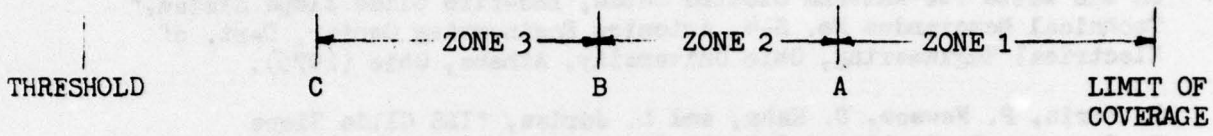

A - 4 nautical miles from threshold

B - 3500 feet from threshold

C - distance at which commissioned glide path is 100 feet above the threshold horizontal plane (901 feet for glide slope angle of 2.86°)

CATEGORY	ZONE	T (μa) (Deviation of the average from the ideal focused, infinite plane glide path, + or -)	t (μa) (Peak deviation from average, + or -)
I	1,2	37.5	30
II	1	37.5	30
	2	37.5	30 at A, 20 at B
	3	37.5 at B to 48.75 at C to 75 at threshold	20

REFERENCES

1. D.A. Hill and R.H. McFarland, "The Effects of Irregular Contour on Image Glide Path Systems," Report EER 5-4, Avionics Research Group, Dept. of Electrical Eng., Ohio University Research Institute, Athens, Ohio (1966).

2. H.B. Tran, "Investigation of the Effects of Irregular Terrain Contour on the Watts Two-Antenna Slotted Cable, End-fire Glide Slope System," Technical Memorandum No. S-4, Avionics Engineering Center, Dept. of Electrical Engineering, Ohio University, Athens, Ohio (1975).

3. S. Morin, P. Newsom, D. Kahn, and L. Jordan, "ILS Glide Slope Performance Prediction," Vol. A, Report No. FAA-RD-74-157.A, Transportation Systems Center, Cambridge, Mass. (1974).*

4. T.B.A. Senior, "The Diffraction of a Dipole Field by a Perfectly Conducting Half-plane," Quart. Journal Mech. and Applied Math., Vol. VI, Pt. 1, p. 101 (1953).

5. B.D. Woods, "The Diffraction of a Dipole Field by a Half-plane," Quart. Journal Mech. and Applied Math., Vol. X, Pt. 1, p.90 (1957).

6. T.J.I'A. Bromwich, Proc. London Math. Soc., 14, p.450 (1915).

7. R.W. Redlich, "Image Radiation from a Finite Ground Plane in Two Dimensions," IEEE Trans. on Antennas and Prop., AP-16, No. 3, p. 334 (1968).

8. R.W. Redlich, "Computed Performance of Glide Slope Arrays on Sites with Limited Ground Planes," IEEE Trans. on Aerospace and Elec. Sys., AES-7, No. 5, p.854 (1971).

9. H. Goldstein, Classical Mechanics, Addison-Wesley Pub. Co., Inc., Reading, Mass., p. 107 (1950).

10. M. Born and E. Wolf, Principals of Optics, Pergamon Press, N.Y., New York, p.564 (1959).

11. S.A. Schelkunoff and H.T. Friis, Antennas: Theory and Practice, Wiley and Sons, Inc., N.Y., New York (1952).

12. DOT/FAA Handbook No. 6750.6A, Installation Instructions for ILS Glide Slope, Federal Aviation Administration, Washington, D.C. (1969). *

13. J.G. Lucas, "The Effect of a Limited Ground Plane on a 2.86 Degree M-Array Glide-path," Air Navigation Group, University of Sidney, Sidney, Australia (1972).

14. R.S. Satterwhite and R.G. Kouyoumjian, "Electromagnetic Diffraction by a Perfectly Conducting Plane Angular Section," Ohio State University Electroscience Laboratory, Columbus, Ohio (1970).

* These documents are available through National Technical Information Service, Springfield, Virginia 22151.

REFERENCES

15. J. T. Godfrey, H. F. Hartley, R. A. Moore, G. J. Moussally, "Capture Effect Array Glide Slope Guidance Study", Westinghouse Defense and Electronic Systems Center rpeort to FAA under Contract DOT-FA74WA-3353 May, 1975.